

**Appendix C**  
**NIWA Report**

# Modelling the effects of coastal reclamation on tidal currents and sedimentation within Mangere Inlet

*Prepared for The East-West Link Alliance*

*October 2016*



Prepared by:

Mark Pritchard  
Glen Reeve  
Richard Gorman  
Ben Robinson


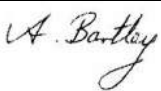

For any information regarding this report please contact:

Mark Pritchard  
Coastal and Estuarine Physical Process Scientist  
Estuarine and Coastal  
+64-7-856 1744  
m.pritchard@niwa.co.nz

National Institute of Water & Atmospheric Research Ltd  
PO Box 11115  
Hamilton 3251

Phone +64 7 856 7026

NIWA CLIENT REPORT No: 2016015HN  
Report date: October 2016  
NIWA Project: GHD16201

Quality Assurance Statement		
	Reviewed by:	Scott Stephens
	Formatting checked by:	Alison Bartley
	Approved for release by:	David Roper

# Contents

- Executive summary ..... 8**
  
- 1 Introduction ..... 10**
  
- 2 Model Applications..... 11**
  
- 3 Hydrodynamic, wave and sediment transport model development ..... 12**
  - 3.1 Delft3D modelling Suite ..... 12
  - 3.2 Model grid..... 12
  - 3.3 Tidal elevations, currents and boundary conditions ..... 15
  - 3.4 Winds ..... 15
  - 3.5 Sediments and sedimentation rates..... 17
  - 3.6 Sediment transport model set up..... 18
  
- 4 Model calibration and validation ..... 20**
  - 4.1 Calibration procedure..... 20
  - 4.2 Hydrodynamic model calibration and validation results..... 21
  
- 5 Model results..... 24**
  - 5.1 Tidal current flows ..... 24
  - 5.2 Sediment transport: pre- and post-reclamation ..... 29
  - 5.3 Predicted area mean ASR in Mangere Inlet pre- and post-coastal reclamation .... 36
  
- 6 Predicted inlet sedimentation rates and sea level rise..... 37**
  - 6.1 Predicted mean ASR in Mangere Inlet with reclamation and SLR..... 38
  
- 7 Effects of mudcrete dredging in entrance channel to Mangere Inlet ..... 39**
  - 7.1 Predicted mean ASR in Mangere Inlet with coastal reclamation and mudcrete dredge..... 41
  
- 8 Point source discharge of suspended sediment plumes ..... 42**
  - 8.1 Suspended sediment plume modelling – model set up ..... 42
  
- 9 Wave climate and extreme wave analysis inside Mangere inlet..... 49**
  - 9.1 Extreme value analysis..... 49
  - 9.2 Results of extreme value analysis of  $H_{sig}$  ..... 50
  
- 10 Conclusions ..... 51**
  
- 11 Acknowledgements ..... 51**



<b>12</b>	<b>References.....</b>	<b>52</b>
<b>Appendix A</b>	<b>Deltares Delft3D modelling suite .....</b>	<b>54</b>
<b>Appendix B</b>	<b>Skill tests .....</b>	<b>56</b>
<b>Appendix C</b>	<b>Tidal Calibration.....</b>	<b>57</b>
<b>Appendix D</b>	<b>Reclamation Scenarios .....</b>	<b>61</b>
<b>Appendix E</b>	<b>Sediment settling velocity experiments .....</b>	<b>71</b>

## Tables

Table 4-1:	Skill test results between observed 2006 water levels at Onehunga tide gauge and S4 mooring and Delft3D model predictions for the coincident 2006 period.	21
Table 4-2:	Skill test results between DHI model 1995 water levels at Onehunga tide gauge and S4 site and Delft3D model predictions for the coincident 1995 period.	22
Table 4-3:	Skill test results between DHI model 1995 currents at Old Mangere Bridge (OMB) and S4 site and Delft3D model predictions for the coincident 1995 period.	23
Table 8-1:	Locations and details of point source sediment discharges sourced from engineering work into Mangere Inlet.	42
Table 9-1:	Maximum predicted significant wave height ( $H_{sig}$ ) for a range of water depth and ARI (years).	50

## Figures

Figure 1-1:	Google earth image of study area showing the geographical limits of the model, tidal boundary, model calibration sites and area of coastal reclamation. Image courtesy of Google Earth®	10
Figure 3-1:	Model computational grid. Model is forced along the western most boundary with time series of tidal elevations or astronomical constants.	13
Figure 3-2:	High resolution model grid developed for region of inlet where coastal reclamation and changes in coastline will be taking place.	13
Figure 3-3:	Pre-reclamation model coastline and bathymetry developed from Ports of Auckland survey data, LINZ charts and LIDAR data.	14
Figure 3-4:	Post-reclamation and bathymetric layout and coastline on the north shore of Mangere Inlet for reclamation version V04.	14
Figure 3-5:	Auckland Airport wind rose for the period 1980 to 2011.	17
Figure 4-1:	Observed (Green and Bell, 1995) and Delft3D modelled tidal hysteresis at Mangere Bridge during a tidal gauging experiment over a complete spring tidal cycle during 1994.	21
Figure 5-1:	Model predicted peak flood current speed and direction on a spring tidal cycle in Mangere Inlet. HW-2 = 2-hours before high water.	24
Figure 5-2:	Model predicted peak ebb current speed and direction on a spring tidal cycle in Mangere Inlet. LW-2 = 2-hours before low water.	25

Figure 5-3:	Model predicted peak flood current speed and direction on a neap tidal cycle in Mangere Inlet. HW-2 = 2-hours before high water.	25
Figure 5-4:	Model predicted peak ebb current speed and direction on a neap tidal cycle in Mangere Inlet. LW-2 = 2-hours before low water.	26
Figure 5-5:	Difference in peak flood current speed due to proposed coastal reclamation in Mangere Inlet during a spring tide.	27
Figure 5-6:	Difference in peak ebb current speed due to proposed coastal reclamation in Mangere Inlet during a spring tide.	27
Figure 5-7:	Difference in peak flood current speed due to proposed coastal reclamation in Mangere inlet during a neap tide.	28
Figure 5-8:	Difference in peak ebb current speed due to proposed coastal reclamation in Mangere inlet during a neap tide.	28
Figure 5-9:	Time series of modelled water levels ( $\eta$ ), bed shear stress ( $\tau$ ), SSC and sediment deposition at the Old Mangere Bridge site for calm, SW and NE wind wave conditions.	29
Figure 5-10:	Predicted $ASR_{CALM}$ (mm/yr) in Mangere Inlet for calm (tide only) conditions for pre-reclamation bathymetry using equation (1).	30
Figure 5-11:	Predicted $ASR_{SW}$ (mm/yr) in Mangere Inlet for SW wind (tide and waves) conditions for pre-reclamation bathymetry using equation (1).	31
Figure 5-12:	Predicted $ASR_{NE}$ (mm/yr) in Mangere Inlet for NE wind (tide and waves) conditions for pre-reclamation bathymetry using equation (1).	32
Figure 5-13:	Predicted wind climate composite $ASR_{WDCLI}$ (mm/yr) in Mangere Inlet from the weighted wind climate using equation (2) for pre-reclamation bathymetry.	32
Figure 5-14:	Predicted ASR rate (mm/yr) in Mangere Inlet from LIDAR data analysis (see Section 3.5).	32
Figure 5-15:	Predicted wind climate composite $ASR_{WDCLI}$ (mm/yr) in Mangere Inlet from the weighted wind climate using equation (2) for V04 post-reclamation coastline and bathymetry.	33
Figure 5-16:	Predicted changes in wind climate composite $ASR_{WDCLI}$ (mm/yr) caused by proposed coastal reclamation in Mangere Inlet using equation (3). Differences in modelled pre- and post-reclamation $\Delta ASR_{WDCLI} \pm 0.5$ mm/yr are blanked out. NE and N2Smark cross-sections where tidal volumetric fluxes are computed.	34
Figure 5-17:	Predicted tidal cumulative volumetric transport (V) and instantaneous volumetric flux (Q) over x-section N2S (see Figure 5-16) for present day (V0) and reclamation (V4) coastlines.	35
Figure 5-18:	Predicted tidal cumulative volumetric transport (V) and instantaneous volumetric flux (Q) over x-section NE (see Figure 5-16) for present day (V0) and reclamation (V04) coastlines.	36
Figure 6-1:	Predicted changes in wind climate composite $ASR_{WDCLI}$ (mm/yr) caused by proposed coastal reclamation in Mangere Inlet using equation (3) and sea-level rise. Differences in modelled pre- and post-reclamation $\Delta ASR_{WDCLI} \pm 0.5$ mm/yr are blanked out.	37
Figure 7-1:	Proposed area of the dredging (black broken line) of bed material to be used for mudcrete in the coastal reclamation. Three locations of point sources of sediment plumes are also shown (see Section 8).	39
Figure 7-2:	Predicted changes in wind climate composite $ASR_{WDCLI}$ (mm/yr) caused by dredging operations in Mangere Inlet with proposed coastal reclamation in place based	

	equation (3). Differences in modelled pre- and post-dredging $ASR_{WDCLI} \pm 0.5$ mm/yr are blanked out.	40
Figure 7-3:	Difference in peak flood current speed due to proposed coastal reclamation and dredging in Mangere inlet on a mean (M2) flood tide.	41
Figure 7-4:	Difference in peak flood current speed due to proposed coastal reclamation and dredging in Mangere inlet on mean (M2) ebb tide.	41
Figure 8-1:	Predicted water column SSC at Source 1 (3.3 m) and 100 m and 200 m east and west of source location during calm, SW and NE winds.	43
Figure 8-2:	Source 1 suspended sediment plumes daily rate of bed deposition.	44
Figure 8-3:	Predicted water column SSC at Source 2 (1.7 m) and 100 m and 200 m east and west of source location during calm, SW and NE winds.	45
Figure 8-4:	Source 2 suspended sediment plumes daily rate of bed deposition.	46
Figure 8-5:	Predicted water column SSC at Source 2 (1.0 m) and 100 m and 200 m east and west of source location during calm, SW and NE winds.	47
Figure 8-6:	Source 3 suspended sediment plumes daily rate of bed deposition.	48
Figure 9-1:	Frequency–magnitude distribution of significant wave height ( $H_{sig}$ ) at 3 nearshore water depths inside Mangere Inlet.	50
Figure C-1:	Water level calibration at Onehunga Wharf and the NIWA S4 mooring site for 2006.	57
Figure C-2:	Model current velocity validation at Onehunga site for 1995 period.	58
Figure C-3:	Model current velocity validation at NIWA S4 mooring site for 1995 period.	59
<b>Figure C-4:</b>	<b>Model water level validation for locations at Onehunga and NIWA S4 mooring site.</b>	60
Figure D-1:	Difference in peak flood current speed due to coastal reclamation design V01 in Mangere Inlet during a mean tide.	61
Figure D-2:	Difference in peak ebb current speed due to coastal reclamation design V01 in Mangere Inlet during a mean tide.	61
Figure D-3:	Predicted changes in wind climate composite $ASR_{WDCLI}$ (mm/yr) caused by coastal reclamation design V01 in Mangere Inlet using equation (3). Differences in modelled pre- and post-reclamation $ASR_{WDCLI} \pm 0.5$ mm/yr are blanked out.	62
Figure D-4:	Difference in peak flood current speed due to coastal reclamation design V02 in Mangere Inlet during a mean tide.	63
Figure D-5:	Difference in peak ebb current speed due to coastal reclamation design V02 in Mangere Inlet during a mean tide.	63
Figure D-6:	Predicted changes in wind climate composite $ASR_{WDCLI}$ (mm/yr) caused by coastal reclamation design V02 in Mangere Inlet using equation (3). Differences in modelled pre- and post-reclamation $ASR_{WDCLI} \pm 0.5$ mm/yr are blanked out.	64
Figure D-7:	Difference in peak flood current speed due to coastal reclamation design V03 in Mangere Inlet during a mean tide.	65
Figure D-8:	Difference in peak ebb current speed due to coastal reclamation design V03 in Mangere Inlet during a mean tide.	65
Figure D-9:	Predicted changes in wind climate composite $ASR_{WDCLI}$ (mm/yr) caused by coastal reclamation design V03 in Mangere Inlet using equation (3).	

	Differences in modelled pre- and post-reclamation $ASR_{WDCLl} \pm 0.5$ mm/yr are blanked out.	66
Figure D-10:	Difference in peak flood current speed due to coastal reclamation design V04 in Mangere Inlet during a mean tide.	67
Figure D-11:	Difference in peak ebb current speed due to coastal reclamation design V04 in Mangere Inlet during a mean tide.	67
Figure D-12:	Predicted changes in wind climate composite $ASR_{WDCLl}$ (mm/yr) caused by coastal reclamation design V04 in Mangere Inlet using equation (3). Differences in modelled pre- and post-reclamation $ASR_{WDCLl} \pm 0.5$ mm/yr are blanked out.	68
Figure D-13:	Difference in peak flood current speed due to coastal reclamation design V05 in Mangere Inlet during a mean tide.	69
Figure D-14:	Difference in peak ebb current speed due to coastal reclamation design V05 in Mangere Inlet during a mean tide.	69
Figure D-15:	Predicted changes in wind climate composite $ASR_{WDCLl}$ (mm/yr) caused by coastal reclamation design V05 in Mangere Inlet using equation (3). Differences in modelled pre- and post-reclamation $ASR_{WDCLl} \pm 0.5$ mm/yr are blanked out.	70

## Executive summary

The East West Link Alliance (NZTA, Beca, GHD, and Buddle Finlay) has been formed to prepare preliminary design, and supporting technical reports and assessment of environmental effects for resource application for a new road link. The road aims to improve freight efficiency and vehicle travel times in the Onehunga, Penrose, Mt Wellington, Mangere, Otahuhu and East Tamaki areas of Auckland. Accommodation of the East West link will require coastal reclamation work along the north coastline of Mangere Inlet.

NIWA was contracted to develop a hydrodynamic and sediment transport model of Mangere Inlet, to model the relative change in tidal flow and sediment deposition following coastal reclamation along the inlet's north shore.

This technical report presents details on the model development and calibration plus model results from a series of tide, wind and wave driven scenarios designed to establish the effects of coastal reclamation on tidal circulation, and sediment transport inside Mangere Inlet. The model scenarios are aimed to assess relative changes inside the inlet (compared to pre-reclamation) in coastal physical processes (hydrodynamic, wave and sediment transport) in the entrance and inside Mangere Inlet.

The model was calibrated and validated using available water level and current measurements. Skill levels (statistical agreement) were high between the observed and modelled water levels. The modelled currents were consistent with the gauging observations, reproducing the shape of the flood-ebb current hysteresis curve through the inlet.

The calibrated hydrodynamic model was run for spring and neap tidal ranges for pre- and post-reclamation coastlines and bathymetries. The main differences in tidal circulation caused by coastal reclamation were predicted adjacent to the reclaimed coastline. The series of new headlands, coves and embayments along the northern stretch of the new coastline act to reduce tidal current speeds and therefore, encouraged slightly more sediment deposition inside the inlet.

The model predicted the inlet to be flood-dominant (infilling). The estimated annual sedimentation rate, averaged over the whole of the existing inlet, was 9.8 mm/yr, which compares closely to an analysis using LIDAR data that estimated an annual sedimentation rate of 10 mm/yr.

The modelled mean annual sedimentation rate after reclamation was similar, being 10.5 mm/yr. The model predicted relative increases in sediment deposition along most of the northern stretch of reclaimed coastline, due to lower current speeds which have less sediment-carrying capacity. Further east along the reclamation there was more relative erosion that resulted from a localised change in the tidal circulation. Analysis of volumetric tidal fluxes in the east section on the inlet showed there was no overall change in the tidal exchange due to the coastal reclamation.

The effects of sea level rise were incorporated into modelling by assuming 1 m increase in sea-level and 0.5 m increase in seabed height due to sedimentation. Results from the modelling predicted a 10.4 mm/yr annual sedimentation rate.

Modelling that investigated the effect of dredging and removing approximately 300,000 m<sup>3</sup> of bed material from the west of Mangere Inlet predicted a decrease in tidal current speeds through the entrance to the inlet. The modelling predicted decreases in tidal current speeds would increase sediment deposition to the north and south of the dredged area. The predicted annual sedimentation rate with both coastal reclamation and dredged area was 10.4 mm/yr.

The model was used to investigate the dispersion of sediment plumes discharged from three point sources during construction and coastal reclamation work in Mangere Inlet. The results from the modelling showed that sediment settled out of the water column almost immediately once a source was turned off. Most of the sediment deposited along the northern and eastern coast of the inlet.

The report includes a table of the expected frequency and magnitude of extreme wave heights in Mangere Inlet, in water depths of 0.5, 1.0 and 2.0 m.

## 1 Introduction

A new east west connection road link project aims to improve freight efficiency and vehicle travel times in the Onehunga, Penrose, Mt Wellington, Mangere, Otahuhu and East Tamaki areas of Auckland. The East West Link Alliance (NZTA, Beca, GHD, and Buddle Finlay) awarded NIWA the contract to develop a hydrodynamic and sediment transport model of Mangere Inlet where there will be coastal reclamation work along the north shore of the inlet (see Figure 1-1) required to accommodate the new road connection and coastal edge.

The numerical model was used to estimate changes in present day tidal circulation and sedimentation rates caused by the proposed coastal reclamation work inside Mangere Inlet.

An extreme-value analysis on wave height inside Mangere Inlet was performed for shallow water regions adjacent to the coast.



**Figure 1-1:** Google earth image of study area showing the geographical limits of the model, tidal boundary, model calibration sites and area of coastal reclamation. Image courtesy of Google Earth®

## 2 Model Applications

The hydrodynamic and sediment transport models developed for this project were used to predict:

1. Tidal flows in the inlet for existing bathymetry during neap tides.
2. Tidal flows in the inlet for existing bathymetry during spring tides.
3. Peak tidal flows in the inlet with coastal reclamation and dredging in place during neap tides.
4. Peak tidal flows in the inlet with coastal reclamation and dredging in place during spring tides.
5. Sedimentation rates over a single mean tide during calm, SW winds and NE winds for existing bathymetry.
6. Sedimentation rates over a single mean tide during calm, SW winds and NE winds with reclamation and dredging in place.
7. Sedimentation rates over a single mean tide during calm, SW winds and NE winds with reclamation and dredging in place and incorporating 100 year sea-level rise.
8. The dispersion of sediment plumes that are discharged from 3 single-point sources.

The study assumes interference of tidal flows around the piles/piers of Old Mangere and the SH20 bridges have no impact on wider scale sediment transport processes in Mangere Inlet. The piles/piers are localised features, and therefore flow (small) headloss near to the bridges only has a minor amount of scour around the piles/piers.

The pre- and post-reclamation model predictions of inlet tidal flows and sedimentation were then used to estimate **relative** changes in:

1. Inlet peak flood and ebb current speeds on a mean spring tidal range (3.80 m at Onehunga Wharf, LINZ CHART 4315).
2. Inlet peak flood and ebb current speeds on a mean neap tidal range (2.11 m at Onehunga Wharf, LINZ CHART 4315).
3. Inlet sedimentation rates over a single mean semidiurnal tide period during calm, SW winds and NE winds for existing bathymetry.
4. Inlet sedimentation rates over a single mean semidiurnal tide period during calm, SW winds and NE winds with reclamation in place.
5. Inlet sedimentation rates over a single mean semidiurnal tide period during calm, SW winds and NE winds with reclamation in place and 100 year sea-level rise.
6. Inlet sedimentation rates over a single mean semidiurnal tide period during calm, SW winds and NE winds with reclamation in place and mudcrete dredge volume removed.

The pre- and post-reclamation tidal period sedimentation rates were weighted and scaled up to provide estimates of annual sedimentation rates. These results were used to provide an estimate on the **relative** changes in sedimentation rates caused by the coastal reclamation.



## 3 Hydrodynamic, wave and sediment transport model development

### 3.1 Delft3D modelling Suite

Tidal dynamics and sediment transport in Mangere Inlet were modelled using the Deltares Delft3D hydrodynamic, wave and sediment transport modelling suite.

The curvi-linear, 2-dimensional (depth averaged) or 3-dimensional sigma coordinate (multi-layer) semi-implicit model suite finds numerical solutions for 2 and/or 3-dimensional flows (Delft3D-FLOW), wave–current interaction (Delft3D-WAVE), non-cohesive/cohesive sediment transport (Delft3D-SED) which can incorporate morphological evolution by scaling the hydrodynamic and sediment transport predictions (Delft3D-MOR) (see Appendix A).

Past studies by NIWA in Manukau Harbour have shown that the harbour is vertically well mixed. Therefore, for the present application in Mangere Inlet, Delft3D-FLOW was set up in 2-dimensional depth-averaged model and run in barotropic mode. This assumes that the inlet's waters are generally vertically well-mixed. The model was used to investigate shallow water tidal dynamics and wave/current interaction and sediment transport in shallow water.

The model grid was developed from bathymetry surveys, navigation charts and LIDAR data. The model was calibrated using archive water level, tidal gauging and comparisons with an existing model of Manukau Harbour. The sedimentation rates predicted by the sediment transport model were compared to the patterns in sedimentation and bulk estimates of annual sedimentation rate estimated from LIDAR surveys of the inlet.

### 3.2 Model grid

The curvi-linear Delft-3D x-y and bathymetric grid (z) of Mangere Inlet was developed for pre-reclamation coastline in ArcGIS using data sourced from:

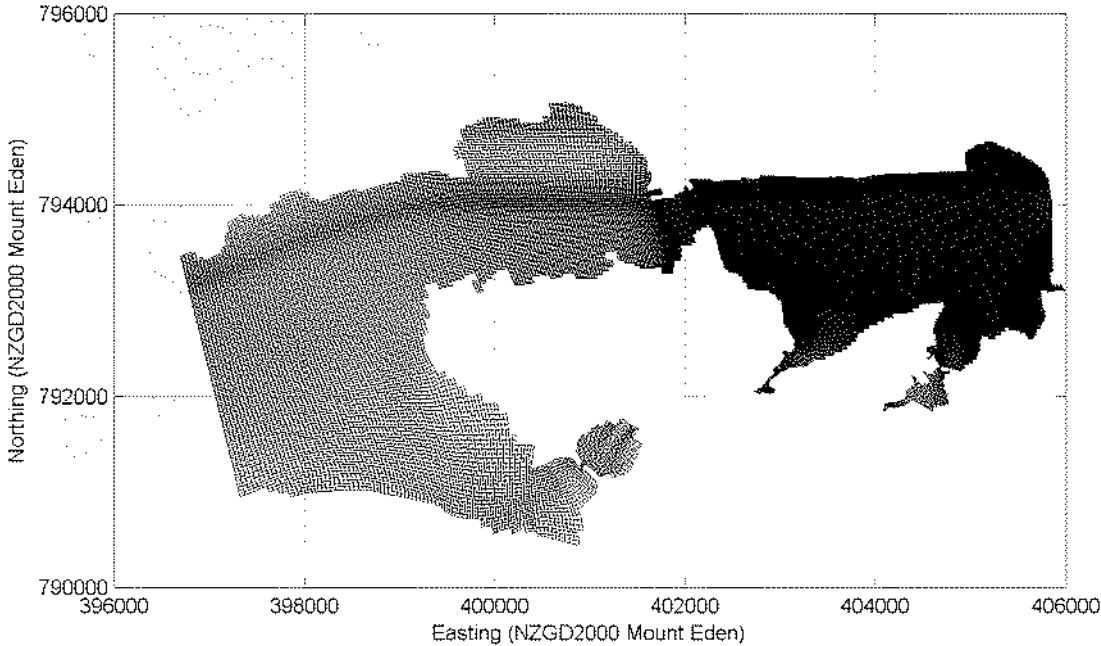
- Google Earth (coast line).
- LINZ Chart 4315 – Approaches to Onehunga.
- Port of Auckland survey data of inner Mangere Inlet (supplied by East-West Alliance).
- LIDAR – NIWA archive data originally supplied by Auckland City Council.

The grid-cell size in the model was about 64 m<sup>2</sup> within the inlet where most of reclamation will take place. The model grid was slightly coarser in the wider inlet and the approaches to Onehunga Bay. The coarser grid away from the main areas of earthworks and reclamation optimises model run times by allocating more computer time to the higher grid resolutions in the inner inlet where detail was required. The model grid was set up relative NZGD 2000 datum, and used Mount Eden Circuit 2000 horizontal coordinates. The model grid has 82,703 grid cells with highest density of cells along the north shore where the future reclamation work will be taking place (see Figure 3-1 and Figure 3-2).

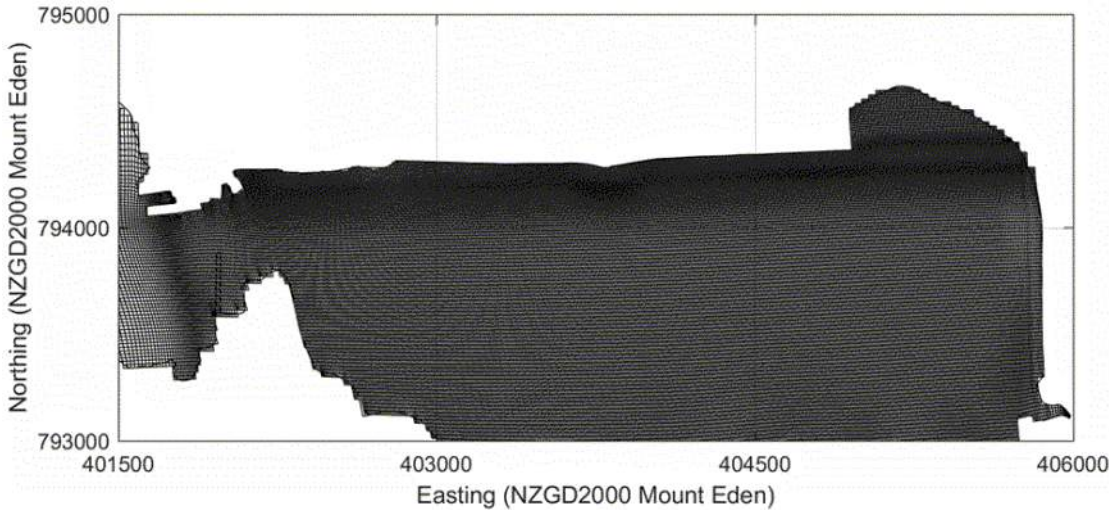
The model's open tidal boundary was set to the west in Manukau Harbour from Wattle Bay to the north and Puketutu Island to the south (see Figure 1-1 and Figure 3-1). The location of the open boundary enabled a full spring-tidal excursion and volume exchange to be simulated between inner Mangere Inlet and outer Onehunga Bay.

A high resolution digital terrain model (DTM) was developed in ArcGIS. This was imported into Deltares modelling suite bathymetry generator and interpolated onto the model grid. A bathymetric contour plot of the inlet is shown in Figure 3-3. This bathymetry and model grid was to be used to investigate pre-reclamation tidal circulation and sediment transport inside Mangere inlet. Model bathymetry was set to Onehunga (Auckland) vertical datum plus the 2016 mean sea-level offset.

A second modified bathymetry (Figure 3-4) and modified shoreline (provided by The East West Alliance) along the north shore of Mangere Inlet that incorporates the proposed reclamation was incorporated into the original model grid. This modified bathymetry was used in a series of simulations to investigate the relative changes (relative to pre-reclamation) in tidal circulation and sediment transport caused by the proposed shoreline reclamation work.

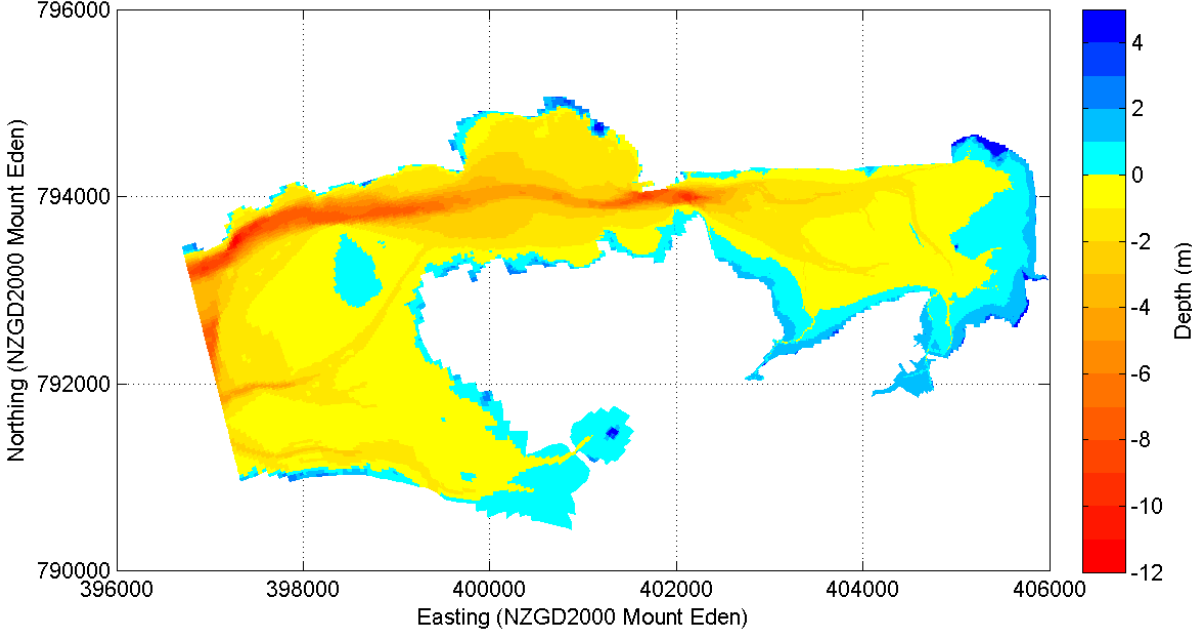


**Figure 3-1: Model computational grid. Model is forced along the western most boundary with time series of tidal elevations or astronomical constants.**

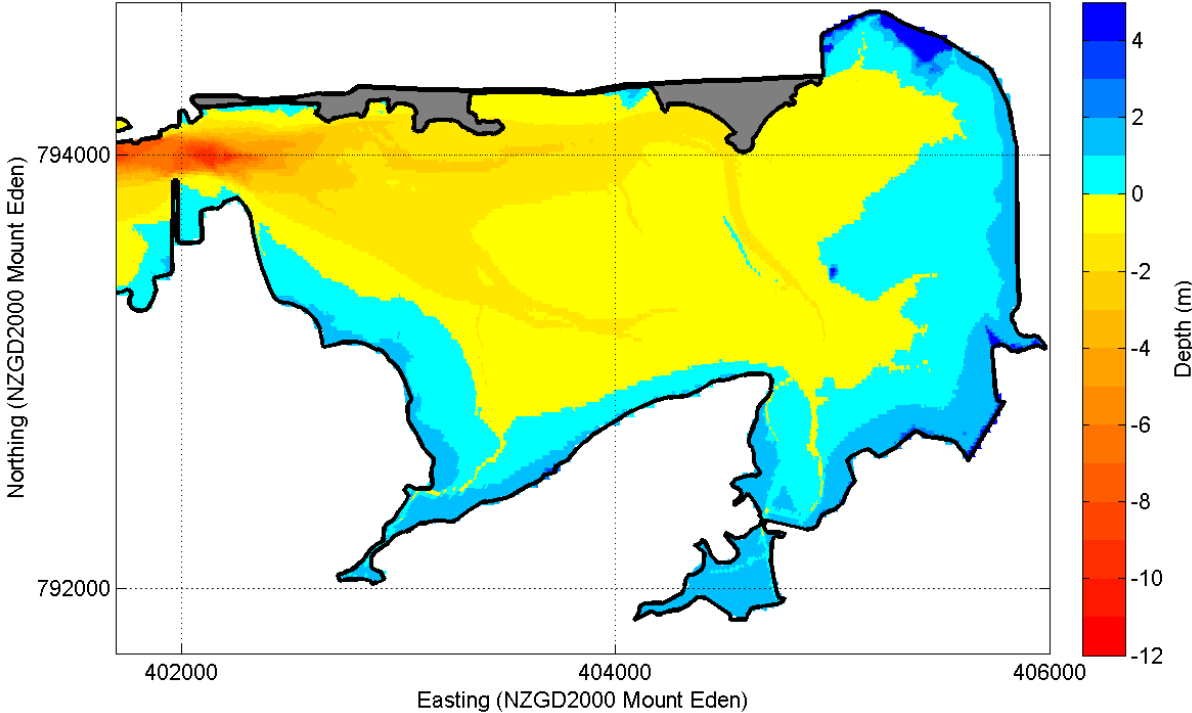


**Figure 3-2: High resolution model grid developed for region of inlet where coastal reclamation and changes in coastline will be taking place.**

The pre-reclamation area of Mangere Inlet is approximately 5.7 km<sup>2</sup>. With reclamation in place this reduces to approximately 5.5 km<sup>2</sup>, or a reduction in total area of 3.5%. Assuming a spring tidal range between 2.05 m to -1.75 m, Mangere Inlet has a pre-reclamation tidal prism volume of approximately 11.9 × 10<sup>6</sup> m<sup>3</sup>. The tidal prism with the proposed reclamation is reduced by approximately 4 × 10<sup>5</sup> m<sup>3</sup> equating to a new tidal prism volume of approximately 11.5 × 10<sup>6</sup> m<sup>3</sup>.



**Figure 3-3: Pre-reclamation model coastline and bathymetry developed from Ports of Auckland survey data, LINZ charts and LIDAR data.**



**Figure 3-4: Post-reclamation and bathymetric layout and coastline on the north shore of Mangere Inlet for reclamation version V04.**

### 3.3 Tidal elevations, currents and boundary conditions

Tidal elevations and currents used in the model calibration/validation and pre- and post-reclamation scenarios were based on archive tidal data recorded at:

- A NIWA “S4” mooring site in Wairopa Channel in the approaches to Onehunga (Bell et al. 1998).
- Onehunga tide gauge records (Ports of Auckland).
- A tidal gauging site located on Old Mangere Bridge (Green and Bell, 1995).
- Numerical model results extracted from a larger calibrated DHI MIKE3-FM regional model of Manukau Harbour (Reeve and Pritchard, 2010).

The tidal boundary water levels for the model were synthesised from least-squares harmonic analysis of Onehunga water-level data because this was the most reliable and best quality controlled data set. However, because of the distance between the model boundary and Onehunga wharf, the phase of each tidal constituent had to be adjusted to compensate for the phase lag between the two sites. Calculations based on shallow water wave speed suggested there is an approximate 8 min phase lag at Onehunga as compared to the phase at the model tidal boundary. This was further verified by comparing phase values extracted from archive MIKE3-FM model runs with the phases at Onehunga wharf and phases predicted at the S4 site by the Delft3D model. The MIKE3-FM model is now not in use at NIWA, so could not be run for other time periods.

Analysis of tidal currents showed that the S4 mooring currents were poor quality and unsuitable for model calibration. However, sea-level elevations from the mooring were used for model calibration. The model was also calibrated against tidal gauging data from Green and Bell (1995). These data included measured current speed and direction plus tidal elevations at Old Mangere bridge over a full  $M_2$  (12.42 hr) tidal cycle.

### 3.4 Winds

Wind speeds were used in the model to generate both wind driven currents and local fetch-limited wind waves. Figure 3-5 shows a wind rose that summaries the time series of wind speed and direction recorded at Auckland Airport between 1980 and 2011. The rose shows the dominance of the prevailing SW wind and also the presence of NE tropical lows that pass through the region.

#### 3.4.1 Effects of wind waves on sediment transport

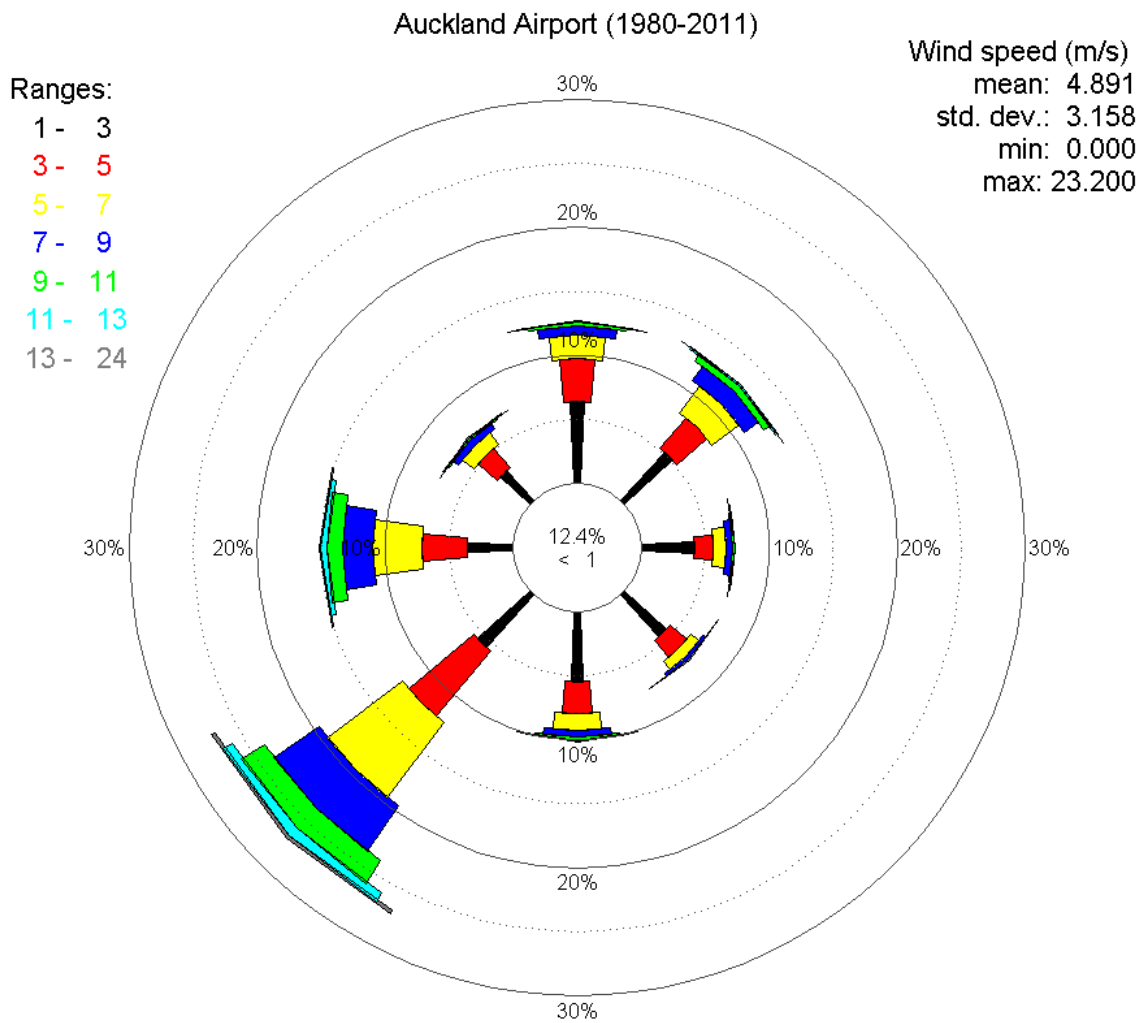
Previous studies have shown that fetch-limited (locally generated) wind waves have an important impact on sediment transport processes in Manukau Harbour and Mangere Inlet (Green et al. 2000). Wind wave generated orbital velocities that ‘feel’ the bed in shallow water increase the total bed shear stress (through non-linear interaction with tidal currents) and consequently can increase the rate of sediment erosion/resuspension at the bed. This process is prevalent at high water on inter-tidal flats and on the edge of tidal channels where the waves tend to erode and ‘stir up’ the bed deposited sediments into suspension. This is often observed as ‘turbid fringe’ that on the ebb tide drains from the flats into the main sub-tidal channels and moves seaward (Green et al. 1997; Green et al. 2000). On the next flood tide the sediments sourced from the flats and now in suspension in the channels is transported and dispersed in a landward direction by the flood tidal currents and the cycle repeats.

We used a representative wind climate to create three wind scenarios, to simulate wind waves and their effect on long-term (annual) sedimentation rates. The winds were superimposed on the tides. Based on Figure 3-5 we assumed a bi-directional wind climate and modelled south westerly, north easterly and calm states. Winds blowing from the south west sector (125–315 °T) and north east sector (315–125 °T) were assigned either a south west (225 °T) or north east (45 °T) angle respectively.

Previous NIWA studies and shallow water sediment transport models developed for Kaipara Harbour and Hauraki Gulf (Pritchard et. al., 2015) found that wind speeds below 7.5 m/s had little effect over and above that of tidal currents on sediment transport. When wind speeds exceeded 7.5 m/s waves become important. Therefore, for this study we assumed that wind speeds below 7.5 m/s are classed (in context of sediment transport) calm and above this wind speed, waves are then generated. The resulting percentage trend in the idealised wind wave climate for sediment transport is then:

- Calm – 80%
- SW – 15%
- NE – 5%

Wind speeds in the model were ramped up from zero to 7.5 m/s, sustained at 7.5 m/s for 72 hours and then ramped down to zero for all scenario simulations. Winds stronger than 7.5 m/s were not simulated – the assumption was made that 7.5 m/s represents the wave impacts for all wind speeds  $\geq 7.5$  m/s. This assumption appears reasonable given the apparent dominance of tidal flows on sediment transport and the good sediment transport calibration that was achieved, as shown in Section 5.2.1.



**Figure 3-5: Auckland Airport wind rose for the period 1980 to 2011.**

### 3.5 Sediments and sedimentation rates

The historical and present day sedimentation rates in Mangere Inlet have a range of reported values in the literature. These values vary from 0.01 mm/yr to 49 mm/yr (Croucher, 2005; Wilcock and Northcott, 1995). No present day coring data was available to verify any of the published rates.

Therefore, in an attempt to gauge the recent sedimentation levels inside Mangere Inlet, a comparison was made of the intertidal seabed levels between the 2006 and 2013 LIDAR information.

Inherent inaccuracies will lie within the LIDAR data and consequently the comparisons. Therefore to obtain some confidence in results, areas of the inlet where a comparison was possible were block averaged. From these estimates the overall average sedimentation rate throughout the entire Inlet was approximately 10mm/yr. Areas of mangroves and exposed intertidal flats had similar rates with an average sedimentation rate of 17mm/yr. In areas near tidal channels, in tidal channels and near islands the average erosion rate was 26 mm/yr. In general the northern coastline had higher sedimentation rates than the southern coastline (Stephen Priestley, BECA, pers. comm.).

## 3.6 Sediment transport model set up

### 3.6.1 Sediment transport model

The coupled hydrodynamic and sediment transport model was run with a mean tide ( $M_2$ ) boundary condition, with waves and without waves for a period of 30 days.

The cohesive sediment transport model was set up with a sediment particle settling velocity ( $W_s$ ) of 0.7 m/hr (See Appendix E). The critical sediment deposition threshold  $\tau_{cd}$ , and critical sediment erosion threshold  $\tau_{ce}$  were set at 0.125 N/m<sup>2</sup> and 0.25 N/m<sup>2</sup> based on literature values (e.g., Whitehouse et.al, 2000). The sediment and specific and dry bed densities were set at 2650 kg/m<sup>3</sup> and 700 kg/m<sup>3</sup> respectively.

Previous work has shown that Mangere Inlet is flood dominated (Green and Bell, 1995). Therefore, the inlet acts as sink for sediment imported from the Manukau Harbour. Based on these observations we initialised the model domain with no deposits of bed sediment. Else if the model was started with an ad hoc bed sediment distribution it could later bias the estimates of the relative changes in present day sediment deposition rate inside the inlet caused by the reclamation work.

Therefore, suspended sediments were introduced into the model domain from a series of 18 point sources in the main Wairoa Channel (see Figure 1-1). The sources mimic the sediment transport flux off the intertidal flats and into the main sub-tidal Wairopia Channel as observed by Green et al. (1997).

The model simulations that matched a modelled suspended sediment concentration (SSC) to a measured SSC of 40 mg/m<sup>3</sup> at Mangere Bridge (Green and Bell, 1995) required a sediment input flux of 0.3 kg/s at each point source plus a source of legacy bed sediment from Onehunga Bay. To incorporate both legacy and instantaneous fluxes into simulations, sediment inputs into the model were started 2 tidal cycles after the model start up to eradicate any effects of hydrodynamic instability on the transport of the sediment in the model domain. The model was then allowed to run for a further 5-days to build up the supply of legacy bed sediment. The new sediments that were introduced into the model 'evolve the bed' through a morphological feedback into Delft3D-Flow and Delft3D-Wave by the model by Delft3D-MOR model.

No model wind climate scenarios were started in a model run until 6 days after the start up. This delay allows a build-up of legacy bed sediments that can be eroded when the scenario begins. This gives the model a physical reality where the existing bed deposition footprints inside the inlet have resulted from transport by tidal currents not an arbitrary allocated bed deposition layer. This gives better confidence in the assessments of relative changes in bed levels later performed using weighted model scenario predictions.

### 3.6.2 Prediction of inlet sedimentation rates for pre- and post-reclamation coastline and bathymetry

Annual sedimentation rate (ASR) inside Mangere Inlet for pre- and post-reclamation bathymetry were predicted from the relative change (+/-mm) in bed level that occurs between the start and the end of 1 complete  $M_2$  (12.42 hr) tidal cycle. The 30-day model simulation was setup for periods (after the 6-day start up period) for calm (tides only), SW and NE wind and wave conditions. The relative change in the bed level over a  $M_2$  tidal period for calm, SW and NE wind were then extracted from model results. The  $M_2$  tidal sedimentation rate was then scaled up to an approximate ASR through (1) :

$$\text{ASR} = \text{Tidal sedimentation rate} \times 1.93 \text{ tides/day} \times 365 \text{ days} \quad (1)$$

A composite ( $\text{ASR}_{\text{WDCLI}}$ ) in the inlet based on annual wind climate is then estimated using the modelled ASR. Each separate modelled ASR for calm and winds was weighted by its percentage annual occurrence (see 3.4) and then all values summed together to produce a single wind climate composite ASR for the inlet. This can be summarised as equation (2):

$$\text{ASR}_{\text{WDCLI}} = \text{ASR}_{\text{CALM}} 0.8 + \text{ASR}_{\text{SW}} 0.15 + \text{ASR}_{\text{NE}} 0.05 \quad (2)$$

The changes in ASR caused by reclamation inside the inlet were investigated through application of equation (2) where  $\Delta\text{ASR}_{\text{WDCLI}}$  gives a measure of the relative change in annual sedimentation (more or less erosion or deposition) due to coastal reclamation as compared to pre-reclamation  $\text{ASR}_{\text{WDCLI}}$ . This can be expressed as equation (3):

$$\Delta\text{ASR}_{\text{WDCLI}} = \text{ASR}_{\text{WDCLI-PRE}} - \text{ASR}_{\text{WDCLI-REC}} \quad (3)$$



## 4 Model calibration and validation

The model was calibrated for:

- 2006 water levels observed at Onehunga and water levels predicted at the S4 site for same period during 2006.
- Tidal currents for the period that coincided with 1994 Old Mangere Bridge gauging experiment.
- Validated with DHI model modelled tidal elevations extracted from archived model results for the period during 1995.
- Regions of sedimentation and erosion were compared to the LIDAR estimates of erosion and sedimentation inside Mangere Inlet.

### 4.1 Calibration procedure

The Delft3d hydrodynamic model was calibrated by adjusting the two main calibration parameters:

- Horizontal Eddy Viscosity ( $K_x$ ,  $K_y$ ) – A time constant (but can be varied in space) parameter used to close the 2-d momentum equations that can be used to damp unexplained variance in modelled flows. Raising the values of  $K_x$  and  $K_y$  causes the modelled amplitude of maximum flows and tidal elevations to reduce.
- Chezy bed roughness formulation – A hydraulic bed roughness parameter used to formulate bottom boundary closure by parameterising energy dissipation at the seabed. This is often used to finely tune and calibrate current and tidal phase. However, correct specification of the bathymetry is the main deterrent of correct model phase.

A measure of ‘model skill’ or ‘best fit’ between the model predictions and observations and/or model predictions and predictions from tidal harmonic analyses of data was then determined through a series of basic statistical measures and tests. These are:

- RMSE – Root Mean Square Error - A measure of the difference in the variance between the observed and predicted signal.
- BIAS - The averaged signed residual offset between two time series. The bias indicates a positive/negative offset i.e., central tendencies in predicted and observed time series data.
- SKILL - where values span 1 (high) to 0 (poor) skill decreases towards zero as described by Warner et al. (2005) and Haidvogel et al. (2008).
- Rxy - Cross-correlation analysis – where 1 = 100 % correlation at zero phase lag is perfect correlation between two time series.

See Appendix B for the complete mathematical description of the above tests.

Model calibration parameters were iteratively changed until the best possible skill measures (indicating fit between observations and model predictions) were obtained. This process fine-tunes the model’s performance to minimise the error between the predictions and the observations.

## 4.2 Hydrodynamic model calibration and validation results

### 4.2.1 2006 Water levels

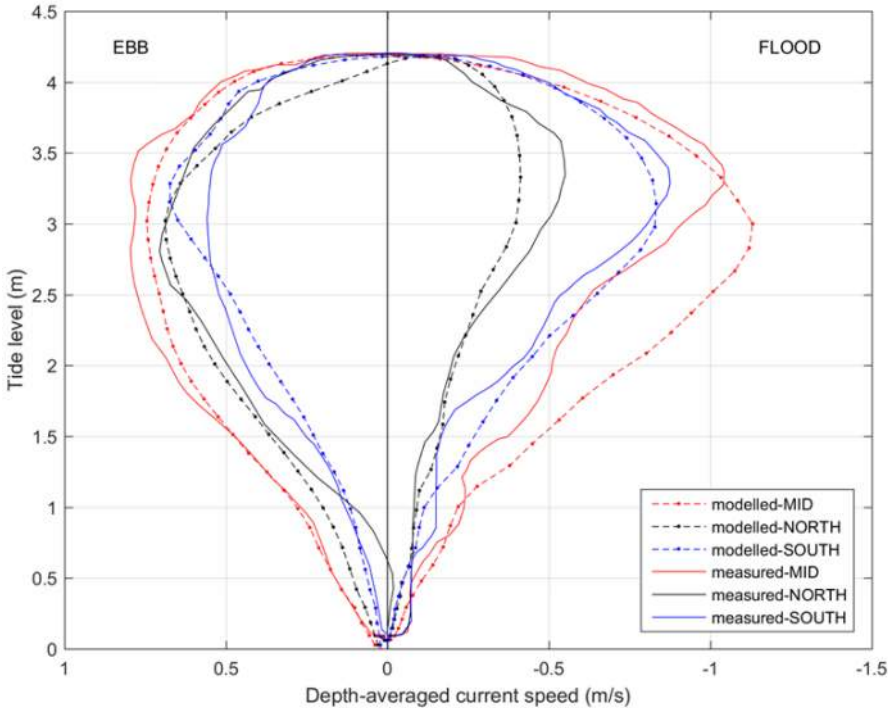
Modelled time series of tidal elevations were extracted from model domain at the locations of the S4 mooring site and Onehunga Wharf tide gauge. Figure C-1 (Appendix C) shows the results from the inter-comparison between modelled-observed and modelled-predicted. Results show close agreement and this is further verified through model skill test results presented in Table 4-1.

**Table 4-1: Skill test results between observed 2006 water levels at Onehunga tide gauge and S4 mooring and Delft3D model predictions for the coincident 2006 period.**

Location	Skill score (%)	RMSE (m)	Bias (m)	Rxy
Onehunga Tide Gauge	0.99	0.08	0	0.98
S4	0.99	0.09	-0.03	0.99

### 4.2.2 1994 tidal gauging

The modelled trend in flood-ebb dominance of tidal currents is an important factor for the transport of sediment. This flood-ebb dominance is illustrated in more detail by Figure 4-1 that shows a comparison between results from the 1994 old Mangere Bridge tidal gauging experiment (Green and Bell, 1995) and the Delft-3D model predictions made at the same location for the same 1994 tide. Figure 4-1 shows the observed and modelled tidal hysteresis (tidal height vs tidal current speed) measured over a single spring-tidal cycle (approximately 12.42 hrs). The modelled currents are consistent with the gauging observations to the degree that can be expected given expected bathymetry differences between the model grid and the harbour and inlet channel shape in 1995.



**Figure 4-1: Observed (Green and Bell, 1995) and Delft3D modelled tidal hysteresis at Mangere Bridge during a tidal gauging experiment over a complete spring tidal cycle during 1994.**

Following Figure 4-1 in a clockwise direction both observations and model show that the highest current speeds are on the flood tide. Furthermore, the hysteresis curve on the flood cycle is more 'peaky' and distorted than hysteresis on the ebb. This suggests there are two processes here that can influence sediment transport:

1. Higher current speeds on the flood than on the ebb implies flood-biased tidal asymmetry. Therefore, this bias has the potential to promote a higher suspended sediment flux by the tide into the inlet than out of the inlet.
2. The peaky flood hysteresis shows that tidal currents accelerate faster on the flood than the ebb. Therefore, because sediment transport is proportional to the cube of velocity, this is an important factor in the erosion, resuspension and transport of bed sediments. Observations and model would suggest a flood tide bias in the transport of sediments.

#### 4.2.3 1995 Model – model tidal height and current validation

Modelled time series of tidal elevations and currents were extracted from an archive MIKE3-FM Manukau Harbour model run for a period during 1995 at the locations of the S4 mooring site and the Onehunga Wharf tide gauge. The Delft3D model was run for this same 1995 period and results compared to the DHI model. High skill test scores on water levels and currents at the two sites shown in Table 4-2 show that the Delft3D model closely matched the MIKE3-FM model.

The skill test results shown in Table 4-3 indicate the Delft3D modelled water levels were a better match with MIKE3-FM than the modelled currents. This is a possible result from that current speed can vary over a very small scale due to localised bathymetric irregularities, such as reef outcrops and channel meanders, sea-surface elevations depend more on volume, which is less sensitive to small-scale irregularities in the bathymetry.

**Table 4-2: Skill test results between DHI model 1995 water levels at Onehunga tide gauge and S4 site and Delft3D model predictions for the coincident 1995 period.**

Location	Skill score (%)	RMSE (m)	Bias (m)	Rxy
Onehunga tide gauge	0.99	0.03	0.01	0.98
S4	0.99	0.06	0.0	0.95

**Table 4-3: Skill test results between DHI model 1995 currents at Old Mangere Bridge (OMB) and S4 site and Delft3D model predictions for the coincident 1995 period.**

Location	Cartesian component of velocity	Skill score (%)	RMSE (m/s)	Bias (m/s)
OMB	u	0.99	0.07	0.01
OMB	v	0.89	0.02	-0.01
S4	u	0.99	0.11	0.01
S4	v	0.98	0.01	0

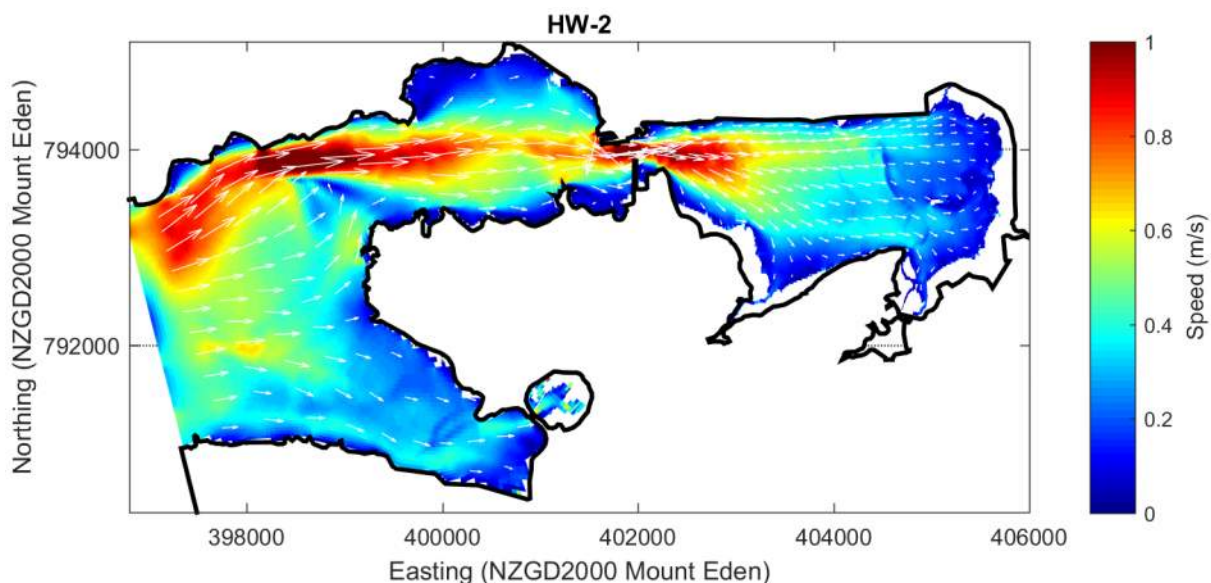
## 5 Model results

### 5.1 Tidal current flows

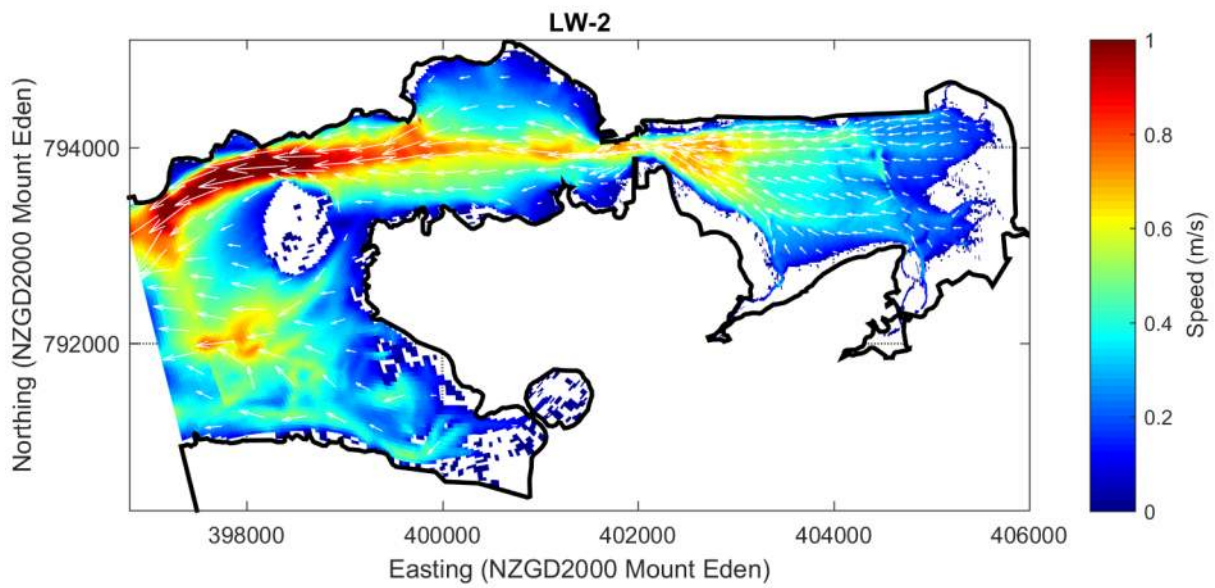
#### 5.1.1 Pre-reclamation tidal circulation

The simulated peak flood and ebb current speeds and directions for a mean spring tide and mean neap tide ranges for the approaches to Onehunga and inside Mangere inlet are presented in Figure 5-1 to Figure 5-4. Peak flood and ebb currents occurred two-hours before local high and low water (respectively) at Onehunga Wharf.

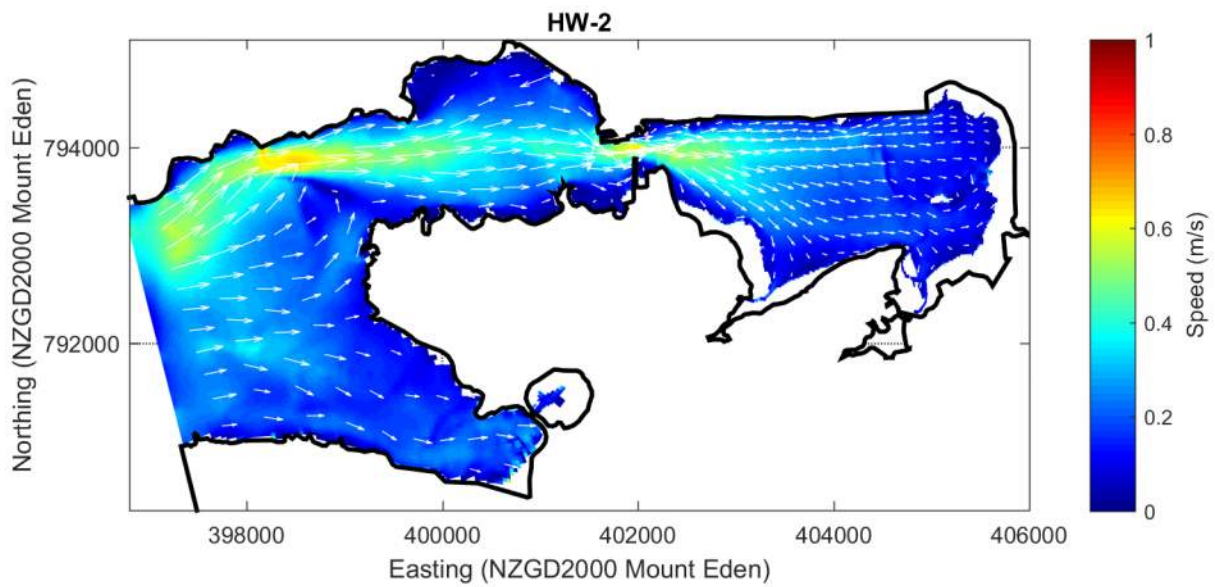
At local low water (LW), currents are slack but as the tide begins to flood current speeds increase and flow towards the east. The tidal currents continue to accelerate through to the mid-flood and, 2 hours before high water, reach peak speeds of over 1 m/s (2 knots) in the main flood channels of Onehunga Bay and through the Mangere inlet tidal channel. Fast currents occur as the water squeezes through the narrow inlet entrance. Inside Mangere inlet, the currents decelerate as the inlet widens out. After local HW, the tide turns and begins to flow towards the west and current speeds peak 2 hours before low water. Notably the model predicts that tidal current speeds in the entrance to Mangere Inlet are slightly slower on the ebb than on the flood. Similar circulation patterns occur on neap tides, although neap current speeds are approximately half the speed of spring tidal current speeds.



**Figure 5-1: Model predicted peak flood current speed and direction on a spring tidal cycle in Mangere Inlet. HW-2 = 2-hours before high water.**

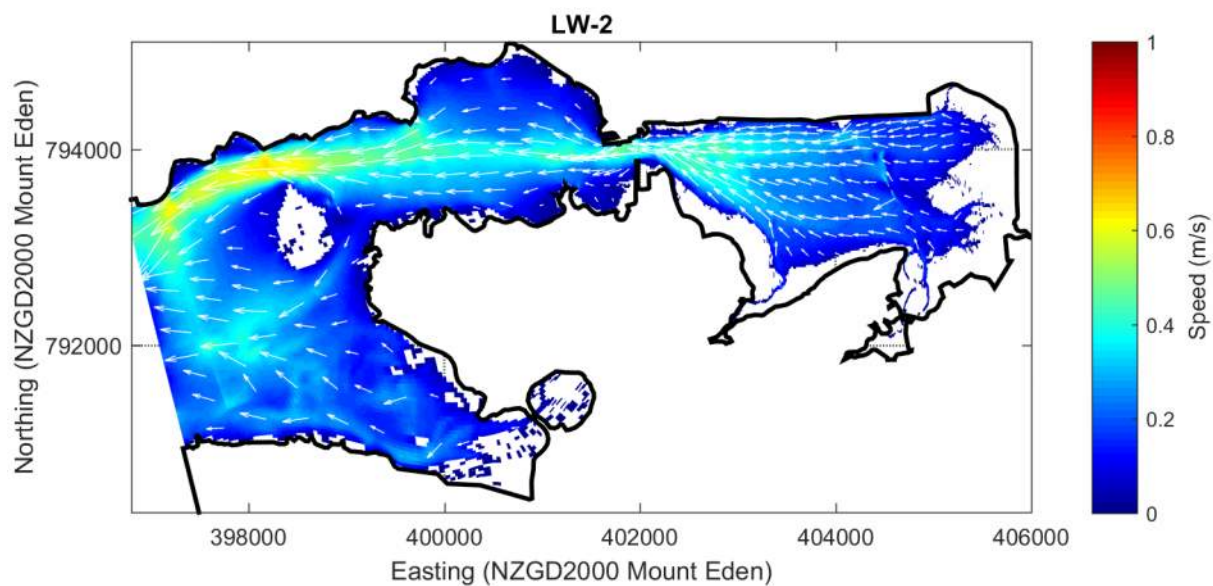


**Figure 5-2: Model predicted peak ebb current speed and direction on a spring tidal cycle in Mangere Inlet. LW-2 = 2-hours before low water.**



**Figure 5-3: Model predicted peak flood current speed and direction on a neap tidal cycle in Mangere Inlet. HW-2 = 2-hours before high water.**

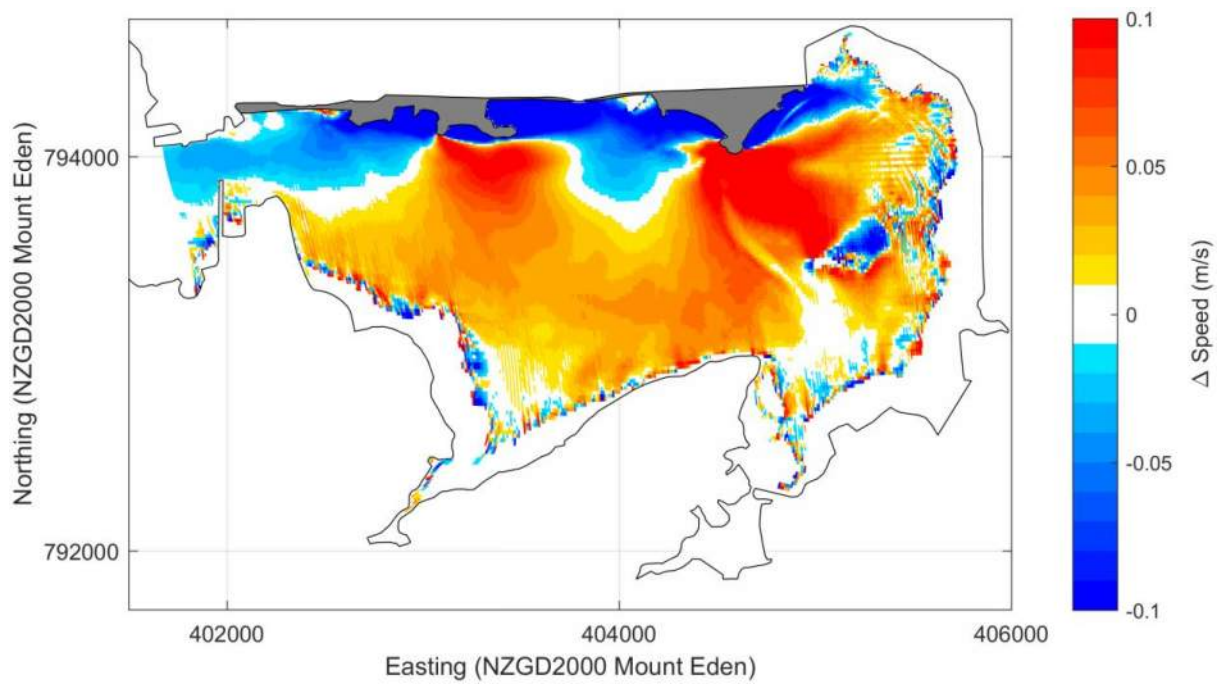




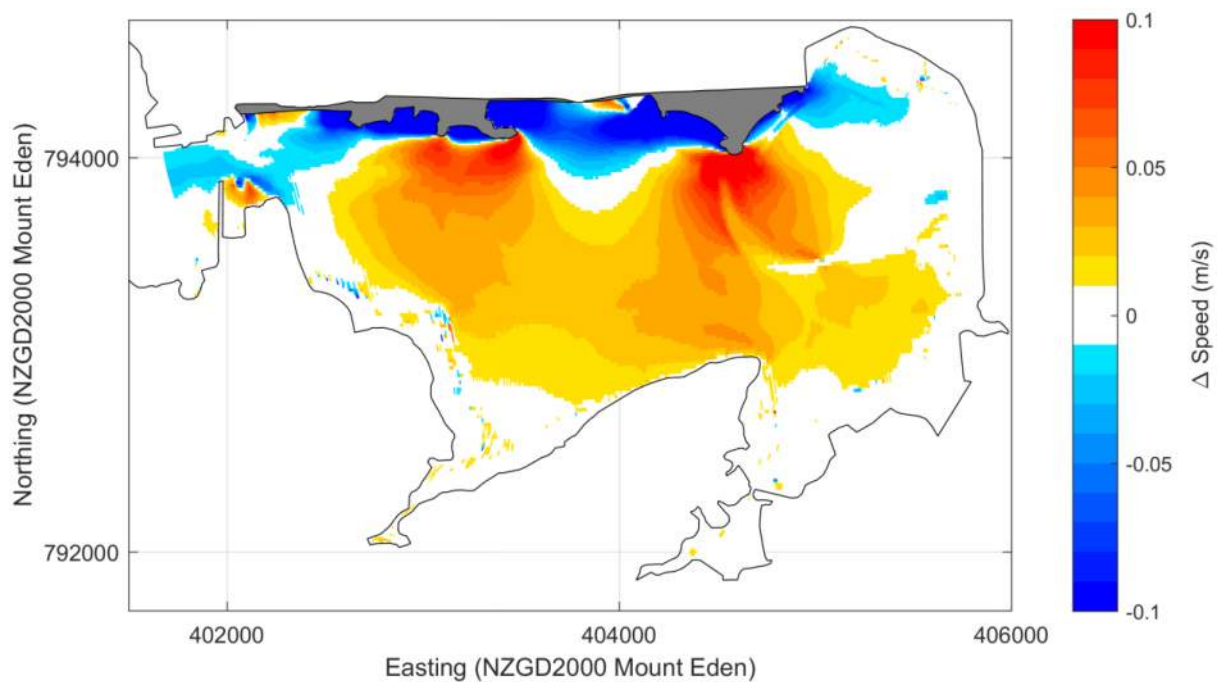
**Figure 5-4: Model predicted peak ebb current speed and direction on a neap tidal cycle in Mangere Inlet. LW-2 = 2-hours before low water.**

### 5.1.2 Predicted changes in tidal circulation due to reclamation

The predicted difference in tidal current speed due to the coastal reclamation is shown for mid-flood and mid-ebb flows for both spring and neap tidal ranges in Figure 5-5 to Figure 5-8. The four plots highlight where there is a predicted increase (yellow to red) or decrease (light blue to dark blue) in peak current speeds due to coastal reclamation. The analysis shows the same general regional changes in peak current speeds for both spring and neap tidal ranges, and for both ebb and flood currents. Due to reclamation there is a small decrease in peak current speeds in the inlet entrance and along the north shore where the reclaimed coastline slows the alongshore tidal flows. The largest decreases in peak current speed are inside the new coves and small embayments of the reclamation. The most striking feature shown in this analysis is decrease in current speeds adjacent the reclamation (in the north of the inlet), and an increase in current speeds south of the reclamation. This is a result of diverting tidal flow from an existing tidal channel (that is infilled during reclamation, see Figure 3-3 and Figure 3-4) to the south into a newly dredged channel that will link the NE corner of the inlet to the main tidal channel.

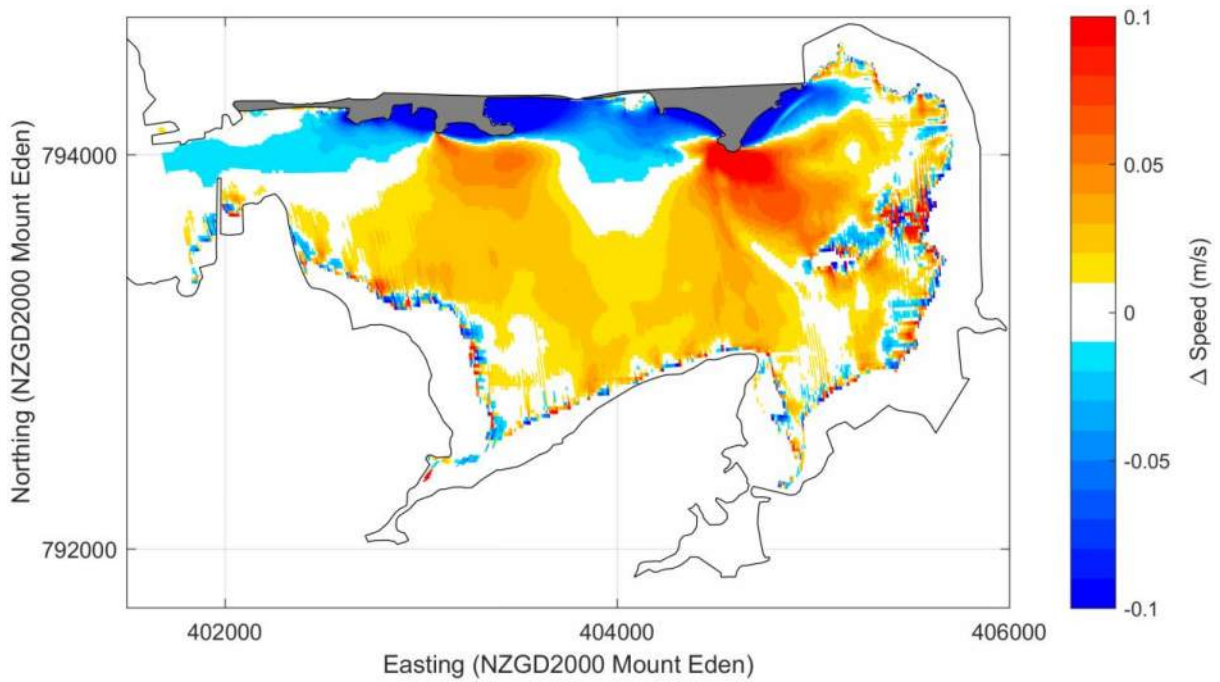


**Figure 5-5: Difference in peak flood current speed due to proposed coastal reclamation in Mangere Inlet during a spring tide.**

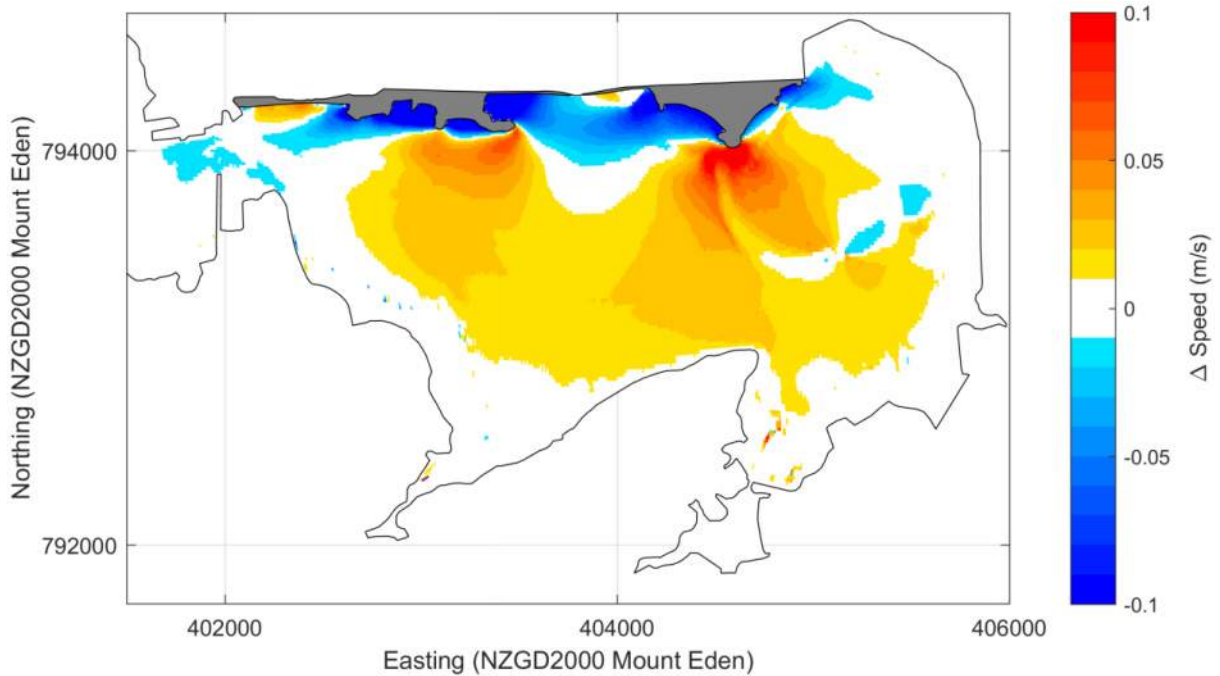


**Figure 5-6: Difference in peak ebb current speed due to proposed coastal reclamation in Mangere Inlet during a spring tide.**





**Figure 5-7: Difference in peak flood current speed due to proposed coastal reclamation in Mangere inlet during a neap tide.**



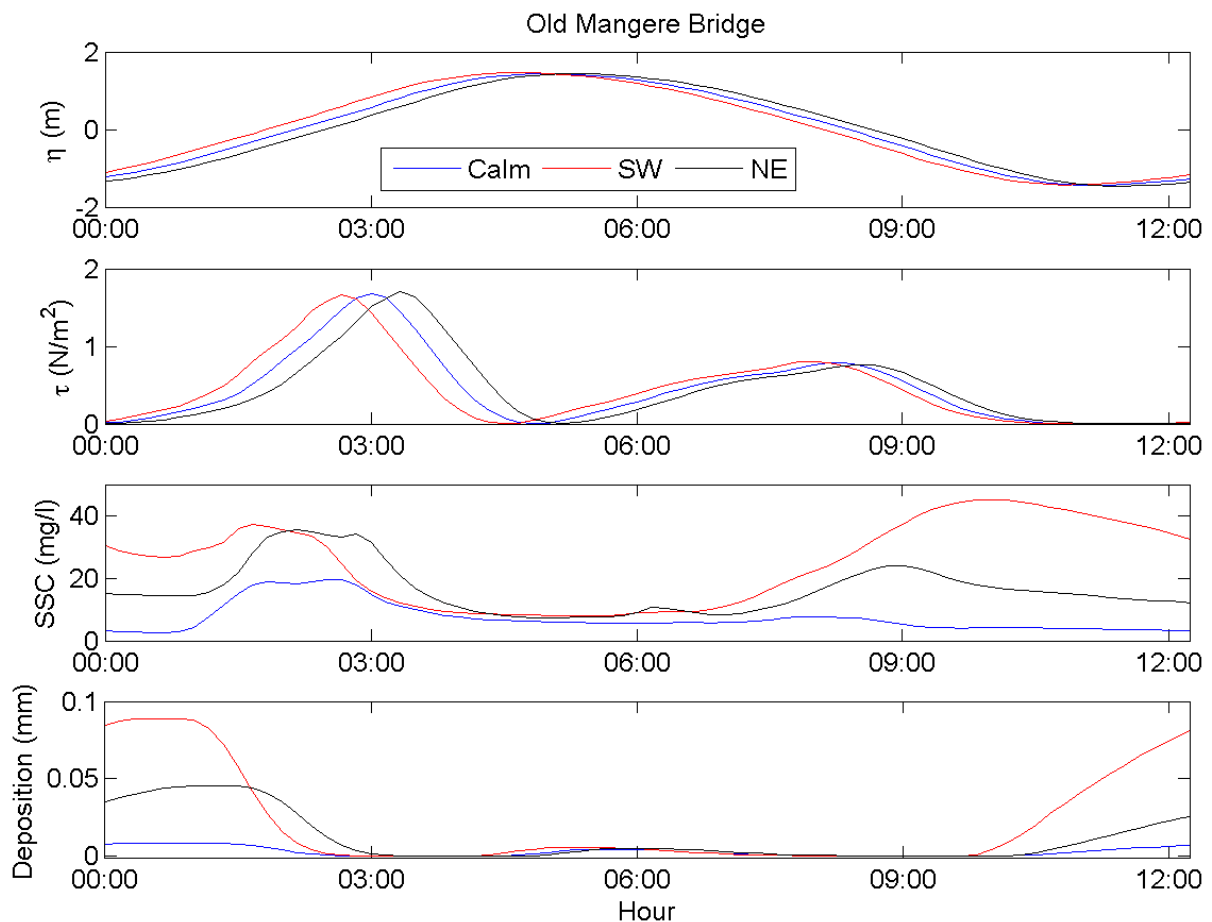
**Figure 5-8: Difference in peak ebb current speed due to proposed coastal reclamation in Mangere inlet during a neap tide.**

## 5.2 Sediment transport: pre- and post-reclamation

The modelled physical and sediment transport processes over a tidal cycle in the main tidal channel at Old Mangere Bridge is shown in Figure 5-9. Bed shear stress ( $\tau$ ) was computed using equation (4):

$$\tau = C_D \rho U^2 \quad (4)$$

Where  $C_D = 0.0025$  and  $\rho = 1026 \text{ kg/m}^3$  and  $U$  is current speed. Figure 5-9 shows that the magnitude of  $\tau$  is nearly double on the flood than that predicted on the ebb. This flood-ebb asymmetry is also shown in predicted SSC at the site which, on the flood are the same order of magnitude as those measured by Auckland Council surveys (Stephen Priestley, BECA, pers. comm.) The modelled peak in SSC was lower than that observed at the site during highly turbid conditions (Green and Bell, 1995; Williamson et al. 1996), but had the same relative flood-ebb trend in SSC. The SSC predictions also show a higher secondary peak on ebb when the effects of wind waves are incorporated into the simulations. This results from higher rates of sediment resuspension and reworking inside the inlet due to higher bed shear stresses due to wave-current interaction – the reworked sediments are then transported through the tidal channel. Predicted sediment deposition and resuspension at the Old Mangere Bridge site is higher during wave events than during calm conditions.



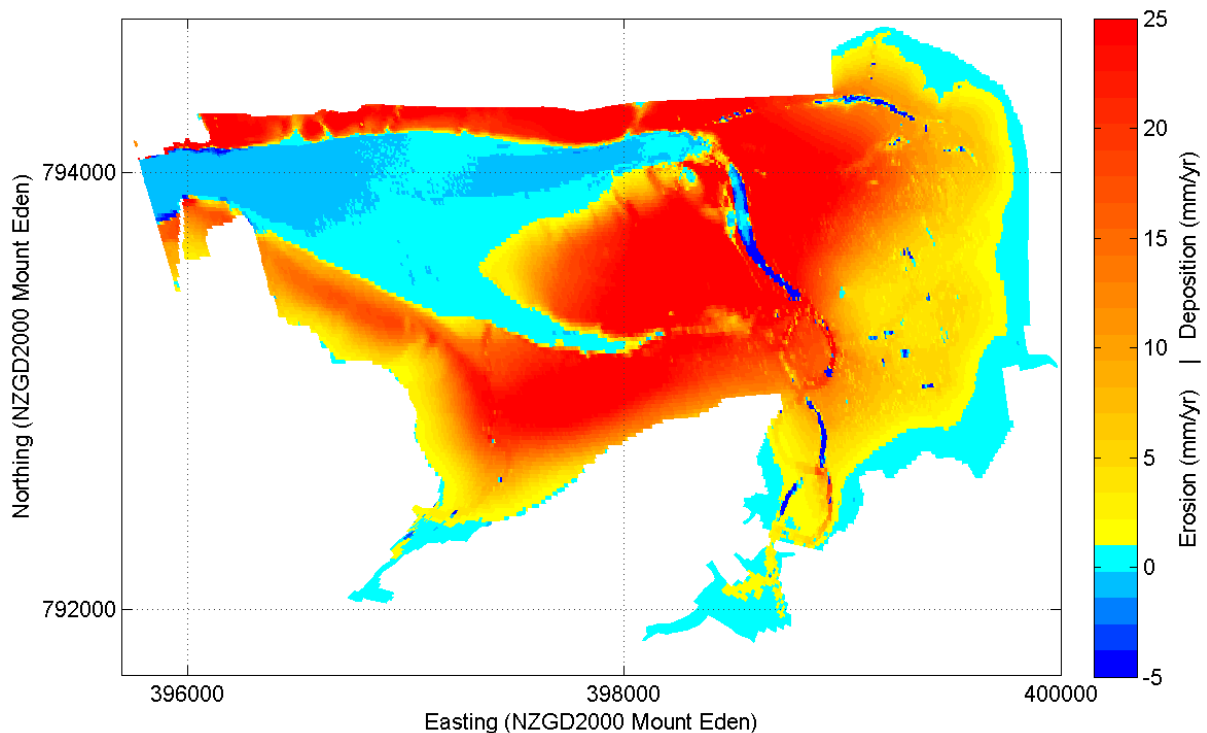
**Figure 5-9: Time series of modelled water levels ( $\eta$ ), bed shear stress ( $\tau$ ), SSC and sediment deposition at the Old Mangere Bridge site for calm, SW and NE wind wave conditions.**

### 5.2.1 Predicted inlet sedimentation rates for pre-reclamation bathymetry

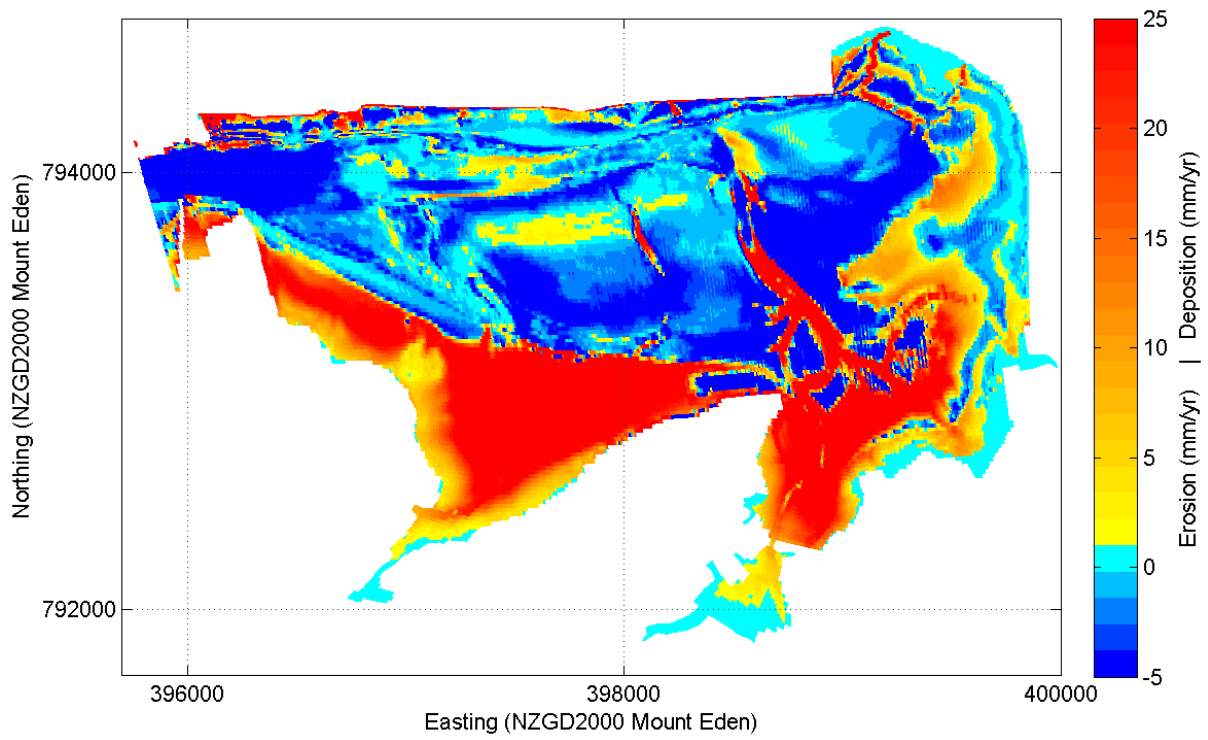
Figure 5-10 to Figure 5-12 illustrate the simulated annual sedimentation rate (ASR) from equation (1) inside Mangere Inlet for pre-reclamation bathymetry during calm (tides only), SW and NE wind and wave conditions.

Figure 5-10 shows that the Mangere inlet is mostly depositional during calm conditions, with exception of the scoured (eroded) fan at the entrance and on the flanks of the inlet. Inclusion of wind and waves into the simulations tends to increase downwind scour (erosion) of sediment especially on the NE and SW edges of the inlet. Furthermore, the wind/waves increased the deposition rate in the tidal channels (Figure 5-11 and Figure 5-12 ) because wave-scoured suspended sediment off the intertidal flats drains on the ebb into the tidal channel. These channel sediment deposits are ultimately reworked by tidal currents.

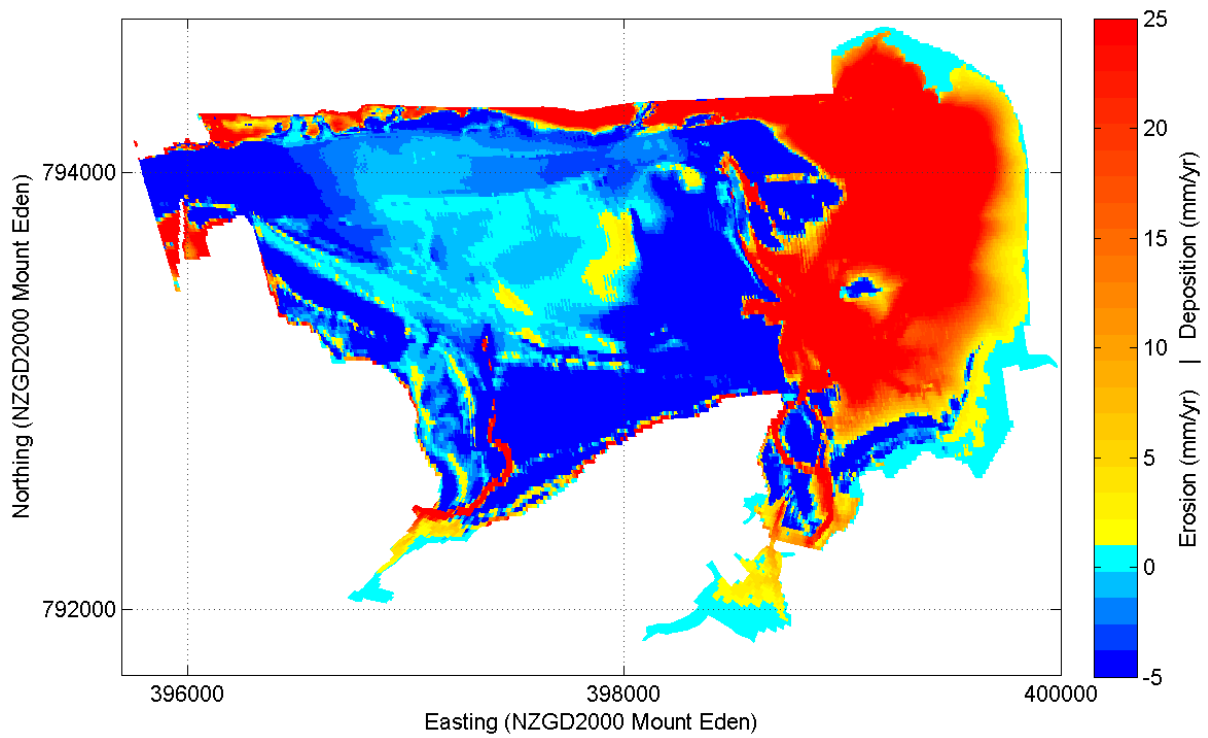
The result composite  $ASR_{WDCL}$  from equation (2) (Figure 5-13) is similar to the calm (tide only) simulation with subtle changes only.



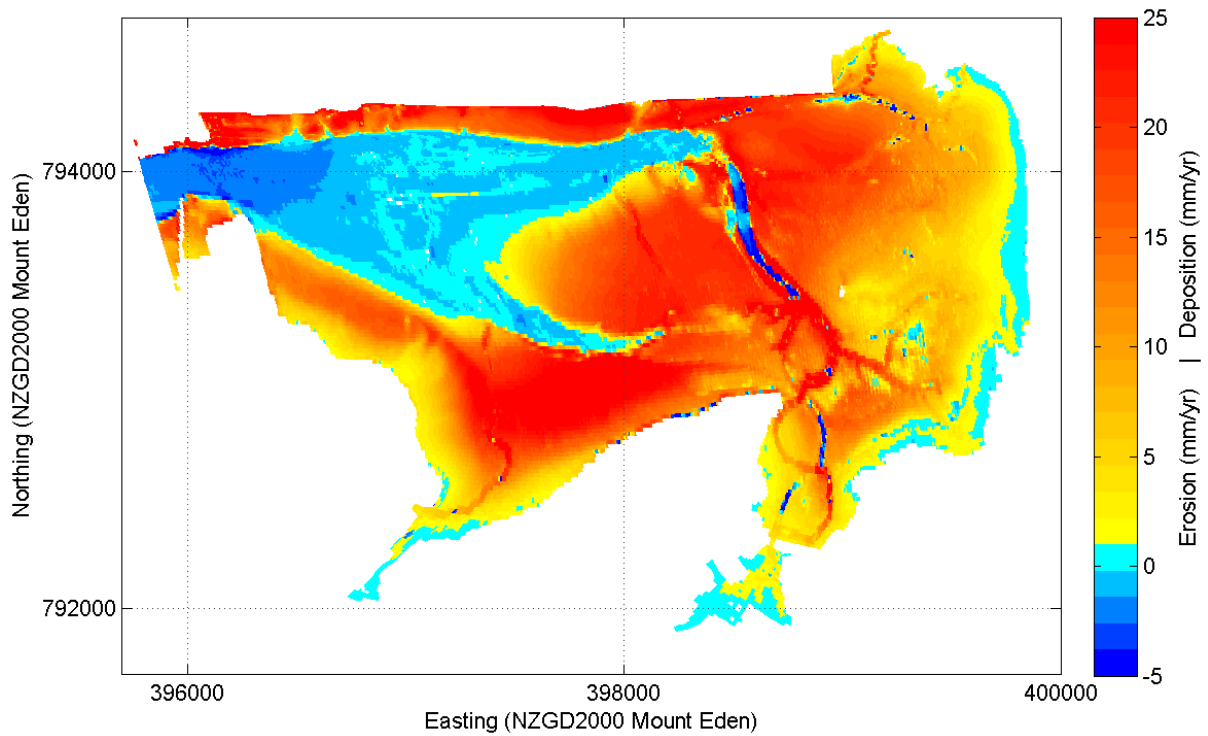
**Figure 5-10: Predicted  $ASR_{CALM}$  (mm/yr) in Mangere Inlet for calm (tide only) conditions for pre-reclamation bathymetry using equation (1).**



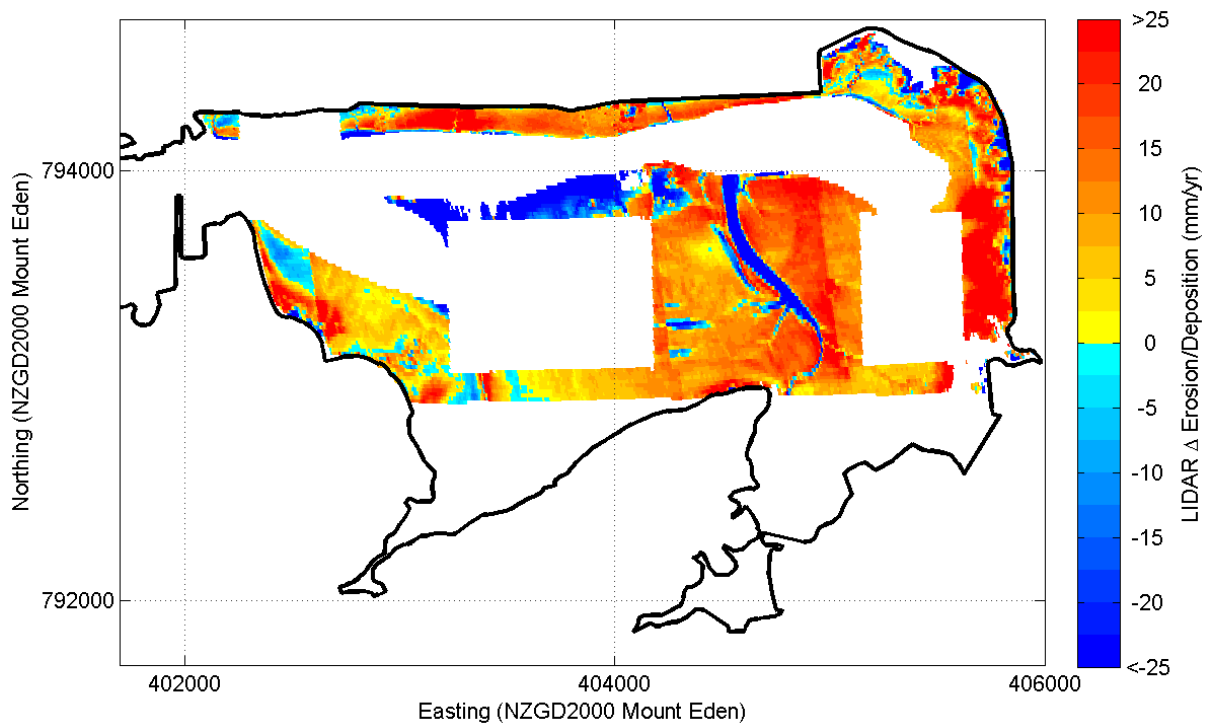
**Figure 5-11: Predicted  $ASR_{sw}$  (mm/yr) in Mangere Inlet for SW wind (tide and waves) conditions for pre-reclamation bathymetry using equation (1).**



**Figure 5-12: Predicted ASR<sub>NE</sub> (mm/yr) in Mangere Inlet for NE wind (tide and waves) conditions for pre-**



**Figure 5-13: Predicted wind climate composite ASR<sub>wDCU</sub> (mm/yr) in Mangere Inlet from the weighted wind climate using equation (2) for pre-reclamation bathymetry.**



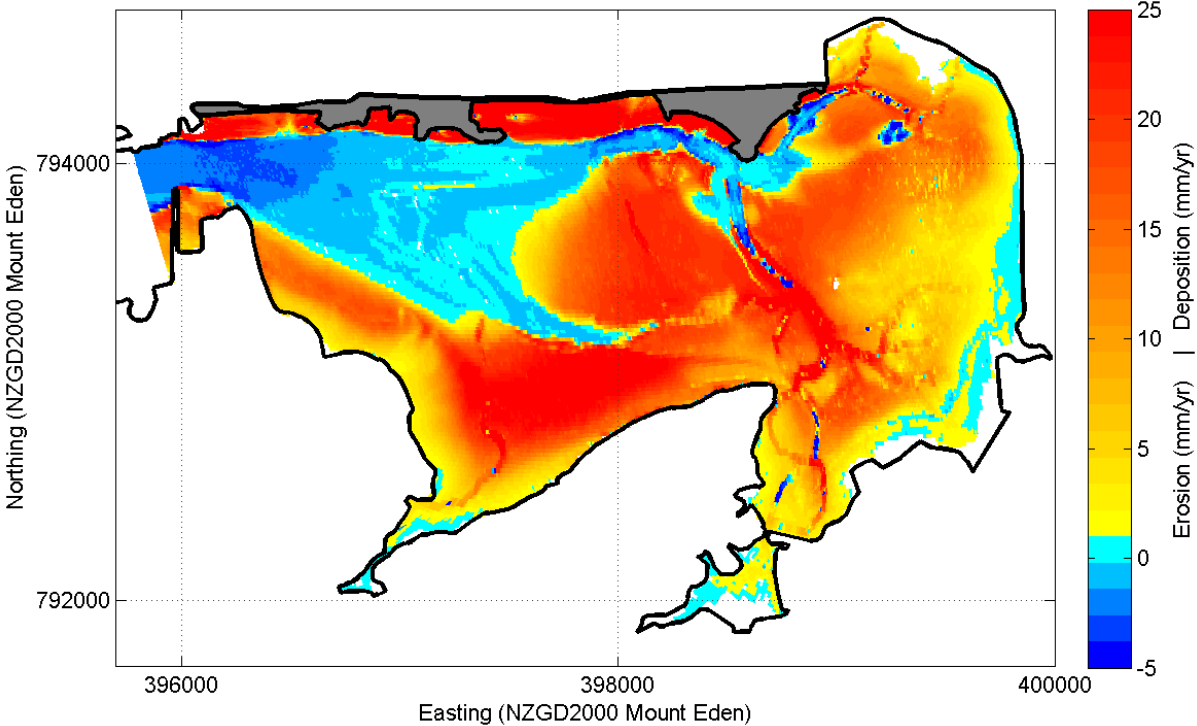
**Figure 5-14: Predicted ASR rate (mm/yr) in Mangere Inlet from LIDAR data analysis (see Section 3.5).**

The comparison of modelled  $ASR_{WDCLI}$  shown in Figure 5-13 with the results from analysis of the LIDAR data (Figure 5-14) shows the model makes a good job of predicting morphological features and ASR throughout the inlet. Most of the inlets shallows (i.e., on the north shore where the proposed reclamation will take place) and inter-tidal regions were predicted as depositional. In contrast in deeper water through the inlet entrance, a bifurcated fan shaped scoured region extends down to the south east and to east where it then couples with a network of sub-tidal channels. The channels are erosional being scoured out by mainly tidal currents (see Figure 5-10).

**5.2.2 Predicted sedimentation rates due to coastal reclamation**

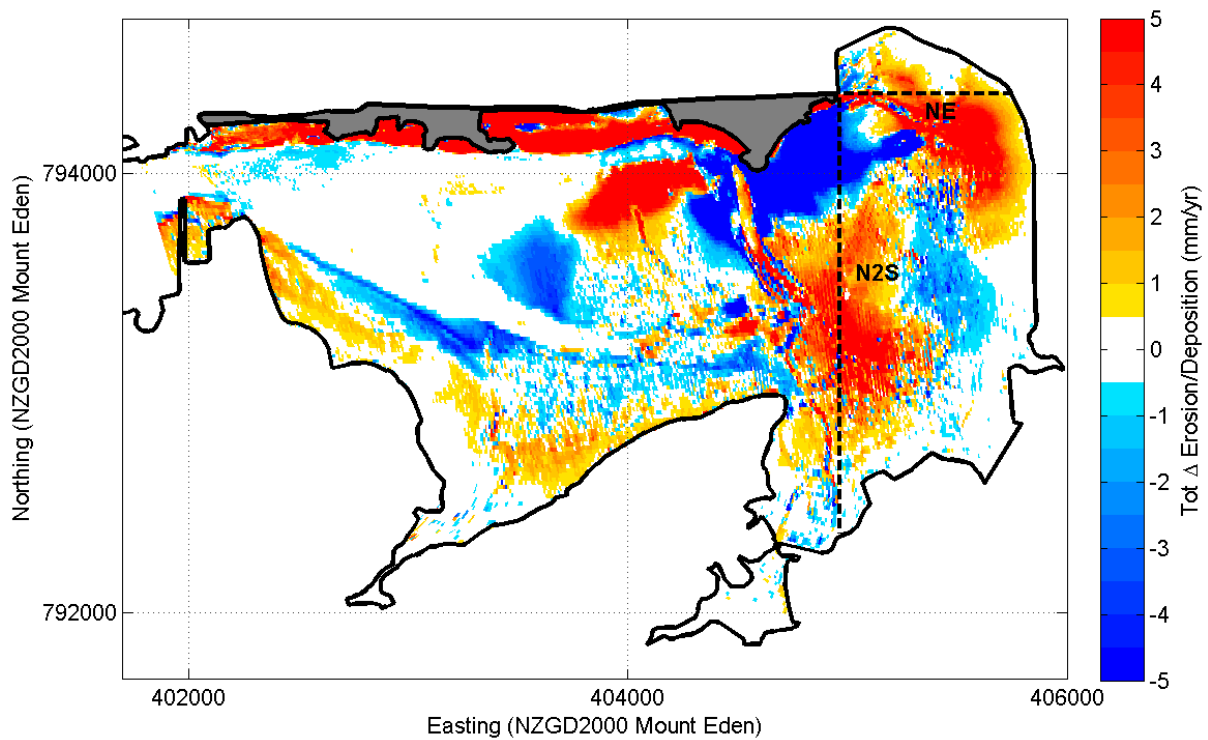
The Mangere Inlet sediment transport model was run with same boundary, sediment source and wind conditions as the pre-reclamation scenarios but with the modified bathymetry and coastline as shown in Figure 3-4.

The changes in ASR caused by reclamation inside the inlet were investigated through application of equation (2) and equation (3) where  $\Delta ASR_{WDCLI}$  gives a measure of the relative change in annual sedimentation.



**Figure 5-15: Predicted wind climate composite  $ASR_{WDCLI}$  (mm/yr) in Mangere Inlet from the weighted wind climate using equation (2) for V04 post-reclamation coastline and bathymetry.**

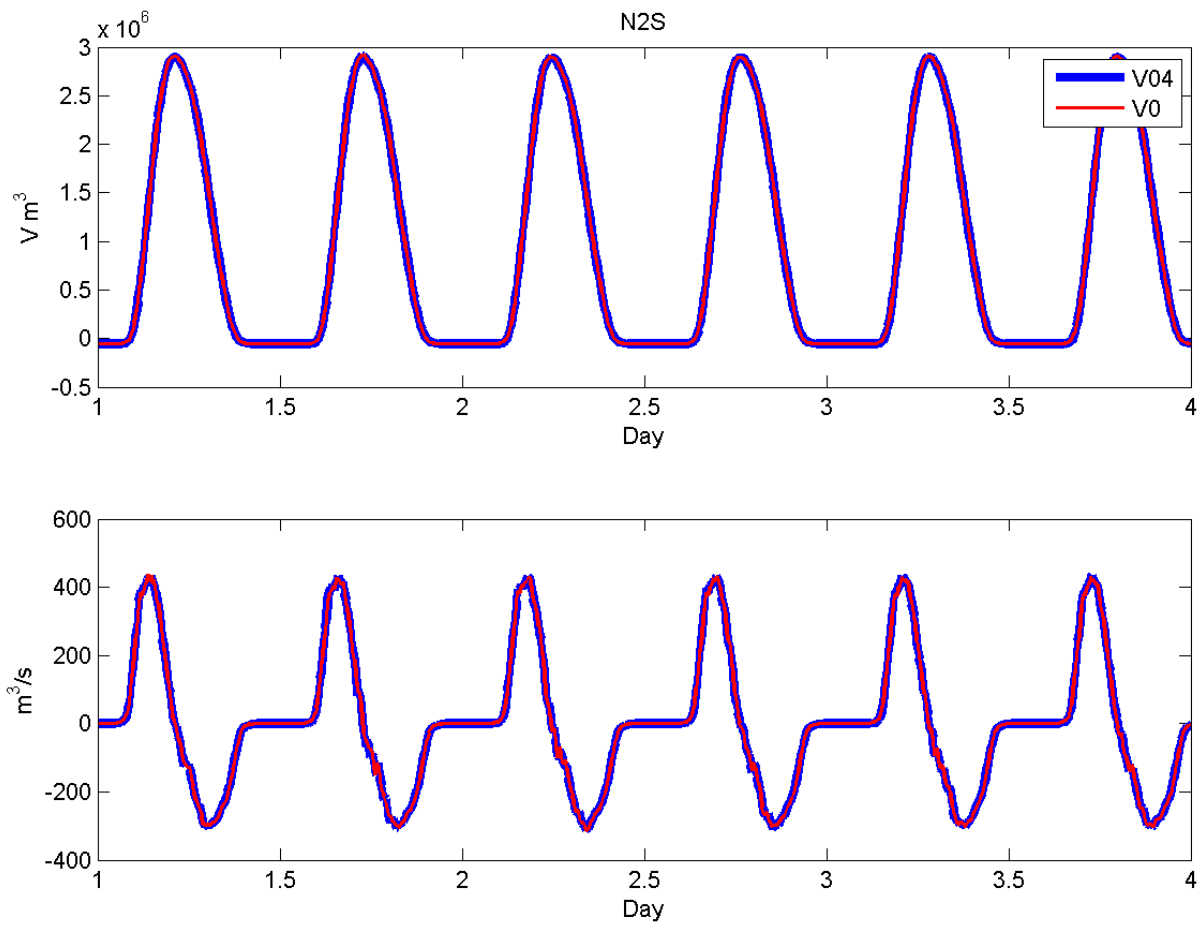
Figure 5-15 and Figure 5-16 displays results from equation (2) and equation (3) respectively. The results show that reclamation promotes an increase in sedimentation rates along most of the coastline where coastal reclamation will take place. The new embayments, coves and headlands along this coast act as sediment traps and decrease tidal flows (see Figure 5-5 to Figure 5-8). This causes a localised increase in ASR of approximately 3-5 mm/yr. The sharp divergence between an increase in accretion (+5mm/yr) and erosion (-5mm/yr) on the east of the reclamation is caused by changes in tidal flows due to the effects of reclamation and the infilling of a sub-tidal channel.



**Figure 5-16:** Predicted changes in wind climate composite  $ASR_{WDCLI}$  (mm/yr) caused by proposed coastal reclamation in Mangere Inlet using equation (3). Differences in modelled pre- and post-reclamation  $\Delta ASR_{WDCLI} \pm 0.5$  mm/yr are blanked out. NE and N2S mark cross-sections where tidal volumetric fluxes are computed.

The implication of the reclamation work on tidal volumetric transport in the eastern end of the inlet was investigated by extracting transport rates through the 2 cross-sections shown in Figure 5-16.

The resultant cumulative volume ( $V$ ) and transport rate ( $Q$ ) for pre- and post-reclamation bathymetric layouts and coastlines over NE (Figure 5-17) and N2S (Figure 5-18) cross-sections shows that there were no notable changes in tidal exchange due to coastal reclamation.



**Figure 5-17: Predicted tidal cumulative volumetric transport (V) and instantaneous volumetric flux (Q) over x-section N2S (see Figure 5-16) for present day (V0) and reclamation (V4) coastlines.**



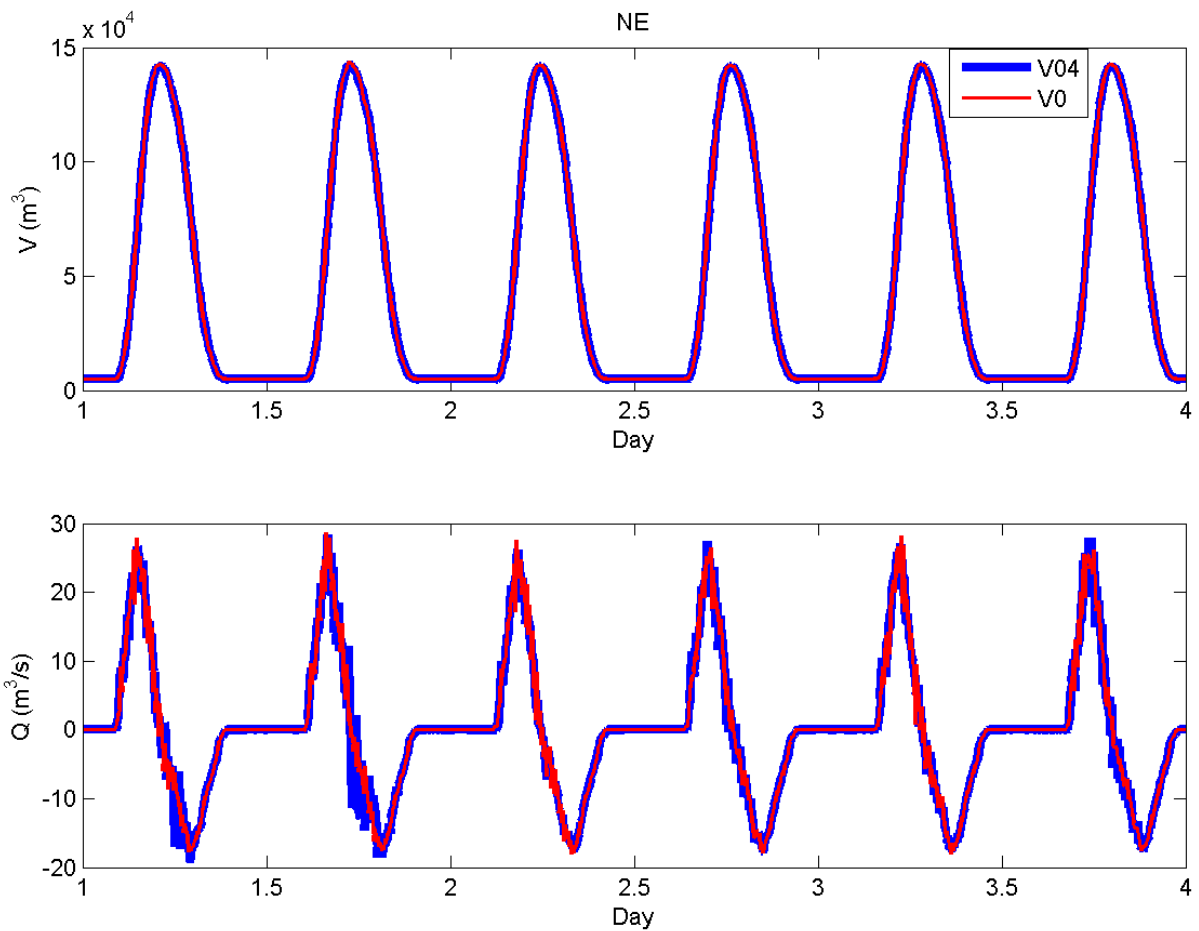


Figure 5-18: Predicted tidal cumulative volumetric transport ( $V$ ) and instantaneous volumetric flux ( $Q$ ) over x-section NE (see Figure 5-16) for present day ( $V0$ ) and reclamation ( $V04$ ) coastlines.

### 5.3 Predicted area mean ASR in Mangere Inlet pre- and post-coastal reclamation

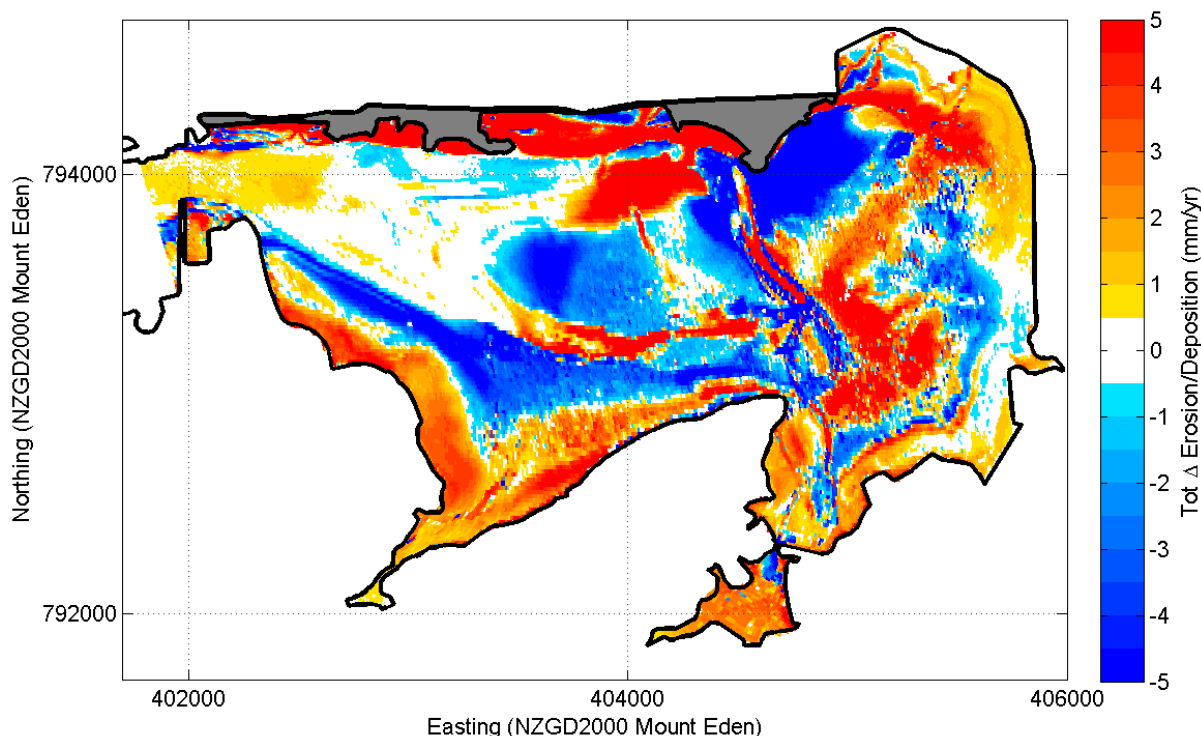
The mean ASR over the area of Mangere Inlet as shown in Figure 5-13 was estimated for pre-reclamation conditions as **9.8 mm/yr** and coastal with reclamation in place **10.5 mm/yr**. This is an increase of 0.7 mm/yr.

## 6 Predicted inlet sedimentation rates and sea level rise

The effect of global sea-level rise (SLR) on Mangere Inlet's sedimentation rates with the coastal reclamation in place were investigated by modelling a 1 m increase in mean sea level and 0.5 m of sediment deposition inside the inlet (scenario agreed with Stephen Priestley of BECA). A SLR of 1 m over the next 100 years is a commonly-applied SLR allowance in New Zealand, and was applied in the Proposed Auckland Unitary Plan. 0.5 m of seabed deposition is an approximation based on 5 mm/year over a 100-year period. The 0.5 m deposition was applied uniformly over the existing bathymetry.

The simulations used in this investigation were set up with coastal reclamation in place, with and without SLR. The series of sediment transport simulations were run, and equation (2) was used to estimate ASR rates inside the inlet. Figure 6-1 shows the predicted  $\Delta ASR_{WDCLI}$  (equation (3)) that results due to SLR.

The effect of SLR and reclamation (Figure 6-1) compared to reclamation only (Figure 5-16) predicts the centre of the inlet becomes more erosional and the edges of the inlet more depositional. These changes occur because of the increase in water depth due to SLR. SLR exposes pre- SLR intertidal regions of the central inlet to permanent submergence or more frequent tidal inundation. Therefore, the central inlet becomes more susceptible to erosion and 'off flat' transport by the tidal currents and waves. Similarly, greater water depths in the south of the inlet increases tidal inundation time and tidal excursion higher up onto the intertidal flats. This encourages more 'on flat' sediment transport in the south of the inlet.



**Figure 6-1:** Predicted changes in wind climate composite  $ASR_{WDCLI}$  (mm/yr) caused by proposed coastal reclamation in Mangere Inlet using equation (3) and sea-level rise. Differences in modelled pre- and post-reclamation  $\Delta ASR_{WDCLI} \pm 0.5$  mm/yr are blanked out.

## 6.1 Predicted mean ASR in Mangere Inlet with reclamation and SLR

The predicted mean ASR for Mangere Inlet with coastal reclamation and SLR is 10.4 mm/yr, compared to 10.5 mm/yr without SLR.

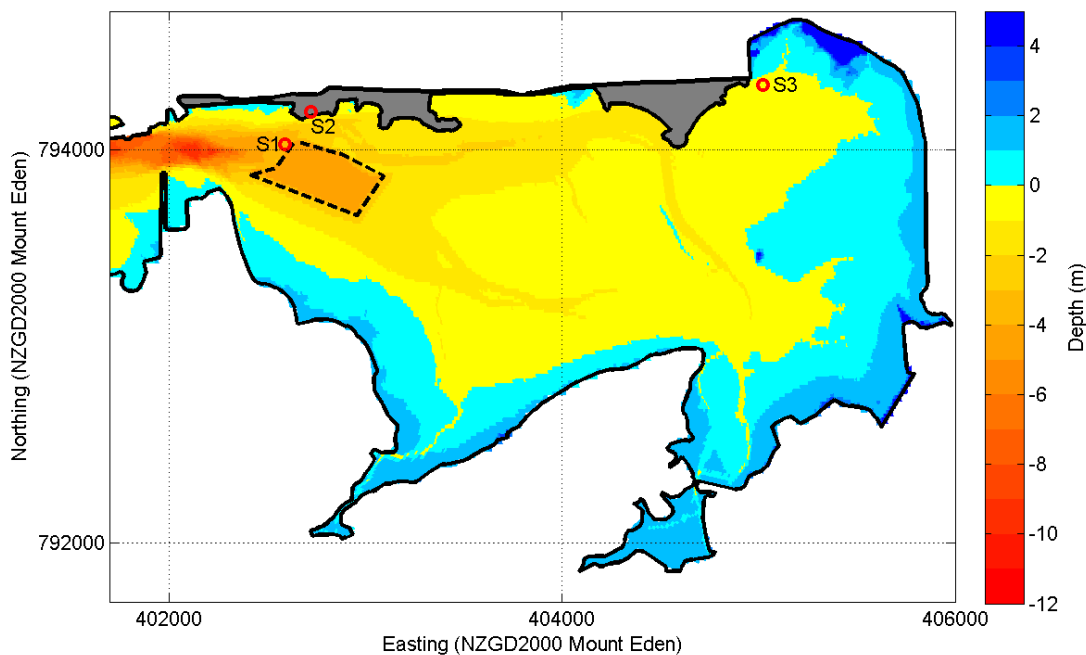
## 7 Effects of mudcrete dredging in entrance channel to Mangere Inlet

The coastal reclamation work in Mangere Inlet will require approximately 300,000 m<sup>3</sup> of dredged mud to produce the mudcrete (a mix of sand and concrete/cement and marine mud) required in the construction of the new coastline. It is proposed that the mud will be dredged from the area shown in Figure 7-1. This area was selected on the basis that it avoids ecologically sensitive areas to the east of the dredge area but also removes an area of the invasive Asian date mussels inside the area of the dredge area.

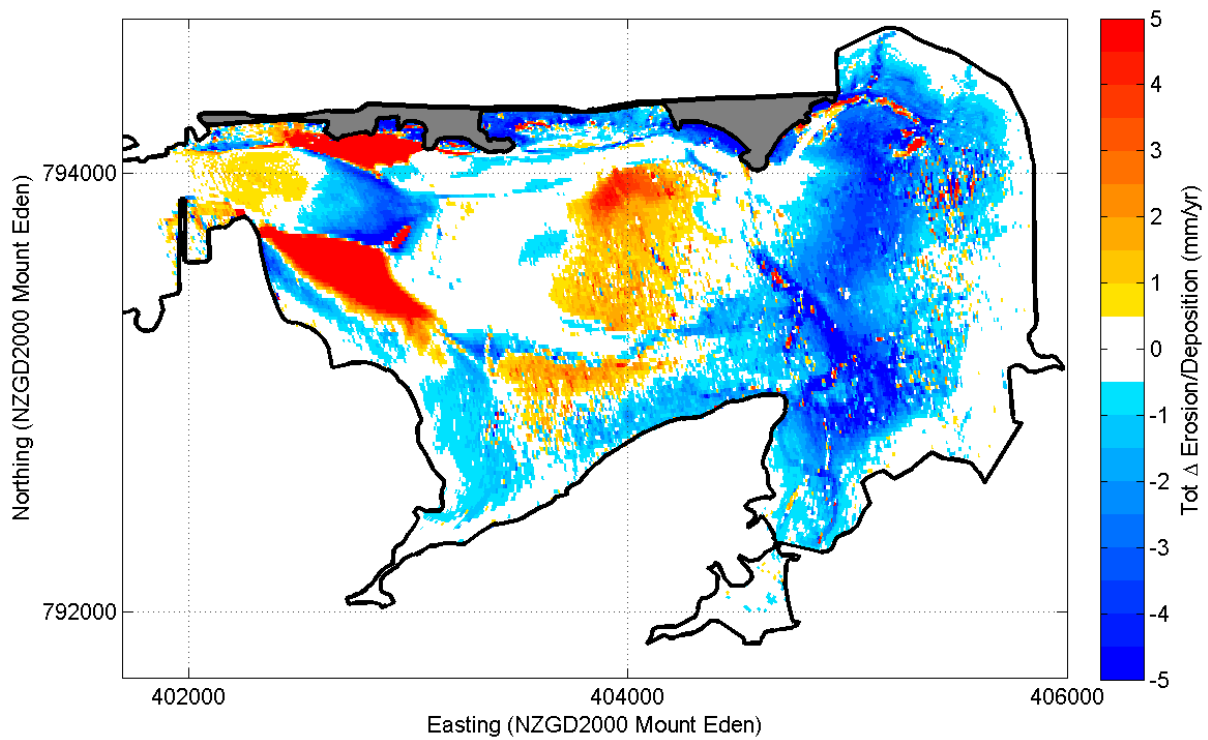
The simulations used in this investigation were set up with coastal reclamation in place, with and without the dredged volume. The series of sediment transport simulations were run using the equation (2) wind climatology weighting methodology to estimate ASR rates inside the inlet. Figure 7-2 shows the predicted  $\Delta ASR_{WDCL}$  (equation (3)) that results due to the dredged volume removed.

Removal of the dredged volume has most impact on ASR in the entrance to the inlet. Figure 7-3 and Figure 7-4 show that the dredge area reduces current speed both on the flood and ebb tide. However, the current speeds and bed shear stress  $\tau$  do not drop below the critical bed erosion threshold  $\tau_{cr}$  in the subtidal channel, therefore, sediment is still scoured in the tidal channel and in the main area of the dredged area. On the shallower flanks of the dredge where there are already lower current speeds, the further reduction in current speed caused by the dredge is enough to cause  $\tau$  to drop below  $\tau_{cr}$  and increase the rate of sediment deposition as shown in Figure 7-2.

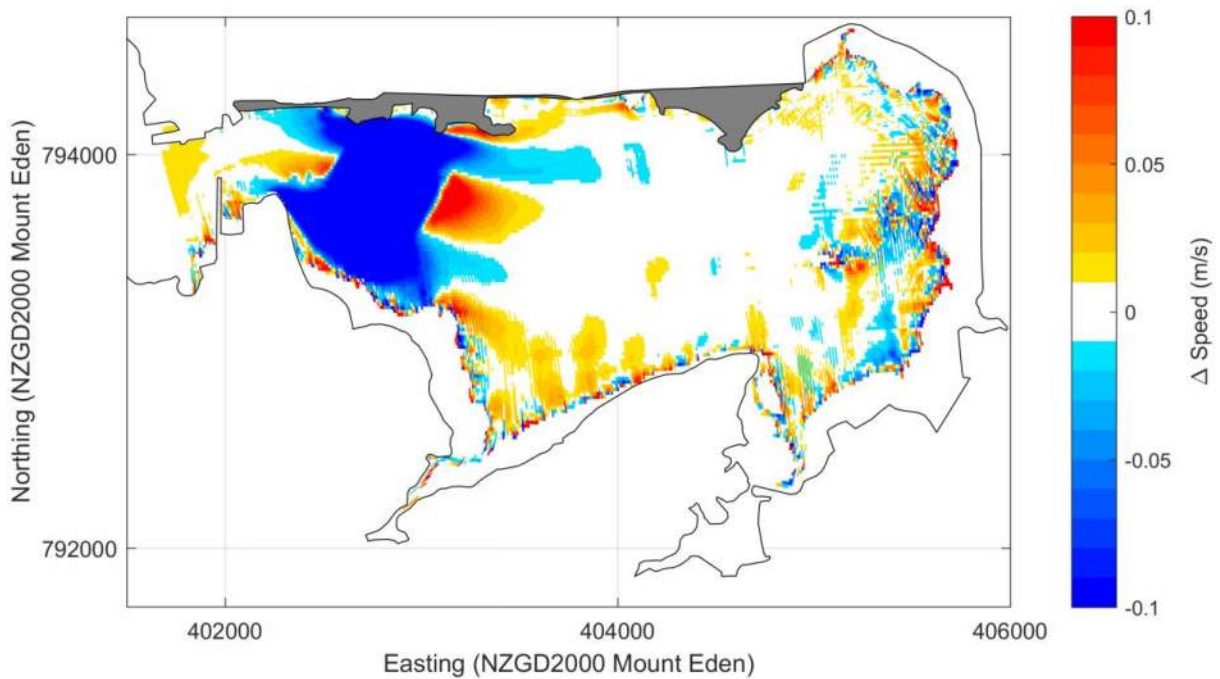
It is expected that over time the sediment deposition (and bed level) will eventually reach an equilibrium depth where the bed becomes susceptible to erosion by waves on the flood tide. The sediment will then be then transported off the flanks on the falling tide (as a turbid fringe) and back into the dredged area (e.g., Green and Bell, 1995).



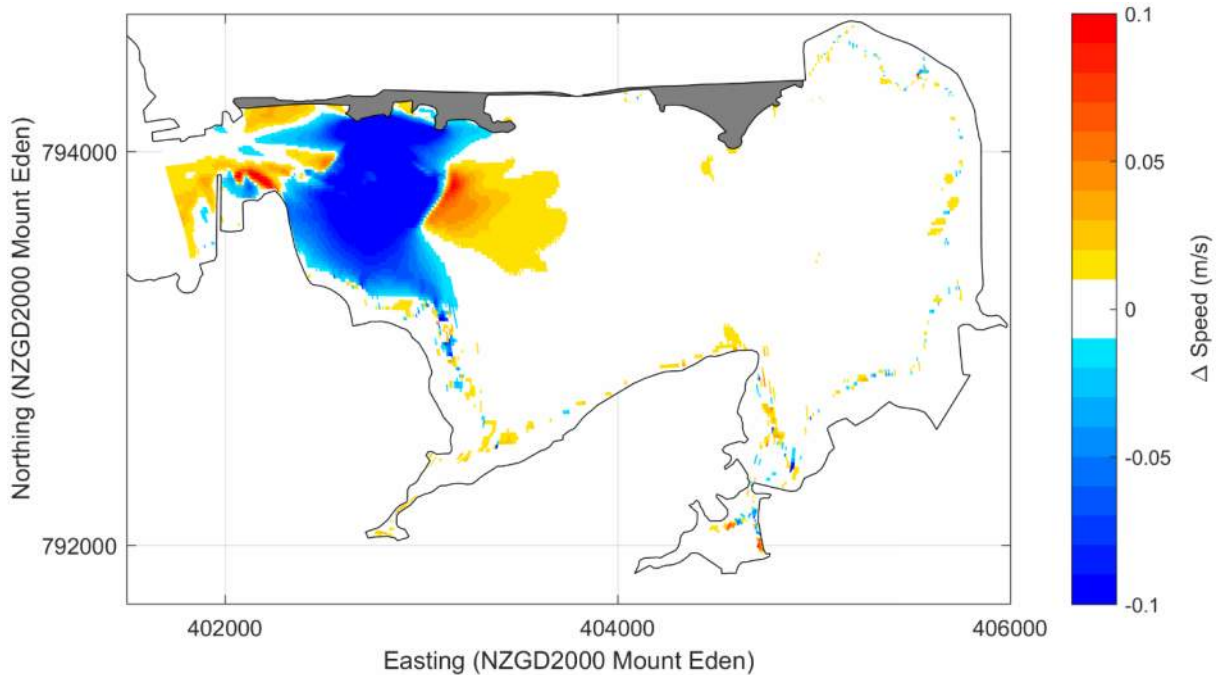
**Figure 7-1:** Proposed area of the dredging (black broken line) of bed material to be used for mudcrete in the coastal reclamation. Three locations of point sources of sediment plumes are also shown (see Section 8).



**Figure 7-2: Predicted changes in wind climate composite ASR<sub>WDCLI</sub> (mm/yr) caused by dredging operations in Mangere Inlet with proposed coastal reclamation in place based equation (3). Differences in modelled pre- and post-dredging ASR<sub>WDCLI</sub>  $\pm$  0.5 mm/yr are blanked out.**



**Figure 7-3: Difference in peak flood current speed due to proposed coastal reclamation and dredging in Mangere inlet on a mean (M2) flood tide.**



**Figure 7-4: Difference in peak flood current speed due to proposed coastal reclamation and dredging in Mangere inlet on mean (M2) ebb tide.**

### 7.1 Predicted mean ASR in Mangere Inlet with coastal reclamation and mudcrete dredge

The predicted mean ASR for Mangere Inlet with coastal reclamation and mudcrete dredge in place is **10.4 mm/yr.**

## 8 Point source discharge of suspended sediment plumes

During the coastal reclamation work inside Mangere Inlet, dredging and earthworks will generate suspended sediment plumes discharged from point sources. These plumes will be dispersed by the tide and wind and will ultimately deposit sediment at locations around the inlet.

The aim of this investigation is to model a point source input of 1kg/s of native sediment (50 percentile settling velocity of about 0.7m/hr) for a 10 hour period every 24 hours. The results from the model simulations will be used to determine:

- The rate SSC decays away with distance from each point source.
- The location of sediment deposits discharged from each source.

### 8.1 Suspended sediment plume modelling – model set up

The location, water depth and discharge rate from 3 point source discharges inside the inlet are shown in Table 8-1 and on Figure 7-1.

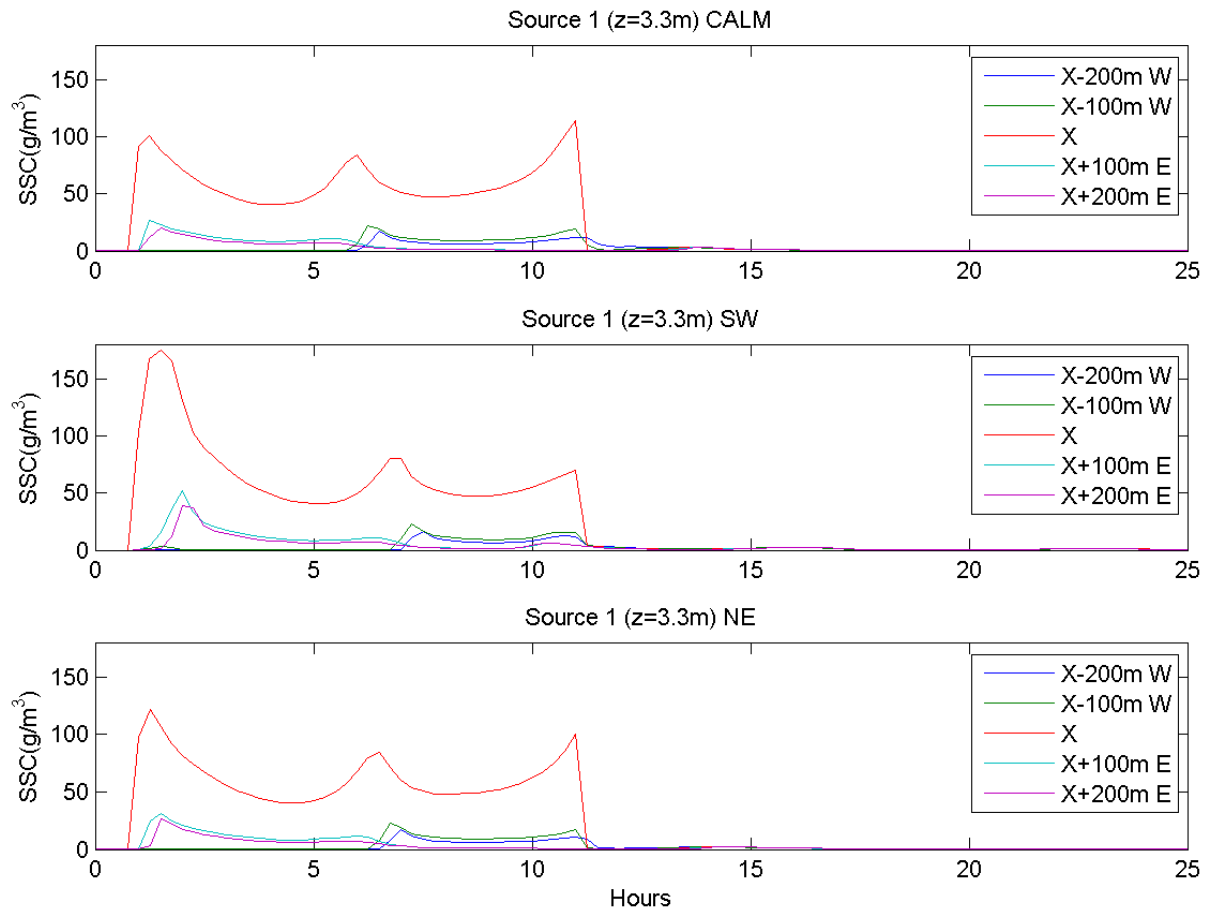
**Table 8-1: Locations and details of point source sediment discharges sourced from engineering work into Mangere Inlet.**

Source	Easting (m)	Northing (m)	Water depth (m)	Discharge rate (kg/s)
S1	402591	794029	3.3	1
S2	402723	794194	1.7	1
S3	405023	794330	1	1

The approach to plume modelling assumes each source will separately discharge a suspended fine sediment flux at a rate of 1 kg /s for a 10 hour period in a day. This equates to a total of 36 tonnes of sediment. The water in the sediment from each source is assumed saline and the receiving water column throughout the inlet is also saline and well mixed. Each model scenario was started at local low water and ran with a mean (M<sub>2</sub>) tide and a 10 hour discharge of suspended sediment. Simulations were run separately for each of calm, and 7.5 m/s SW and NE wind conditions simulations.

The predicted SSC at sites 100 m and 200 m east and west of the 3 sources were extracted from the model and plotted as a 24 hour time series. The corresponding daily depositional rate for each wind scenario was also extracted from the model 24 hrs after the initial start of discharge i.e., 14 hours after the discharge is turned off, and spatially mapped inside the inlet.

#### 8.1.1 Suspended sediment plume – Source 1

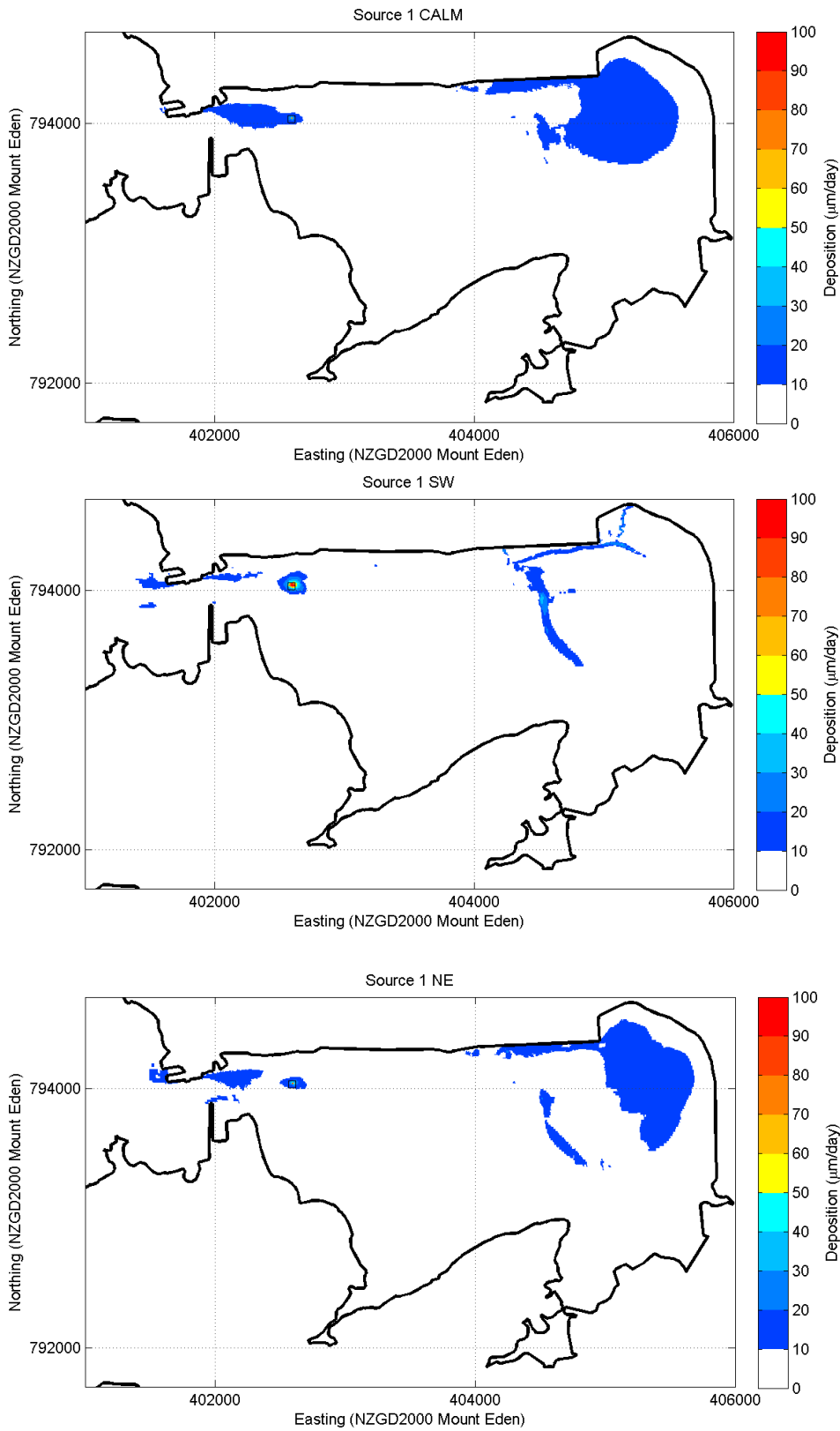


**Figure 8-1: Predicted water column SSC at Source 1 (3.3 m) and 100 m and 200 m east and west of source location during calm, SW and NE winds.**

Figure 8-1 shows the predicted SSC time series during calm, SW and NE wind conditions for a Source 1 plume discharge (see Figure 7-1). The highest SSC values were predicted at the location of the source input and the SSC quickly decayed with distance from the source for all wind conditions. The highest overall SSC was predicted during SW winds reaching SSC of 180 g/m<sup>3</sup> because of the SW wind forcing on an eastward flowing flood tide. Once the discharge was terminated, SSC at all locations dropped to zero.

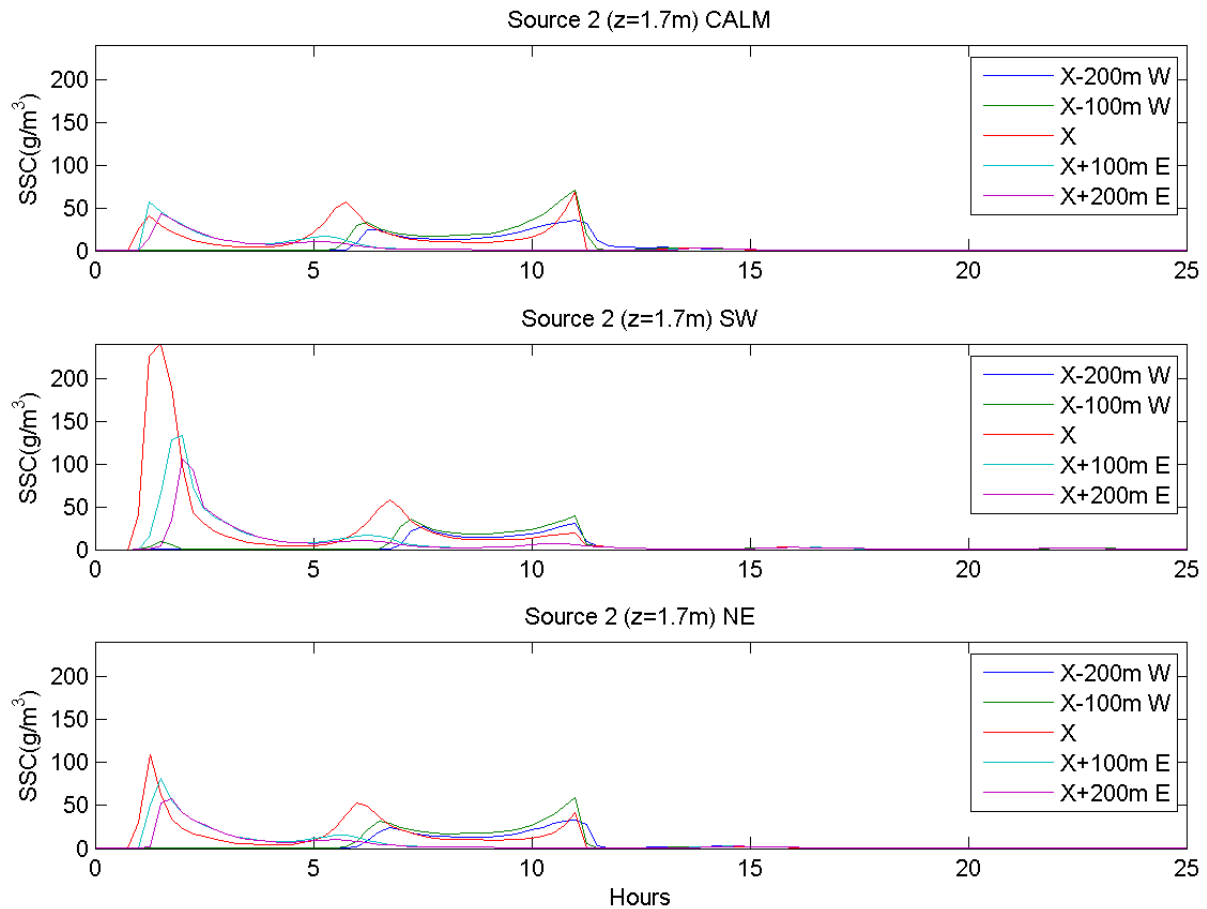
Figure 8-2 shows the predicted locality and daily rate of sediment deposition for a Source 1 sediment plume that is discharged during calm, SW and NE wind conditions. The predicted highest rate of bed deposition was always close to the source but the extent of the plume spreading depended on the wind. During calm and NE winds, plume deposits end up on the intertidal flats to the north east of the inlet and also to the west in the throat of inlet entrance. During a SW wind wave action reduces sedimentation on the intertidal flats and so most sediment is deposited close to the source and in the deeper sub-tidal channels on the north east of the inlet.





**Figure 8-2: Source 1 suspended sediment plumes daily rate of bed deposition.**

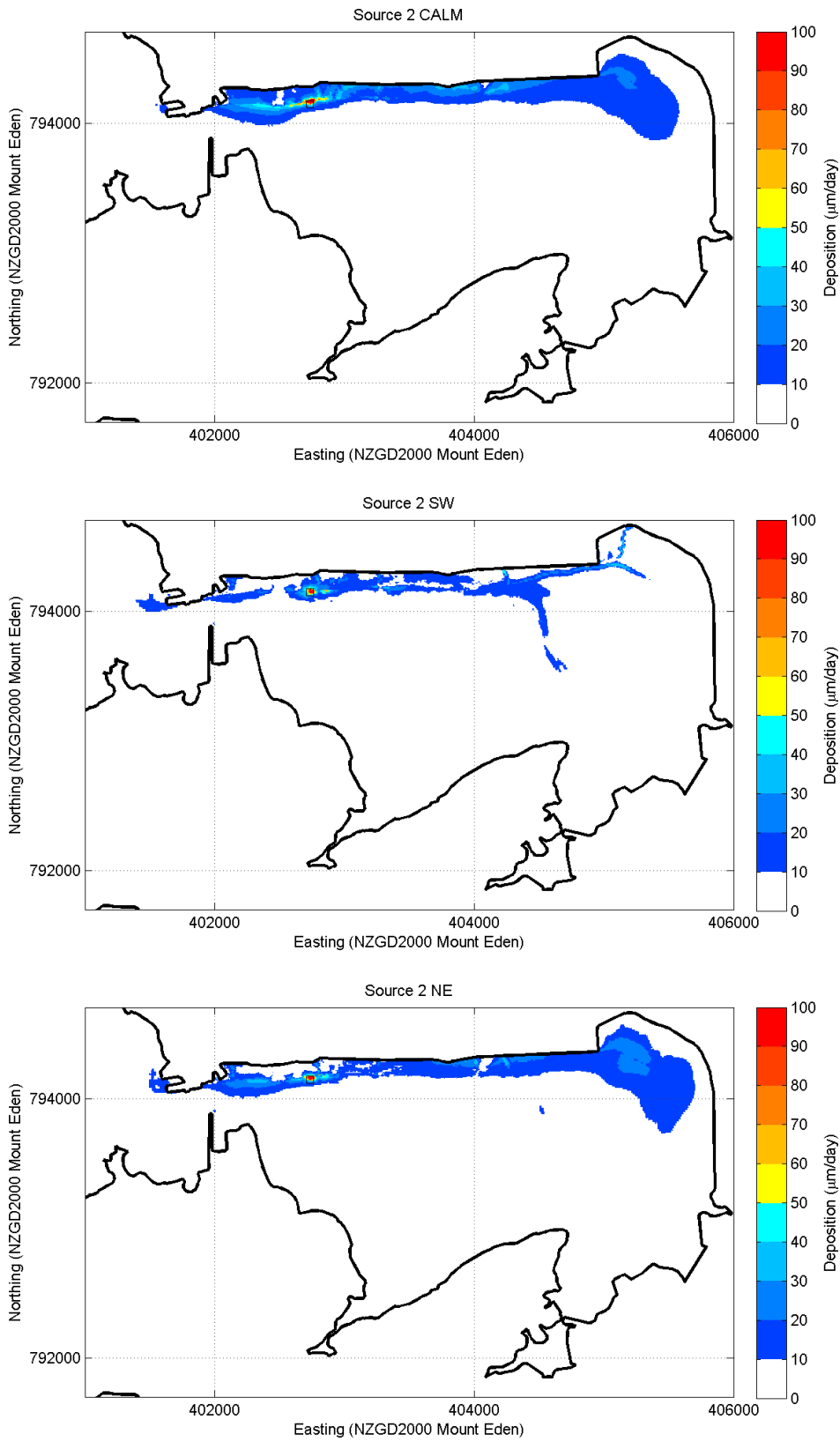
### 8.1.2 Suspended sediment plume – Source 2



**Figure 8-3: Predicted water column SSC at Source 2 (1.7 m) and 100 m and 200 m east and west of source location during calm, SW and NE winds.**

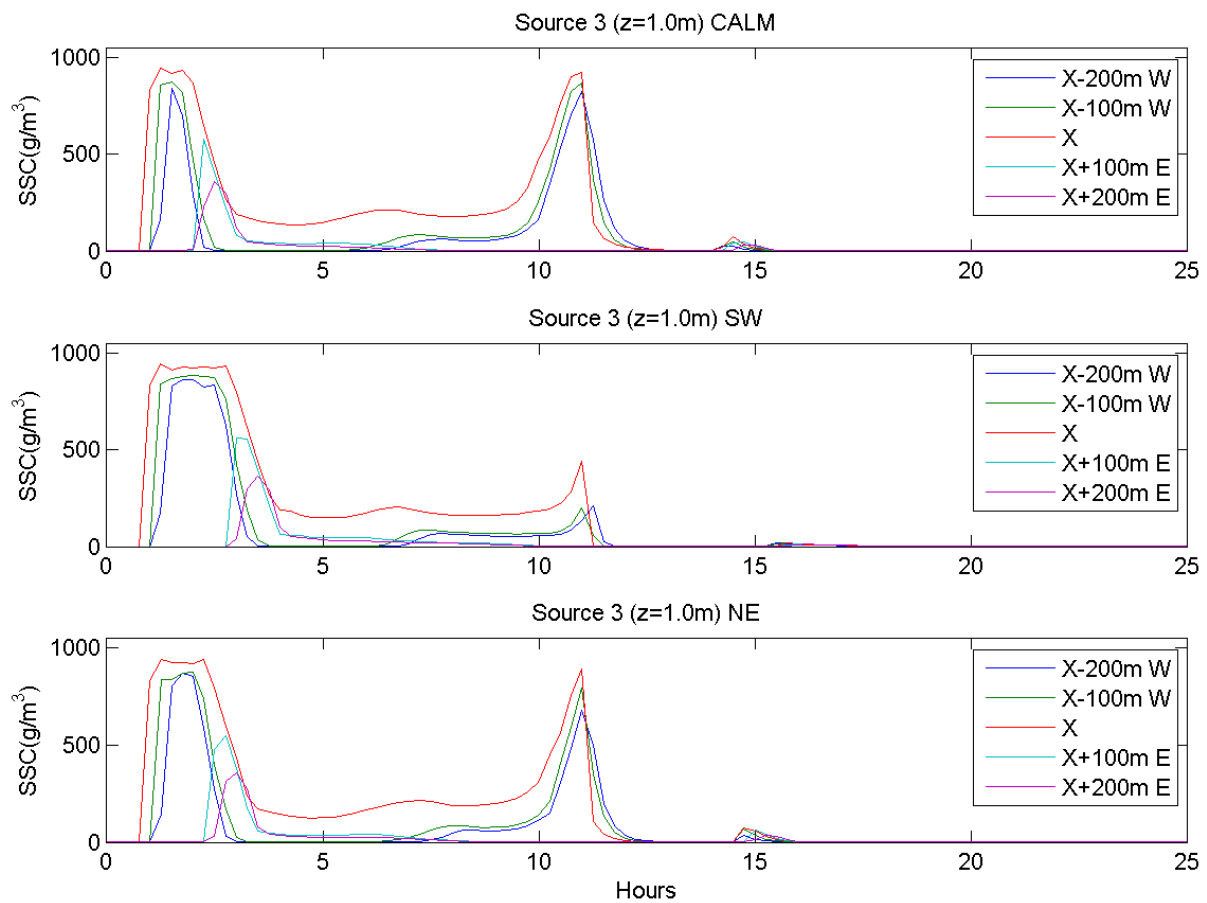
Figure 8-3 shows the predicted SSC time series during calm, SW and NE wind conditions for a Source 2 plume discharge. The peaks in the SSC time series largely reflect the effects to tidal advection that is transporting sediments up and down the main inlet channel. The highest single peak of approximately  $240 \text{ g/m}^3$  is close to the discharge source and results from the effects of ‘wind on tide’ at the start of the sediment discharge. After the initial release peaks in SSC drop down to approximately  $50 \text{ g/m}^3$  for all conditions. Once sediment Source 2 is terminated SSC decreases towards zero.

Figure 8-4 shows the predicted locality and daily rate of sediment deposition for a Source 2 sediment plume that is discharged during calm, SW and NE wind conditions. The highest rate of bed deposition was predicted close to the source for all wind conditions. Low levels of sediment deposition ( $<20 \text{ um}$ ) were predicted all along the northern coast of the inlet, on the north eastern intertidal flats and some small deposits in the inlet entrance. During a SW wind sediment also deposited along the northern coast of the inlet but the deposits to the north east were mainly confined to the subtidal channels.



**Figure 8-4: Source 2 suspended sediment plumes daily rate of bed deposition.**

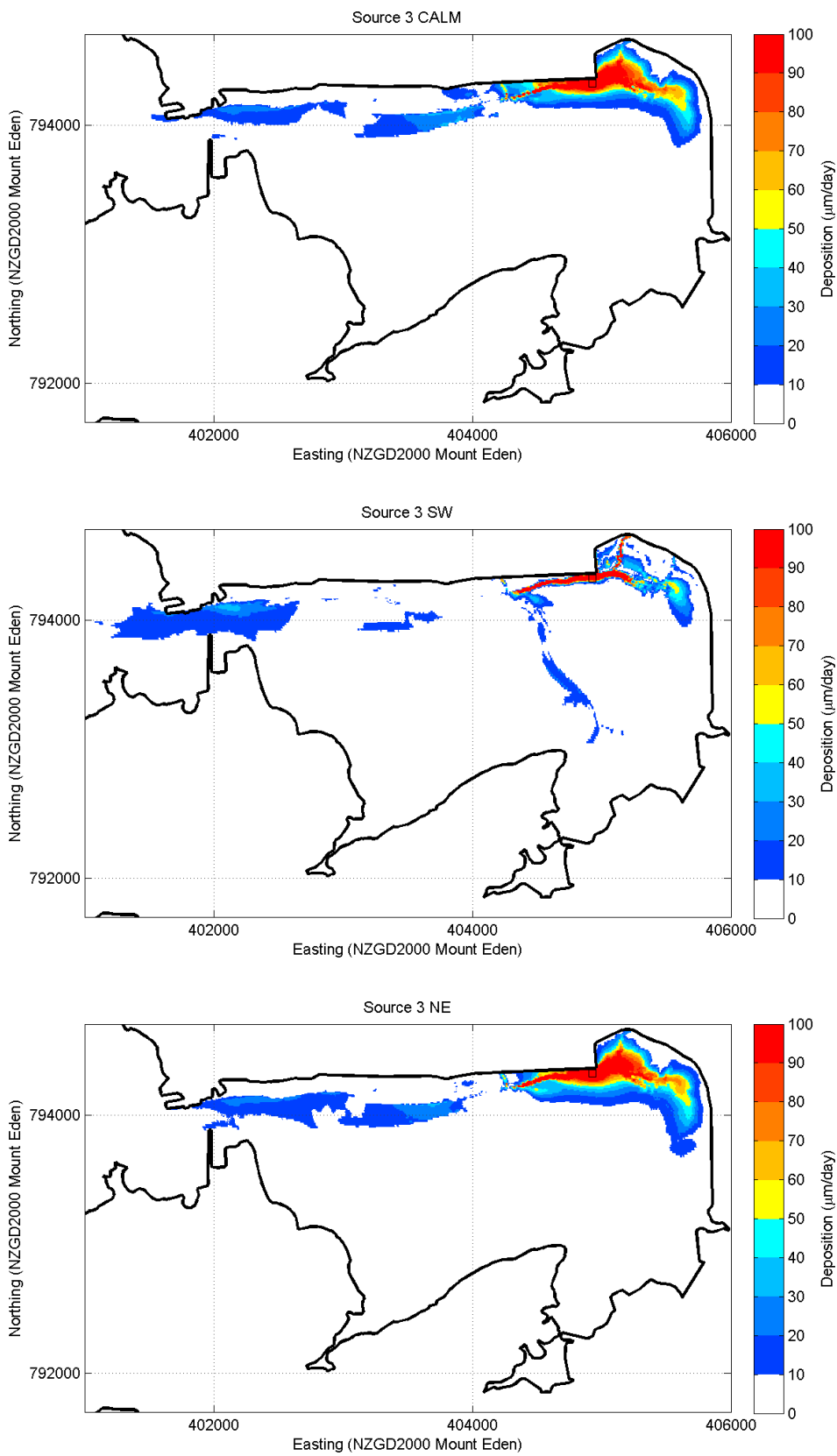
### 8.1.3 Suspended sediment plume – Source 3



**Figure 8-5: Predicted water column SSC at Source 2 (1.0 m) and 100 m and 200 m east and west of source location during calm, SW and NE winds.**

Figure 8-5 shows the predicted SSC time series during calm, SW and NE wind conditions for a Source 3 plume discharge. High levels of SSC that approach  $1000\text{g/m}^3$  were predicted to the west of the source for all wind conditions. In contrast, close to the source and east of the source SSC levels were relatively low.

Figure 8-6 shows through the predicted locality and daily rate of sediment deposition that there is relatively thick sediment deposition to the east of the source on the north eastern intertidal flat during calm and NE winds. Sediment that deposits is trapped on the flat and does not resuspend as reflected by the SSC (Figure 8-5). The high rates of bed deposition on the north eastern intertidal flats coincide with calm and NE winds when there is either no wind (and no waves) or wave height is fetch limited (NE). During a SW wind, less sediment deposits on the north eastern flat because of wave driven resuspension – consequently most of the sediment deposits in the tidal channels only.



**Figure 8-6: Source 3 suspended sediment plumes daily rate of bed deposition.**

## 9 Wave climate and extreme wave analysis inside Mangere inlet

The wind wave climatology (1980-2011) inside Mangere Inlet was estimated for nearshore water depths (assuming near to the area of coast where reclamation will take place) of 50 cm, 1 m and 2 m. Significant wave heights ( $H_s$ ) at these water depth were estimated from the wind data using the empirical formula of Young and Verhagen (1996). The formula estimates the growth of fetch limited waves in water of finite depth from measurements of wind speed and fetch length.

The wave height computations were made using a time series of wind speeds approaching from either the southwest or northeast direction, as described in Section 3.4. Winds blowing from the southwest sector (125–315 °T) and northeast sector (315–125 °T) were assigned either a southwest (225 °T) or northeast (45 °T) angle respectively. A fetch distance of 3 km was used, which approximates the maximum span across the basin in the northeast–southwest direction. The results were insensitive to the relatively short reduction in fetch length caused by the coastline reclamation work.

### 9.1 Extreme value analysis

An extreme value model commonly applied to analyse extreme wave heights is the generalised Pareto distribution (GPD). This is fitted to independent data peaks that exceed a given high threshold (known as peaks over threshold, or POT).

#### 9.1.1 GPD fitting to significant wave heights ( $H_{sig}$ ) over a threshold

The GPD/POT method was used to estimate the extreme wave height frequency–magnitude distribution from the predictions of  $H_s$  at each water depth. The POT method was applied to the hourly  $H_s$  data, and involved separating the time series into independent wave peaks that were at least 3 days apart and above a specified threshold. A generalised Pareto distribution (GPD) was then fitted to the peaks, and used to estimate the frequency–magnitude distribution.

In summary the POT approach is:

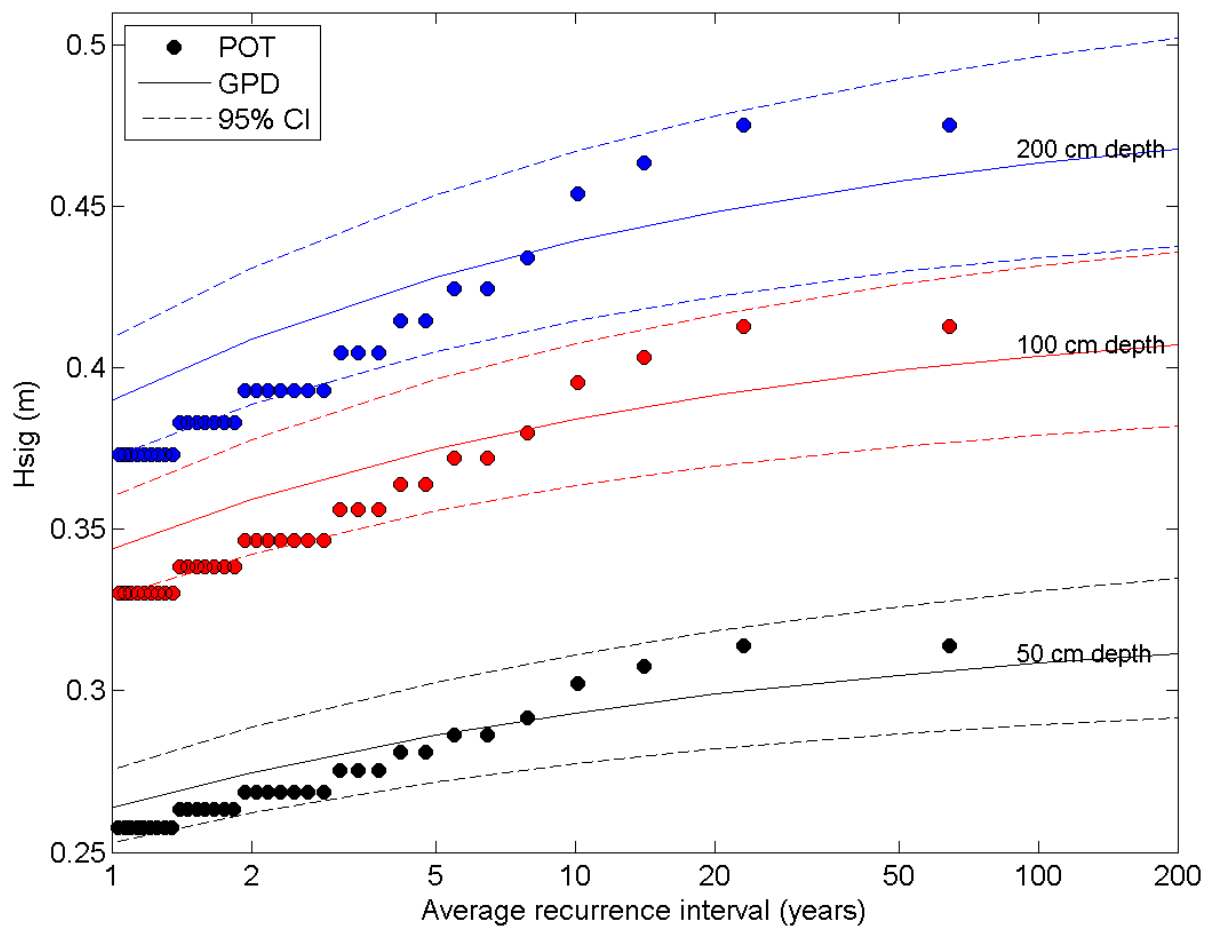
1. With various wave height thresholds, calculate the shape and scale parameters of a GPD fitted to wave heights above that threshold. Plot the variability of the shape and scale parameters against varied threshold.
2. At each site, choose the lowest threshold for which the shape parameter approximately stabilises. The scale parameter should have an approximately linear relationship with wave height at this threshold.
3. Using a 3 day window to separate the wave peaks into independent events, the peak wave heights above the chosen threshold were extracted from each window.
4. The number of observations above the threshold per year ( $S_y$ ) were determined, where  $S_y = \text{total number of peaks} / \text{record length (years)}$ .
5. Fit a GPD to the wave height peaks, and determine the annual exceedance probability (AEP) of the projected significant wave heights.

## 9.2 Results of extreme value analysis of $H_{sig}$

The results from the extreme analysis of  $H_{sig}$  at 3 different water depth are presented in Table 9-1 and Figure 9-1. The results show the typical increase in  $H_s$  with an increasing recurrence interval and an increasing  $H_{sig}$  with increasing water depth.

**Table 9-1: Maximum predicted significant wave height ( $H_{sig}$ ) for a range of water depth and ARI (years).**

Water depth (m)	ARI (yr)						
	2	5	10	20	50	100	200
0.5	0.27	0.29	0.29	0.30	0.30	0.31	0.31
1	0.36	0.37	0.38	0.39	0.40	0.40	0.41
2	0.41	0.43	0.44	0.45	0.46	0.46	0.41



**Figure 9-1: Frequency–magnitude distribution of significant wave height ( $H_{sig}$ ) at 3 nearshore water depths inside Mangere Inlet.**

## 10 Conclusions

This study developed and applied a hydrodynamic, wave and sediment transport model of Mangere Inlet, to model the relative change in tidal flow and sediment deposition following coastal reclamation along the inlet's north shore.

The main differences in tidal circulation caused by coastal reclamation were predicted adjacent to the reclaimed coastline. The series of new coves and embayments along the western stretch of the new coastline act to reduce tidal current speeds. The most notable change in relative current speeds was predicted on the eastern side on the reclamation where the reclamation will infill a tidal channel.

The estimated inlet mean annual sedimentation rate, averaged over the existing inlet, was 9.8 mm/yr. The mean annual sedimentation rate after reclamation was similar, being 10.5 mm/yr. This is an increase in sedimentation of 0.7 mm/yr. The model predicted relative increases in sediment deposition along most of the western stretch of reclaimed coastline, due to the lower current speeds which have less sediment-carrying capacity. Further east along the reclamation there was more relative erosion that resulted from a change in the tidal current speeds and circulation.

The effects of sea-level rise were incorporated into modelling by assuming 1 m increase in sea-level and 0.5 m increase in seabed height due to sedimentation. Results from the modelling predicted a 10.4 mm/yr annual sedimentation rate after sea-level rise.

Modelling that investigated the effect of dredging and removing approximately 300,000 m<sup>3</sup> of bed material from the west of Mangere Inlet predicted a decrease in tidal current speeds through the entrance to the inlet. The modelling predicted decreases in tidal current speeds would increase sediment deposition to the north and south of the dredged area. The predicted annual sedimentation rate with both coastal reclamation and dredged area was 10.4 mm/yr.

The model was used to investigate the dispersion of sediment plumes discharged from three point sources during construction and coastal reclamation work in Mangere Inlet. The results from the modelling showed that sediment settled out of the water column almost immediately once a source was turned off. Most of the sediment deposited along the northern and eastern coast of the inlet.

The report includes a table of the expected frequency and magnitude of extreme wave heights in Mangere Inlet, in water depths of 0.5, 1.0 and 2.0 m.

## 11 Acknowledgements

East-west Alliance provided bathymetric survey data, new coastline projections and physical characteristics and properties of the sediments. Archived current-meter and tidal gauging data were supplied by NIWA (via Rob Bell). Ports of Auckland provided tidal height records at Onehunga Wharf.



## 12 References

- Bell, R.G., Dumnov, S.V., Williams, B.L., Greig, M.J. (1998) Hydrodynamics of Manukau Harbour, New Zealand. *New Zealand Journal of Marine and Freshwater Research*, 32(1): 81-100.
- Booji, N. (1981) Gravity waves on water with non-uniform depth and current. The Netherlands, Technical University of Delft.
- Booij, N., Ris, R.C., Holthuijsen, L.H. (1999) A third-generation wave model for coastal regions 1. Model description and validation. *Journal of Geophysical Research*, 104(C4): 7649-7666.
- Croucher, A.E., Bogle, M.G.V., O'Sullivan, M.J. (2005) Coastal receiving environment assessment (CREA). *Report 1. Modelling framework*. Uniservices, Auckland.
- Deltares (2011) Delft-3D-Flow: Simulation of multi-dimensional hydrodynamic flows and transport phenomena, including sediments. *User Manual Version 3.15*: 672.
- Fredsøe, J. (1984) Turbulent boundary layer in wave-current motion. *Journal of Hydraulic Engineering (ASCE)*, 110(8): 1103-1120.
- Green, M.O., Bell, R.G. (1995) Wave Influence on Suspended Sediment Fluxes in an Estuary (Manukau Harbour, New Zealand). *Conference proceedings for 12th Australasian Conference on Coastal and Ocean Engineering*, Melbourne: 275-78. National Conference Publ. No. 95/5, The Institution of Engineers, Canberra, Australia.
- Green, M.O., Black, K.P., Amos, C.L. (1997) Control of estuarine sediment dynamics by interactions between currents and waves at several scales. *Marine Geology*, 144(1): 97-116.
- Green, M.O., Bell, R.G., Dolphin, T.J., Swales, A. (2000) Silt and sand transport in a deep tidal channel of a large estuary (Manukau Harbour, New Zealand). *Marine Geology*, 163(1): 217-240.
- Haidvogel, D.B., Arango, H., Budgell, W.P., Cornuelle, B.D., Curchitser, E., Di Lorenzo, E., Fennel, K., Geyer, W.R., Hermann, A.J., Lanerolle, L., Levin, J., McWilliams, J.C., Miller, A.J., Moore, A.M., Powell, T.M., Shchepetkin, A.F., Sherwood, C.R., Signell, R.P., Warner, J.C., Wilkin, J. (2008) Ocean forecasting in terrain-following coordinates: Formulation and skill assessment of the Regional Ocean Modelling System. *Journal of Computational Physics*, 227: 3595–3624.
- Lesser, G.R., Roelvink, J.A., van Kester, J.A.T.M., Stelling, G.S. (2004) Development and validation of a three-dimensional morphological model. *Coastal Engineering*, 51(8-9): 883-915. doi:10.1016/j.coastaleng.2004.07.014.
- Pritchard, M., Swales A., Green, M. (2015) Influence of buoyancy- and wind-coupling on sediment dispersal and deposition in the Firth of Thames, New Zealand. *Proceedings of Australasian Coasts & Ports Conference 2015*, 15 - 18 September 2015, Auckland, New Zealand.

- Reeve, G., Pritchard, M. (2010). Manukau Harbour Enhancement Project: Hydrodynamic Modelling Calibration Report. *NIWA Hamilton Client Report HAM2010-019*.
- Ris, R.C., Holthuijsen, L.H., Booij, N. (1999) A third-generation wave model for coastal regions 2. Verification. *Journal of Geophysical Research*, 104(C4): 7667-7681.
- Warner, J.C., Geyer, W.R., Lerczak, J.A. (2005) Numerical modeling of an estuary: A comprehensive skill assessment. *J. Geophys. Res.*, 110, C05001, doi: 10.1029/2004JC002691.
- Whitehouse, R.J.S., Soulsby, R.L., Roberts, W., Mitchener, H.J. (2000). *Dynamics of estuarine muds*.
- Wilcock, R.J., Northcott, G.L. (1995) Polycyclic aromatic hydrocarbons in deep cores from Mangere Inlet, New Zealand. *New Zealand Journal of Marine and Freshwater Research*, 29(1): 107-116.
- Williamson, R.B., Van Dam, L.F., Bell, R.G., Green, M.O., Kim, J.P. (1996) Heavy metal and suspended sediment fluxes from a contaminated, intertidal inlet (Manukau Harbour, New Zealand). *Marine Pollution Bulletin*, 32(11): 812-822.
- Young, I.R., Verhagen, L.A. (1996) The growth of fetch limited waves in water of finite depth. Part 1. Total energy and peak frequency. *Coastal Engineering*, 29: 47-78.

## Appendix A Deltares Delft3D modelling suite

### Delft3D-FLOW

Delft3D-FLOW solves the Navier-Stokes equations for momentum whilst conserving mass through the principle of continuity (Deltares, 2011). Physical processes in the model can be parameterised and simulated through specifying for example, eddy scales, turbulent-closure schemes, surface and bottom boundary conditions, surface winds and pressure fields, wave-current interaction, surface heating, salinity & temperature structure and the earth's rotational effects.

The Delft3D-FLOW model can be forced at open and source input boundaries by oceanic tides, freshwater and heat sources. These forcing mechanisms produce the essential boundary physics required to simulate barotropic (surface-pressure gradients) and baroclinic (internal pressure gradients driven by horizontal and vertical water-density gradients) in the model domain which allow variation in seawater density to be included in model solutions. The superimposed effect of currents and waves on the bed shear stress is taken into account by means of the current-wave interaction model of Fredsøe (1984).

### Delft3D-WAVE

Within the Delft3D modelling suite, the wave module Delft3D-WAVE simulates the evolution of random, short-crested wind-generated waves in estuaries and tidal inlets and based on the third-generation Simulating WAVes Nearshore or SWAN model (see Booij et al. 1999; Ris et al. 1999).

The SWAN model is a spectral wave model intended for shallow water applications in coastal and estuarine environments (Booij et al. 1999; Ris et al. 1999). It computes the evolution of the wave energy spectrum in position (x,y) and time (t), explicitly taking into account the various physical processes acting on waves in shallow water. These include the effects of refraction by currents and bottom variation, and the processes of wind generation, white-capping, bottom friction, quadruplet wave-wave interactions, triad wave-wave interactions and depth-induced breaking. The model can incorporate boundary conditions representing waves arriving from outside the model domain.

For all model simulations of sediment transport predictions, Delft3D-FLOW was 'online' coupled with Delft3D-WAVE which has a two way wave-current interaction i.e., the effect of flow on the waves (via set-up, current refraction and enhanced bottom friction) and the effect of waves on current (via forcing, enhanced turbulence and enhanced bed shear stress).

### Delft3D-SED

The transport of scalars i.e., salinity and temperature (density), and sediments, is solved using a coupled three-dimensional advection-diffusion equation. Horizontal and vertical variations in density in the model caused by, for example, freshwater from rivers, are initially transported and mixed by the coupled advection and diffusion (A-D) equation. The model solution assumes the Boussinesq approximation where the variations in the density are only dynamically accounted for in the pressure terms of the Navier-Stokes equation. In the Delft3d vertical sigma co-ordinate system, this reduces the immediate effects of buoyancy on vertical flows by assuming this is taken into account through the effects of the horizontal pressure gradient and vertical turbulent closure scheme (Deltares, 2011).

Cohesive suspended sediments are transported by the same A-D transport methodology where suspensions are advected by the flow and diffused vertically by turbulent mixing. In addition, sediment fractions have a specified settling velocity (related to particle size via the Stokes settling equation), bed power of erosion, a critical bed erosion threshold and critical deposition threshold (related to bed shear stresses at the bottom boundary layer) that may be varied through the model domain. The velocities used in these computations are provided by the flow fields predicted by Delft3D flow and if coupled, Delft3D-WAVE.

Sediment sample analysis by BECA showed the majority of bed sediments in Mangere Inlet were in the size fraction of muds/fine silts. Therefore, all sediment transport simulations in this study used the Delft3d cohesive sediment transport model.

### Delft3D-MOR

The Delft3D-MOR module applies sediment transport formulae (both suspended and/or bed total load) to estimate the morphological change through the model domain (Lesser et al. 2004). Throughout a simulation, elevation of the sea-bed is dynamically updated at each computational time-step by computing the change in the mass of bed material that has occurred as a result of the sediment sink and source terms and the sediment-transport gradients. The mass is then translated into a bed level change based on the dry-bed densities of the sediment fraction (mud in the case of Mangere Inlet). This means that subsequent hydrodynamic calculations are always carried out using the continually-updated bathymetry as the sea-bed erodes or accretes.

## Appendix B Skill tests

### Bias

$$Bias = \frac{1}{n} \sum_{i=1}^n (y_i - x_i)$$

Where:  $x_i$  is the  $i^{th}$  modelled value,  $y_i$  the  $i^{th}$  measured value, and  $n$  the number of values being compared.

### Root Mean Square Error (RMSE)

$$RMSE = \sqrt{\frac{1}{n} \sum_{i=1}^n (y_i - x_i)^2}$$

Where:  $x_i$  is the  $i^{th}$  prediction and  $y_i$  the  $i^{th}$  true value and  $n$  the number of values being compared.

### Cross Correlation Function ( $R_{xy}$ )

Cross correlation function ( $R_{xy}$ ) is computed from the cross-covariance function:

$$C_{xy}(\tau) \equiv E\{[y(t) - \mu_y][x(t + \tau) - \mu_x]\}$$

Where:  $C_{xy}$  is the cross-covariance function,  $E$  is the expected value,  $x(t)$  and  $y(t)$  are discrete variables at time  $t$ ,  $\mu_y$  and  $\mu_x$  are means of the two time series, and  $\tau$  is the time lag between them.

The cross correlation function ( $R_{xy}$ ) is a non-dimensional summary of this analysis which ranges from 0 to 1, where 1 infers a strong in-phase agreement between the two signals.

$$R_{xy} \equiv \frac{C_{xy}(\tau)}{\sigma_x \sigma_y}$$

Where:  $\sigma_x$ ,  $\sigma_y$  are the standard deviations of each time series.

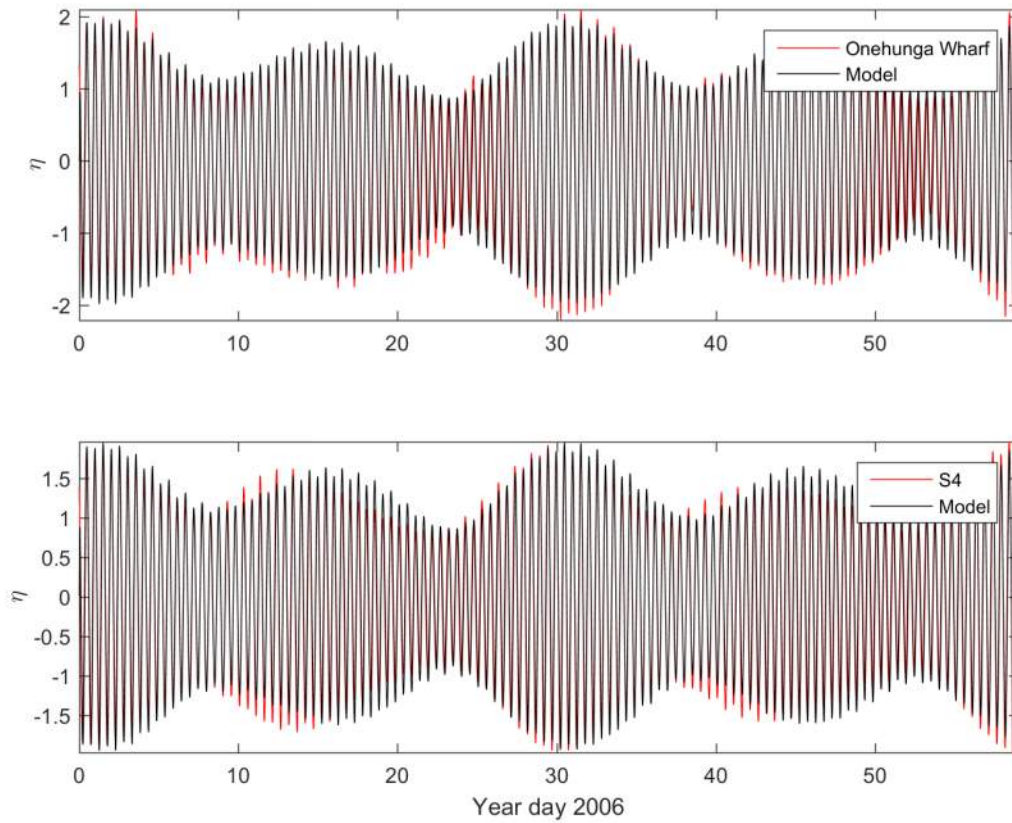
Measures of model performance were bias (*BIAS*), root mean square error (*RMSE*) and model skill (*SKILL*).

*SKILL* is defined as:

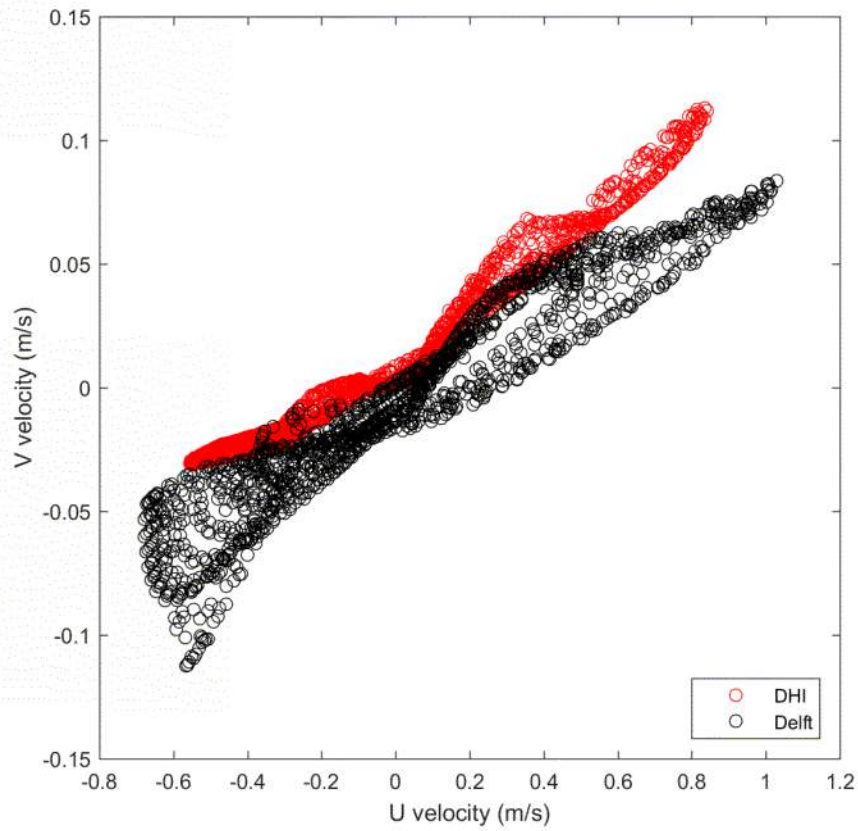
$$SKILL = 1 - [|X_m - X_o|^2] / \left[ \sum_{i=1}^N (|X_{mi} - \bar{X}_o| + |X_{oi} - \bar{X}_o|)^2 \right]. \quad (1)$$

(Warner et al. 2005; Haidvogel et al. 2008) where  $X$  is the variable (in our case, either water level, current speed or current direction),  $\bar{X}$  is the time average of  $X$ , the subscripts  $m$  and  $o$  denote model and observed values respectively,  $i$  is  $i^{th}$  value, and  $0 \leq SKILL \leq 1$ .

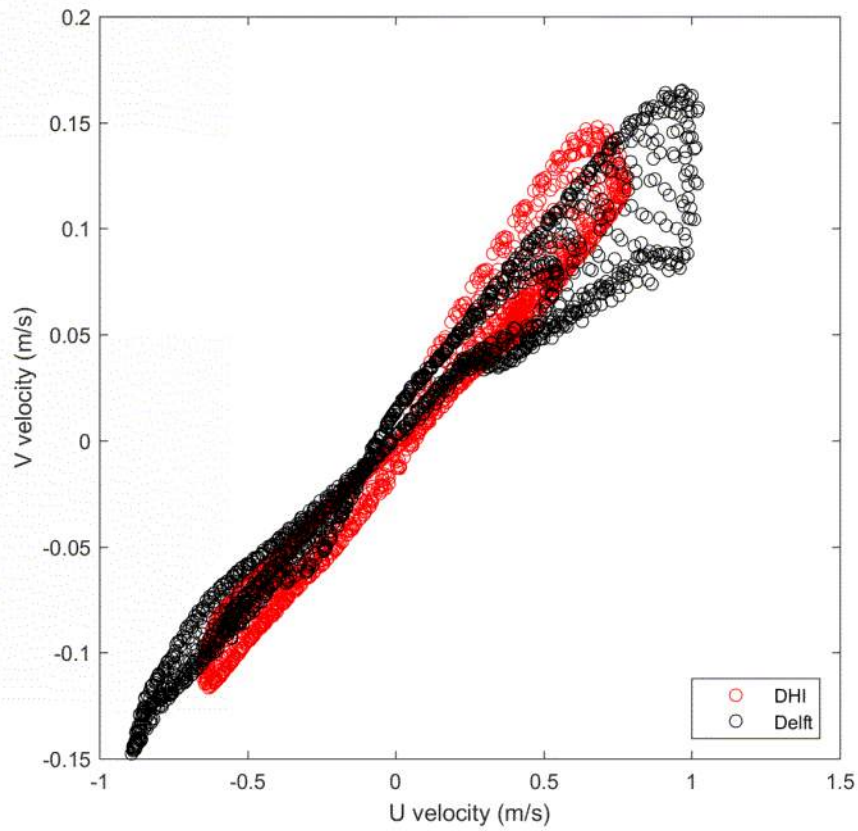
## Appendix C Tidal Calibration



**Figure C-1: Water level calibration at Onehunga Wharf and the NIWA S4 mooring site for 2006.**

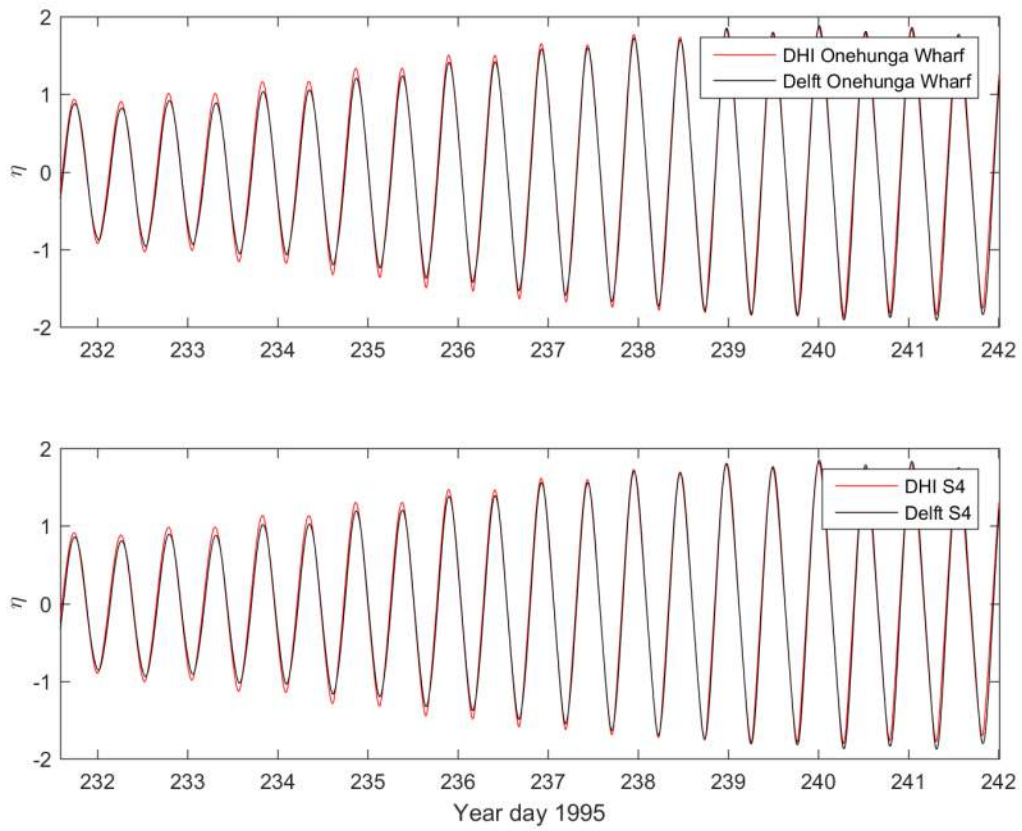


**Figure C-2: Model current velocity validation at Onehunga site for 1995 period.** The comparison is between the present model (Delft), and the DHI model applied by Reeve and Pritchard (2010).



**Figure C-3: Model current velocity validation at NIWA S4 mooring site for 1995 period.** The comparison is between the present model (Delft), and the DHI model applied by Reeve and Pritchard (2010).



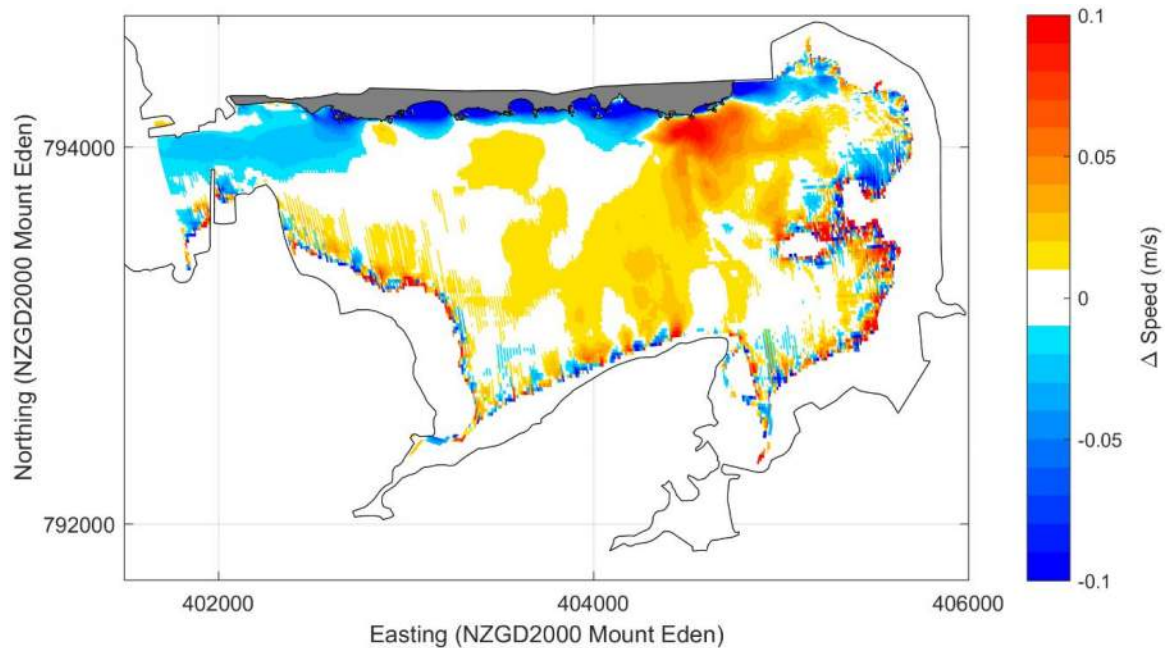


**Figure C-4: Model water level validation for locations at Onehunga and NIWA S4 mooring site.** The comparison is between the present model (Delft), and the DHI model applied by Reeve and Pritchard (2010).

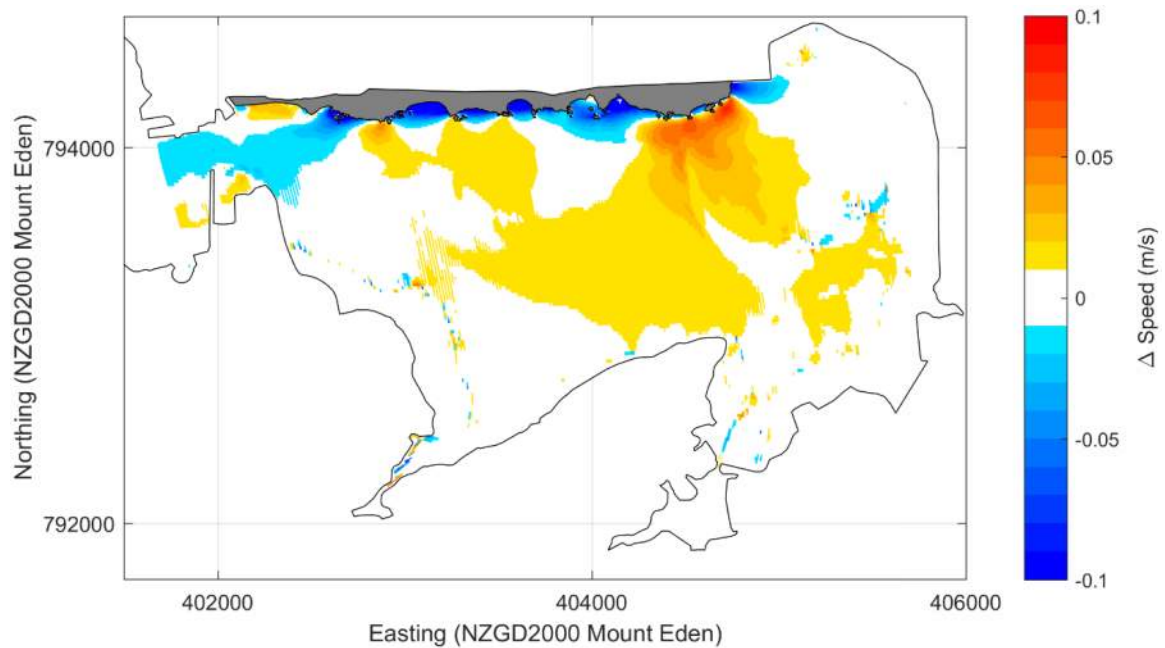
## Appendix D Reclamation Scenarios

The East-West Alliance provided 5 versions coastal reclamation to NIWA for modelling. Through this iterative process, the Alliance selected version 4 (V04) as the preferred new coastline.

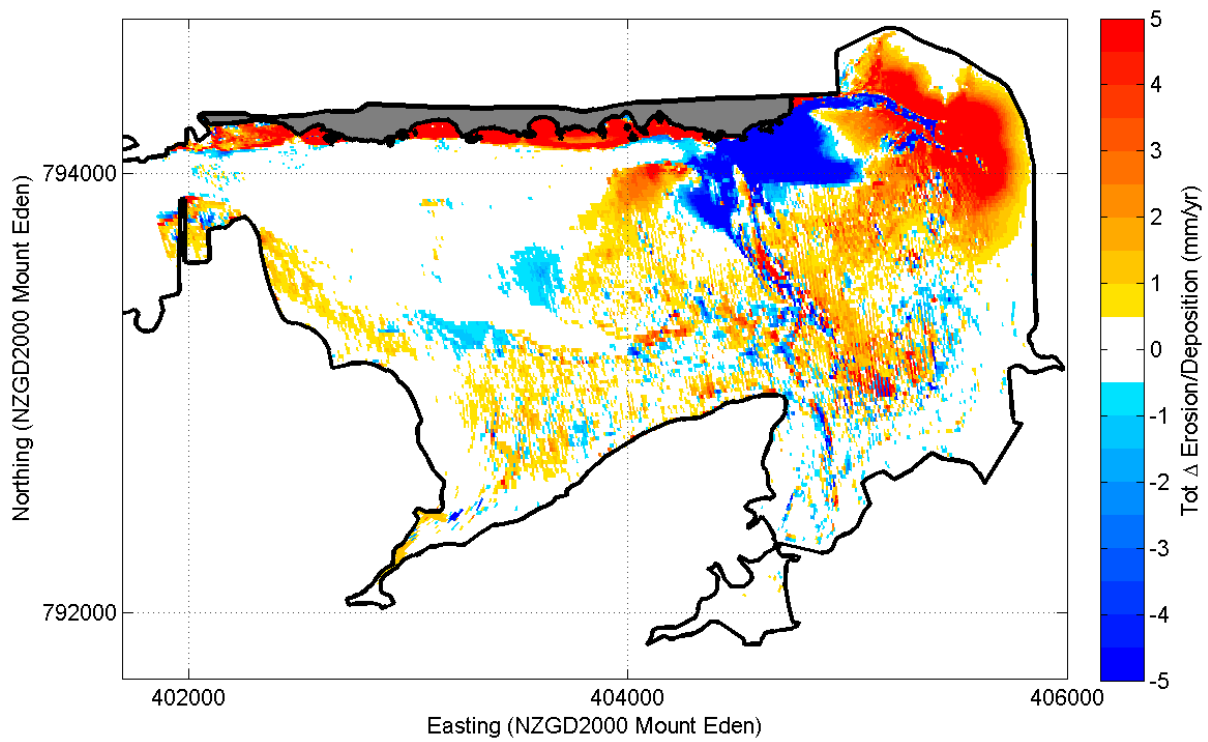
### Reclamation Version V01



**Figure D-1:** Difference in peak flood current speed due to coastal reclamation design V01 in Mangere Inlet during a mean tide.

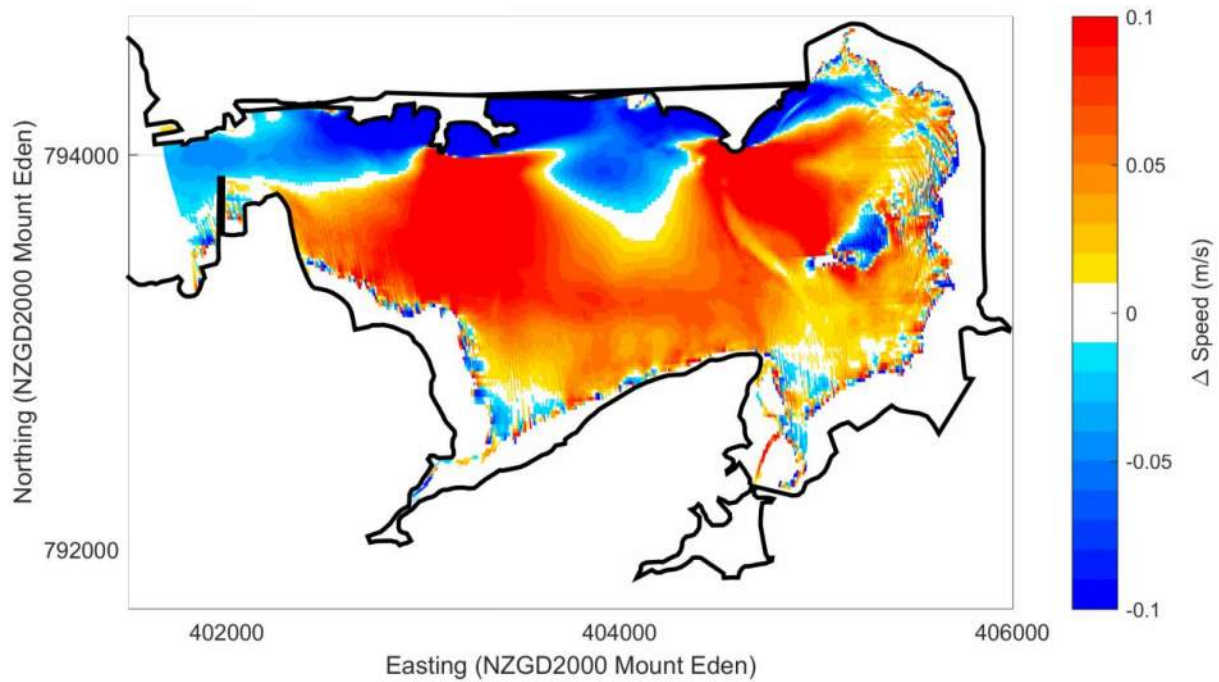


**Figure D-2:** Difference in peak ebb current speed due to coastal reclamation design V01 in Mangere Inlet during a mean tide.

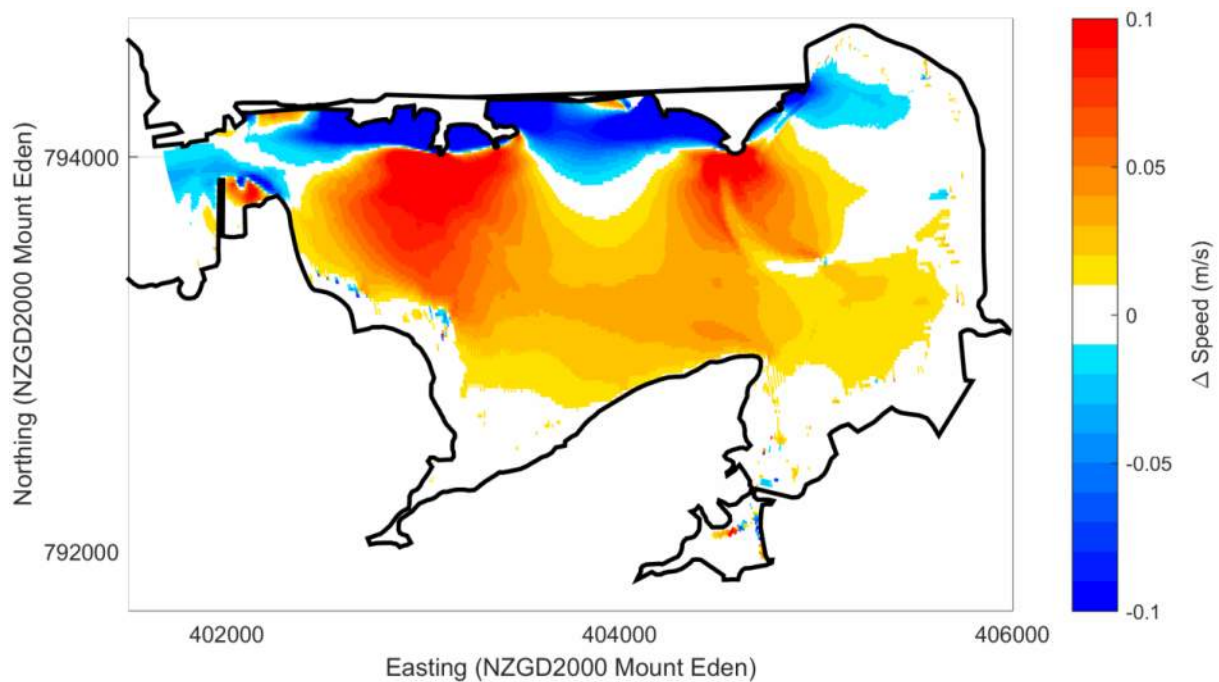


**Figure D-3:** Predicted changes in wind climate composite  $ASR_{WDCLI}$  (mm/yr) caused by coastal reclamation design V01 in Mangere Inlet using equation (3). Differences in modelled pre- and post-reclamation  $ASR_{WDCLI} \pm 0.5$  mm/yr are blanked out.

## Reclamation Version V02



**Figure D-4:** Difference in peak flood current speed due to coastal reclamation design V02 in Mangere Inlet during a mean tide.



**Figure D-5:** Difference in peak ebb current speed due to coastal reclamation design V02 in Mangere Inlet during a mean tide.

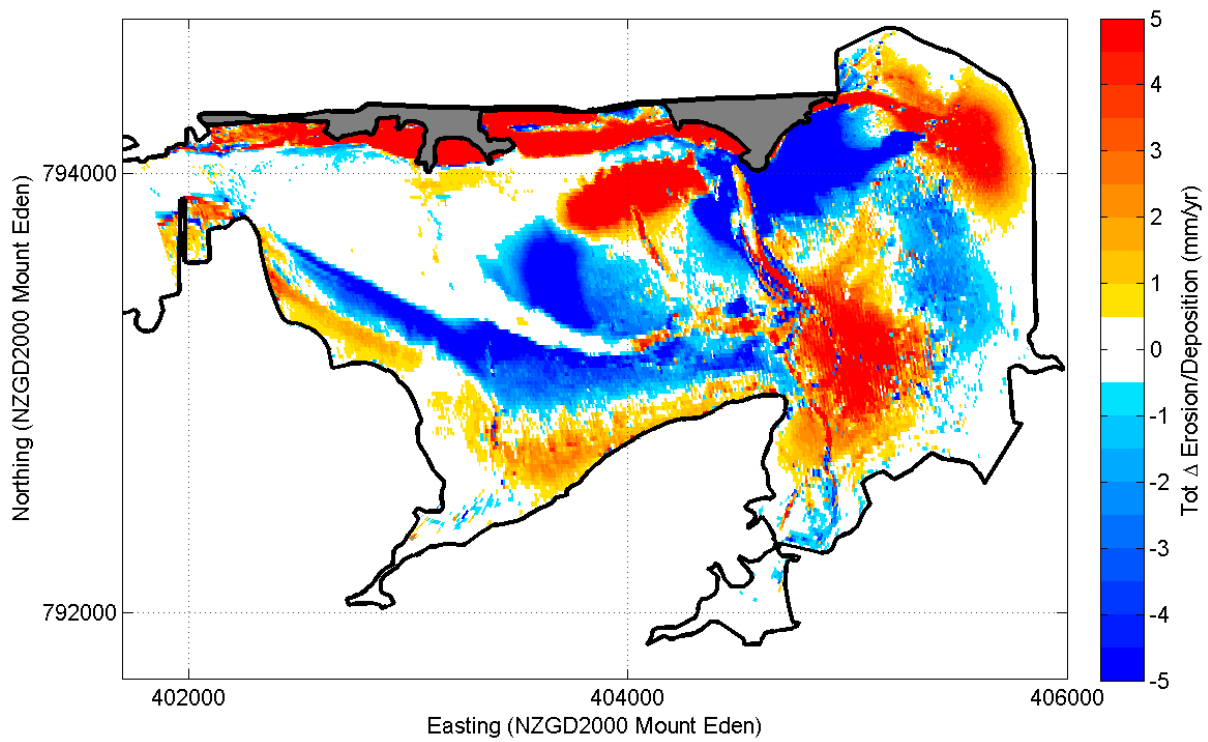
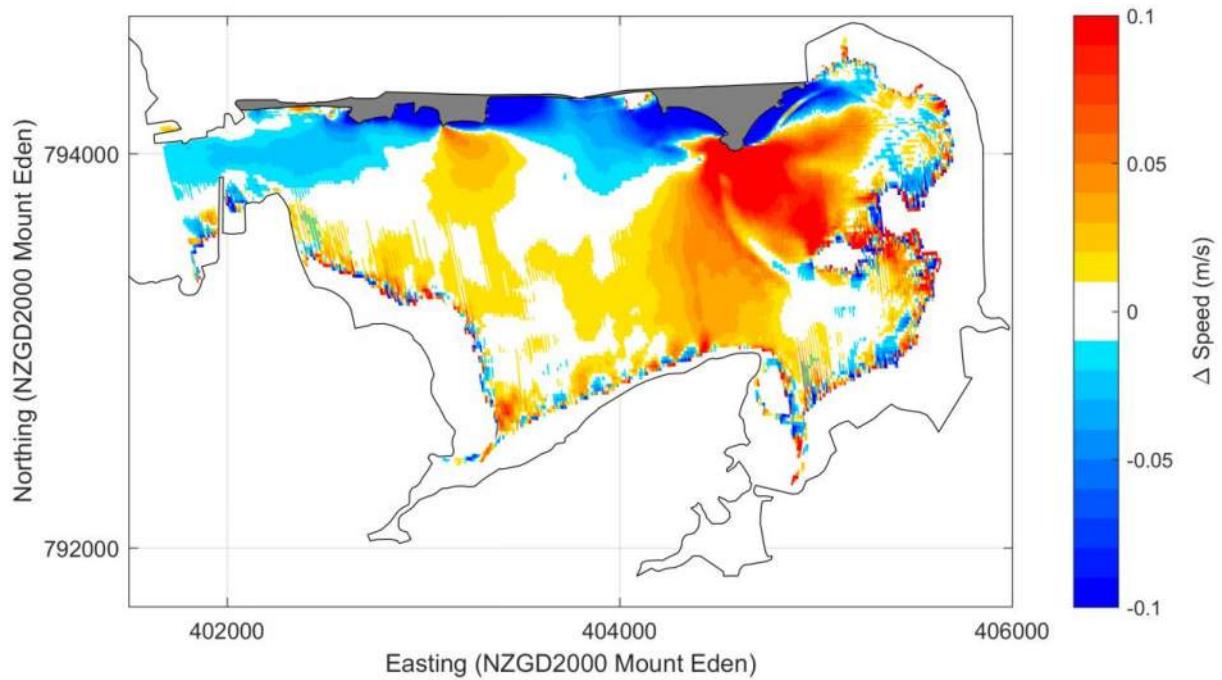
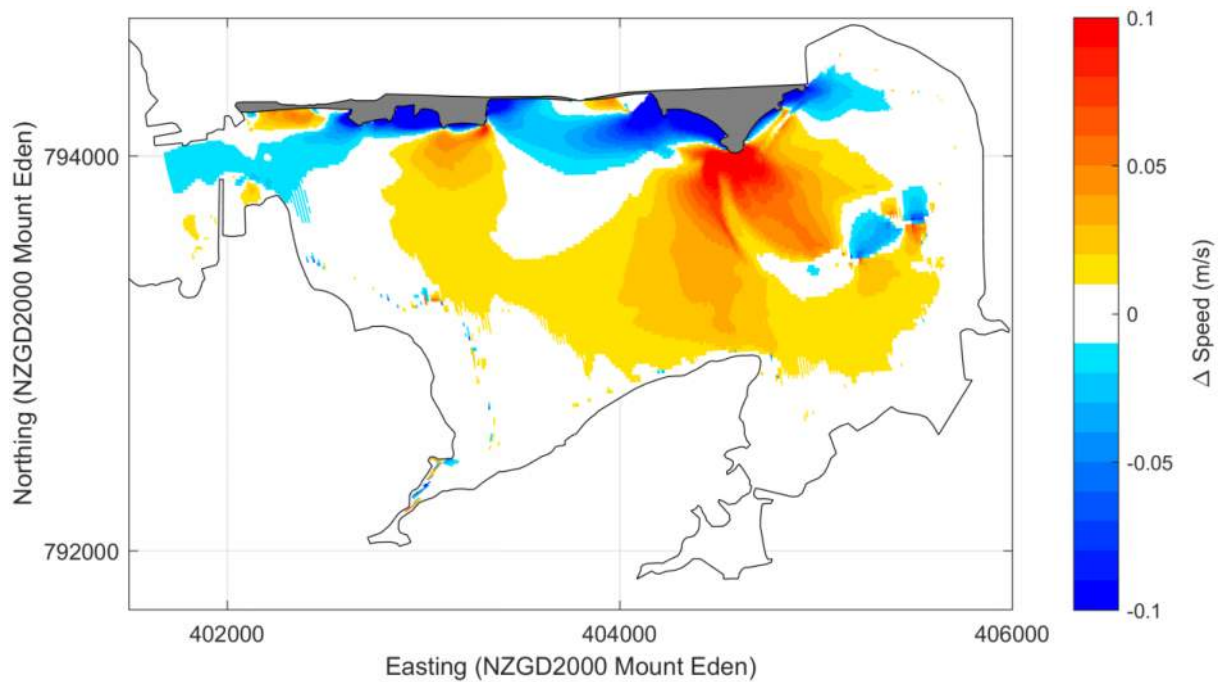


Figure D-6: Predicted changes in wind climate composite  $ASR_{WDCLI}$  (mm/yr) caused by coastal reclamation design V02 in Mangere Inlet using equation (3). Differences in modelled pre- and post-reclamation  $ASR_{WDCLI} \pm 0.5$  mm/yr are blanked out.

## Reclamation Version V03

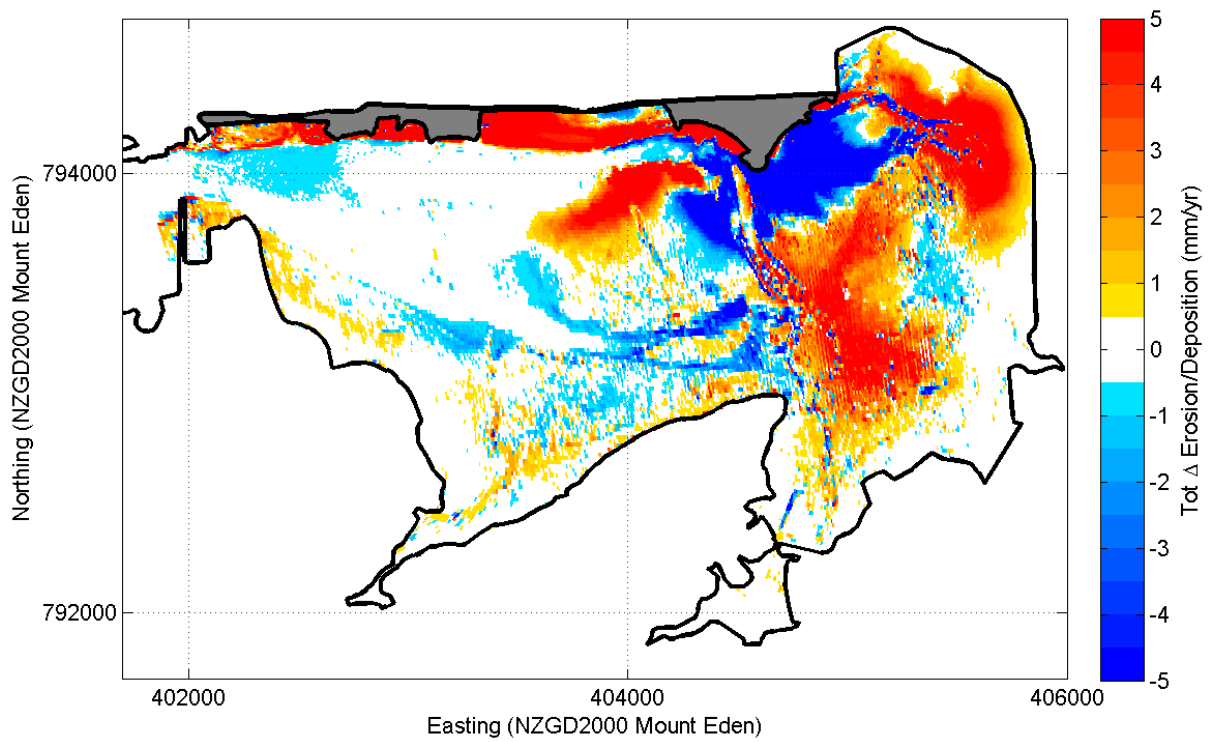


**Figure D-7:** Difference in peak flood current speed due to coastal reclamation design V03 in Mangere Inlet during a mean tide.



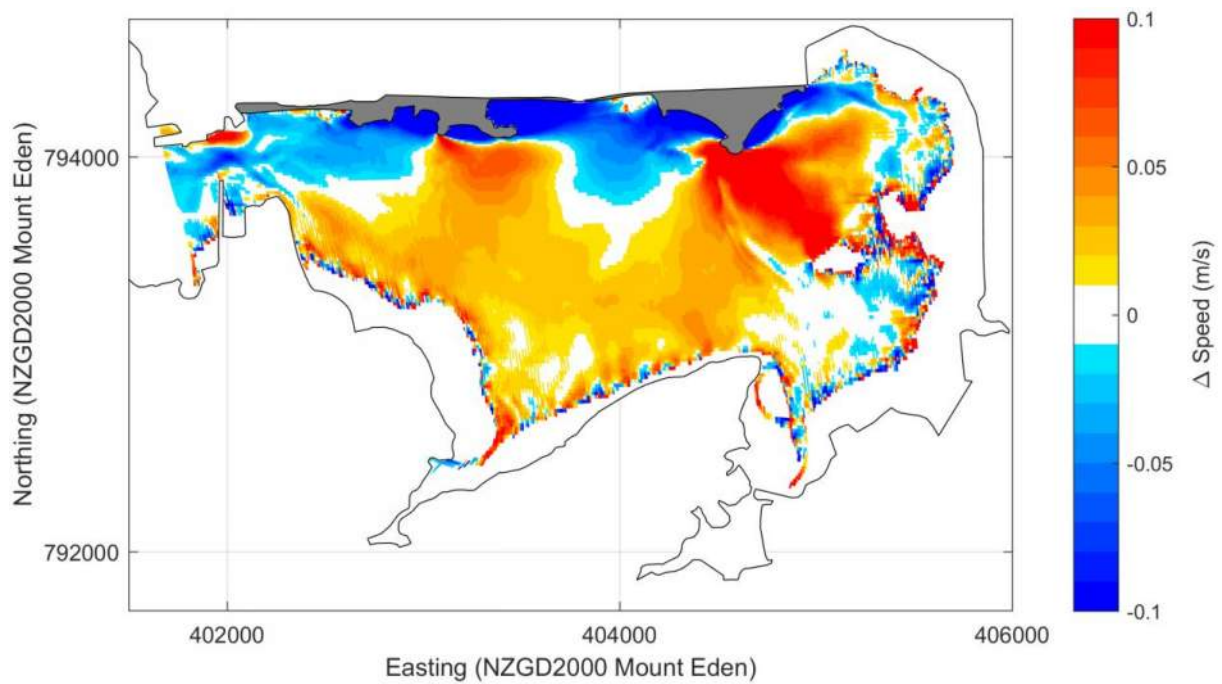
**Figure D-8:** Difference in peak ebb current speed due to coastal reclamation design V03 in Mangere Inlet during a mean tide.



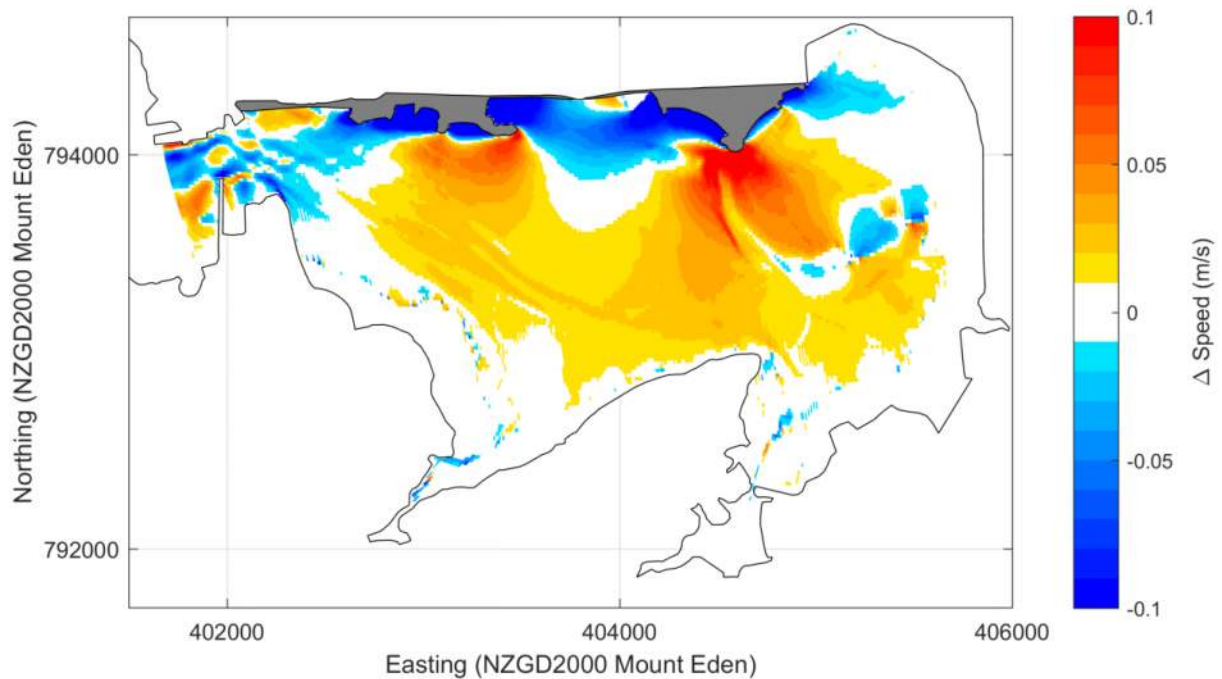


**Figure D-9:** Predicted changes in wind climate composite  $ASR_{WDCLI}$  (mm/yr) caused by coastal reclamation design V03 in Mangere Inlet using equation (3). Differences in modelled pre- and post-reclamation  $ASR_{WDCLI} \pm 0.5$  mm/yr are blanked out.

## Reclamation Version V04

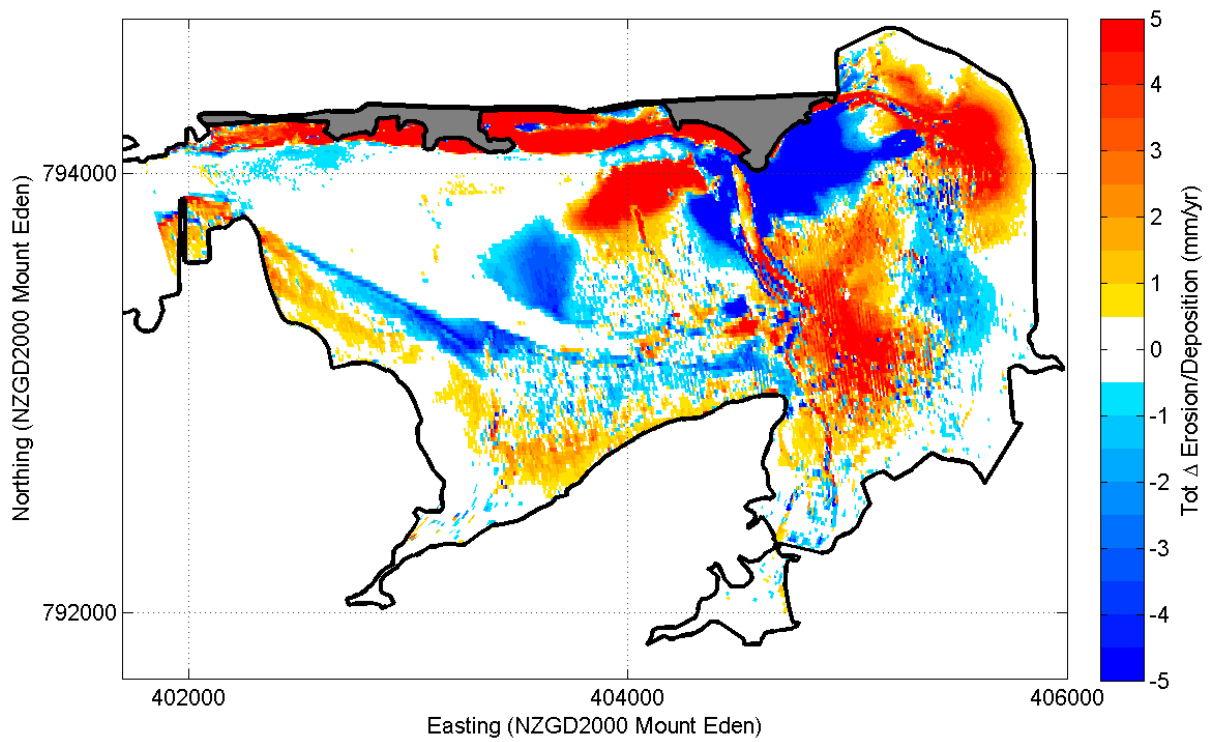


**Figure D-10: Difference in peak flood current speed due to coastal reclamation design V04 in Mangere Inlet during a mean tide.**



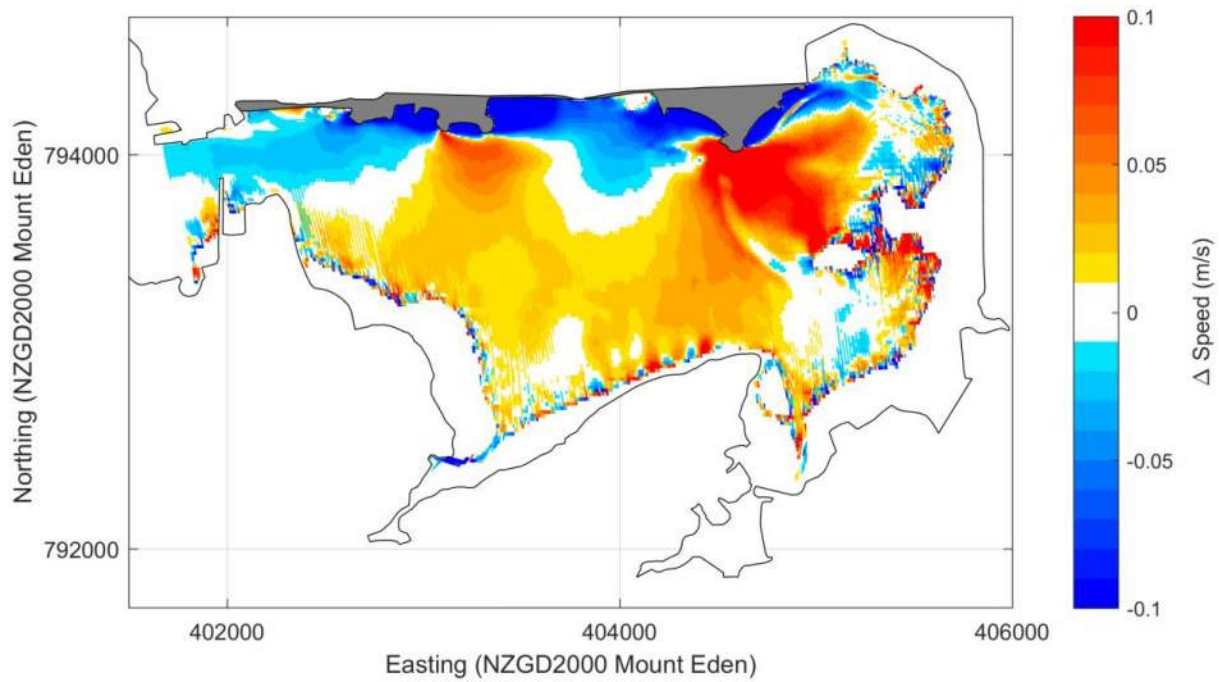
**Figure D-11: Difference in peak ebb current speed due to coastal reclamation design V04 in Mangere Inlet during a mean tide.**



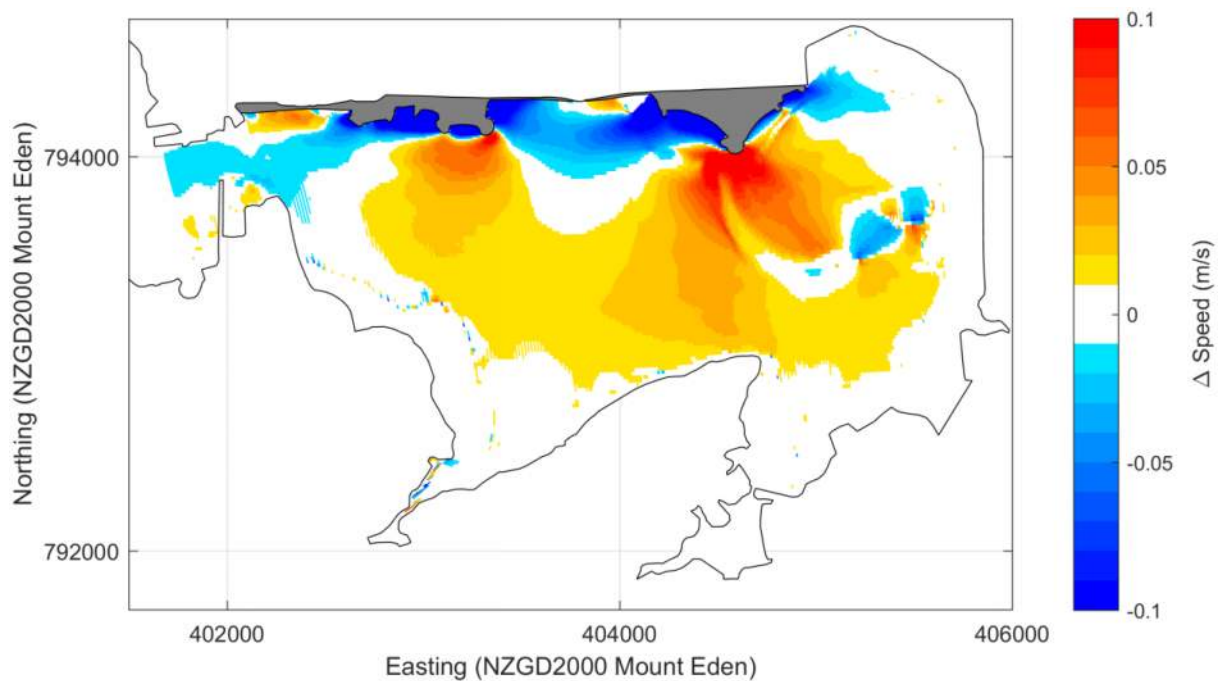


**Figure D-12:** Predicted changes in wind climate composite  $ASR_{WDCLI}$  (mm/yr) caused by coastal reclamation design V04 in Mangere Inlet using equation (3). Differences in modelled pre- and post-reclamation  $ASR_{WDCLI} \pm 0.5$  mm/yr are blanked out.

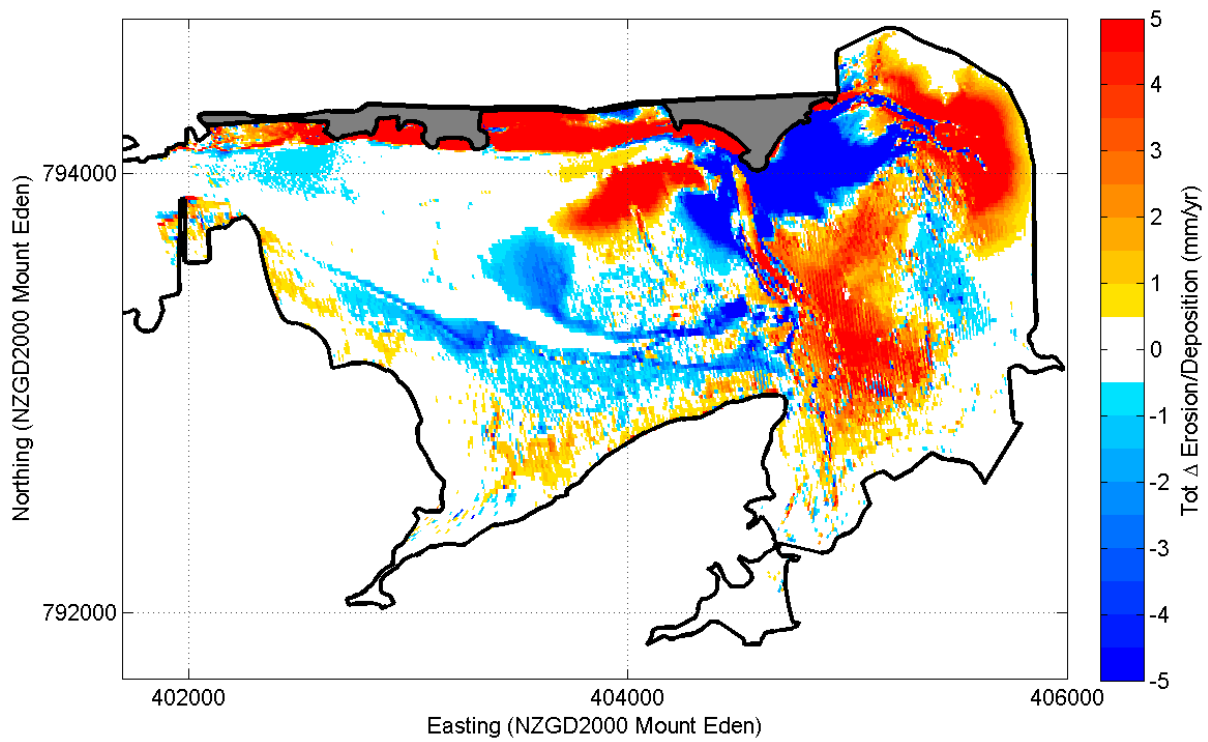
## Reclamation Version V05



**Figure D-13: Difference in peak flood current speed due to coastal reclamation design V05 in Mangere Inlet during a mean tide.**



**Figure D-14: Difference in peak ebb current speed due to coastal reclamation design V05 in Mangere Inlet during a mean tide.**



**Figure D-15: Predicted changes in wind climate composite  $ASR_{WDCLI}$  (mm/yr) caused by coastal reclamation design V05 in Mangere Inlet using equation (3). Differences in modelled pre- and post-reclamation  $ASR_{WDCLI} \pm 0.5$  mm/yr are blanked out.**

## Appendix E Sediment settling velocity experiments



21 Pitt Street <Originator Address Line 2>  
PO Box 6345, Auckland 1141, New Zealand  
T: +64 9 300 9000 // F: +64 9 300 9300  
E: [info@beca.com](mailto:info@beca.com) // [www.beca.com](http://www.beca.com)

Transport Infrastructure - BL  
21 Pitt Street  
PO Box 6345  
Auckland 1141  
New Zealand

2 June 2016

**Attention: Stephen Priestley**

**Report: 16:040**

Dear Stephen,

### **Results of Manukau Harbour Marine Sediment Settling Velocity Testing - May 2016**

Beca Ltd trading as Envirolab was commissioned by the NZ Transport Agency as part of the East West Link Alliance to undertake determination of particle settling velocity on marine sediment samples using a Bottom Withdrawal Tube Method. The testing was undertaken on Marine sediment samples from the Manukau Harbour, this report presents the testing results.

This report relates only to the samples as tested, sampling was undertaken by others.

#### **Bottom Withdrawal Tube Method Summary**

*Detailed Test Procedure for Bottom Withdrawal Tube; Measurement and Analysis of Sediment Loads in Streams, Report 7; St Paul U.S. Engineer District Sub-Office Hydraulic Laboratory, University of Iowa; 1943.*

The device is a glass tube of 100cm in length, graduated with volumetric scale and a quick-acting tap outlet at the bottom of the tube. A sample is uniformly dispersed in the tube. The tube is then placed in an upright position and a series of samples of known volumes are drawn from the bottom at known time intervals (increasingly spaced). The sediment weight of each sample fraction is determined. Based on Stokes Principle that a particle of 1mm will fall 90cm in six seconds and a 62 micron particle will take 5 minutes to fall the same height, the particle size distribution can be calculated with the aid of an Oden curve.

As consecutive samples are taken, the fall height reduces and allows for the calculated sediment load to be extrapolated for longer sampling periods. Hence, a sediment load of fine silt and clay material, which may normally take over 24 hours to settle, can be reduced to within a 2 hour sampling programme due to the falling head height. This method can be applied to lower sediment loads (~10g/L) unlike the particle size determination method using an hydrometer, which requires a high sediment load (~300g/L)

#### **Deviation from Method**

The method was investigated by the St Paul U.S. Engineer District Sub-Office Hydraulic Laboratory for the use of sediment loads in streams. We have undertaken the testing on solid sediment material suspended in seawater.

Our Ref: 4216210  
NZ1-12803139-4 0.4

### Sample Description

Detailed in Table 1 are the samples presented for testing.

**Table 1 – Sample Details Summary**

Envirolab Reference	Description (as given)					
	Bed Depth (m)	Vibrocore	Top	Bottom	Sample Number	Material
16:040-11					EWL S04	Sea floor characteristic
16:040-14					EWL S07	Sea floor characteristic
16:040-3					EWL S53	Sea floor characteristic

### Sample Preparation

Materials were received as moist sediments. A sub-sample of approximately 30 – 40 g was taken and mixed with seawater in a container. The containers of mixed material were placed on a rolling table for a number of hours to aid the breakup of the aggregate to allow dispersal of the material. The resulting slurry was passed through a 2mm sieve to remove large material (e.g. shell fragments) and transferred into the testing tube with the aid of additional seawater until the tube was filled to a fixed mark (0.67 litres).

The tube was then mixed as per the procedure, by repeatedly inverting until the material was dispersed uniformly, at which point the tube was placed upright in a stand and a timer started. At each specific time interval the bottom fraction (of 55mL) was sampled from the tube.

The timed fractions were taken at 10 & 30 seconds, 1, 3, 7, 10, 16, 40, 80, 100, 120 minutes.

Each sampled fraction was tested for total suspended solid content and calculated to represent the % suspended, depth factor and time to settle 100cm. Data was plotted to form the Oden curve from which a tangent line is drawn to the Y-intercept to determine the % solid in suspension. From this, the particle distribution can be determined as it relates to the settling velocity of particles.

## Results

The results of the settling velocity, Oden curve and particle distributions are detailed in **Tables 2 to 4** and **Plots 2 to 4**.

The Oden curve is presented with two time scales, one showing 24 hours (1,440 minutes), the other 2 hours (120 minutes).

Classification of the fraction size is based on the Wentworth Scale, 1922 which is included in **Appendix A**.

**Table 2: Sample EWL-S04**

Lab Ref	Bed Depth (m)	Vibrocore	Top	Bottom	Sample Number	Material
16:040-11					S04	Sea floor characteristic
Time [min, decimal]	Fall Height [cm]	Cumulative Suspended Sediment (Measured) [mg/L]	Depth Factor to 100cm	Sediment in Suspension 100cm tube (Corrected) [mg/L]	% Sediment in Suspension	Time to Settle 100cm [minutes]
0	110	500.8	0.9	455.3	100.00	0.0
0.167	100	460.1	1.0	460.1	91.86	0.2
0.5	90	423.5	1.1	470.6	84.56	0.6
1	80	357.6	1.3	447.0	71.39	1.3
3	70	298.3	1.4	426.1	59.55	4.3
7	60	228.0	1.7	380.0	45.53	11.7
10	50	159.0	2.0	318.0	31.74	20.0
16	40	111.9	2.5	279.8	22.35	40.0
40	30	69.2	3.3	230.7	13.82	133
80	20	21.8	5.0	109.1	4.36	400
100	10	0.0	10	0.3	0.01	1,000
120	1	0.0	100.0	0.7	0.00	12,000

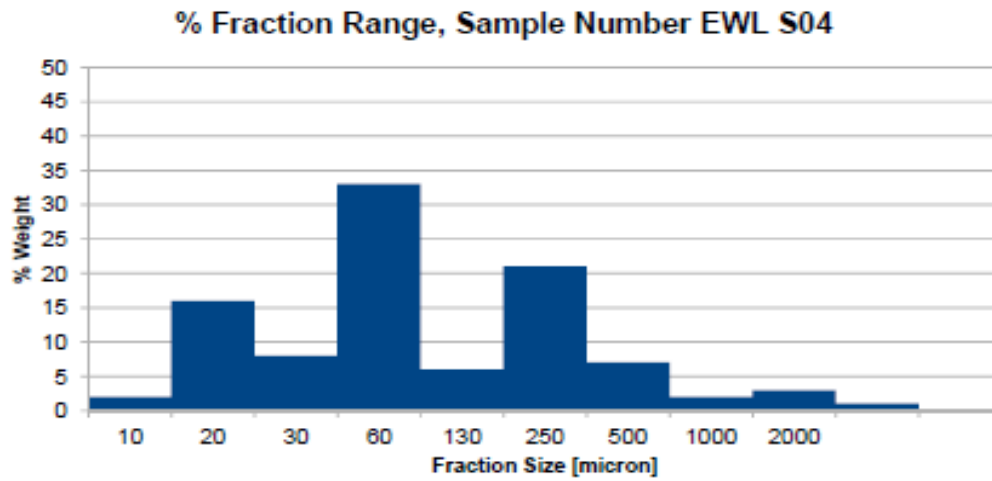
**Table 2b: Sample S04**

Particle Fraction [micron]	% in Fraction [weight]
2	2
4	16
8	8
16	33
31	6
62	21
125	7
250	2
500	3
1,000	1
2,000	0

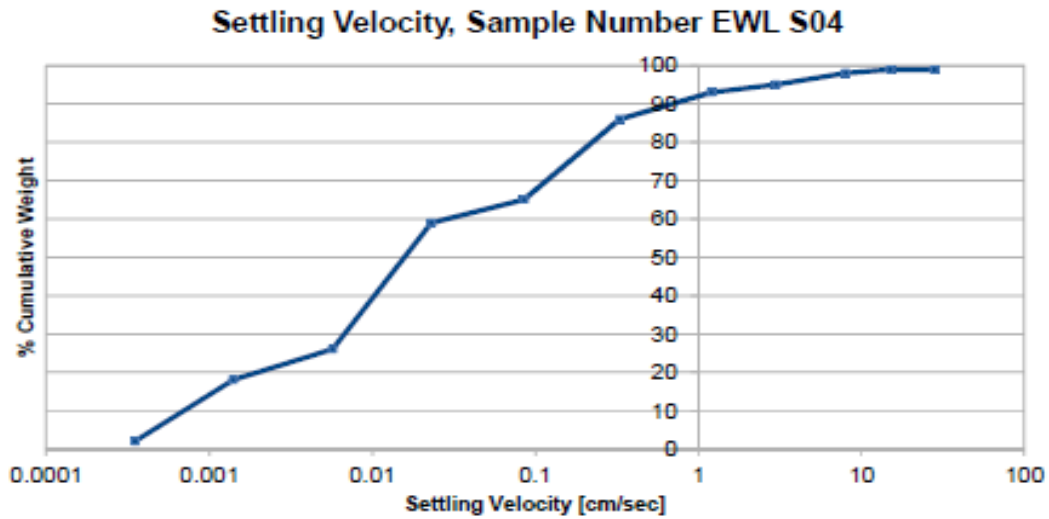
**Table 2c: Sample S04**

Settling Velocity [cm/sec]	% Cumulative Weight
0.00035	0.8
0.0014	1.3
0.0057	1.8
0.023	15.3
0.085	39.8
0.329	68.8
1.2	95.3
3	97.3
8	98.8
15	99.8
28	100.0

Plot 2a: Sample EWL S04: % Fraction Range

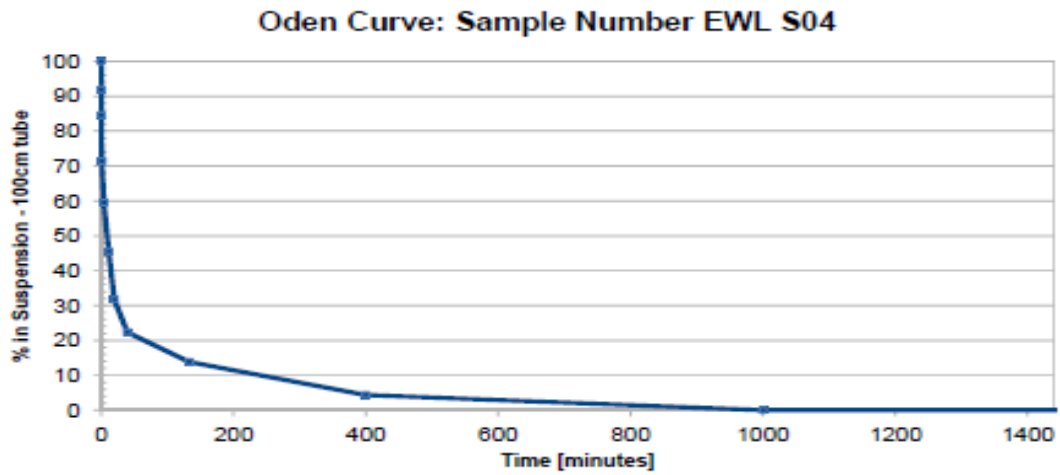


Plot 2b: Sample EWL S04: Settling Velocity

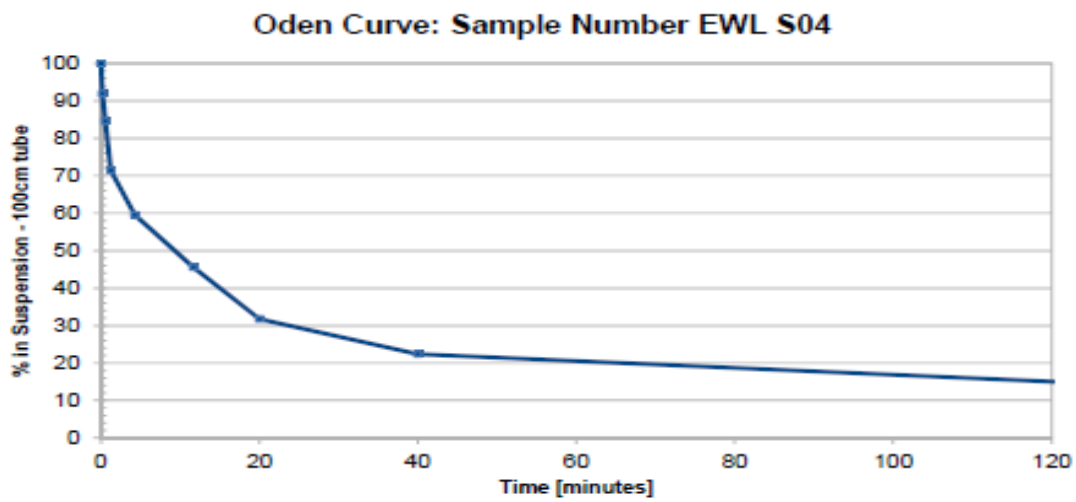




Plot 2c: Sample EWL S04: Oden Curve



Plot 2d: Sample EWL S04b: Oden Curve



**Table 3: Sample S07**

Lab Ref	Bed Depth (m)	Vibrocore	Top	Bottom	Sample Number	Material
16:040-14					EWL S07	Sea floor characteristic
Time [min, decimal]	Fall Height [cm]	Cumulative Suspended Sediment (Measured) [mg/L]	Depth Factor to 100cm	Sediment in Suspension 100cm tube (Corrected) [mg/L]	% Sediment in Suspension	Time to Settle 100cm [minutes]
0	110	675.2	0.9	613.8	100.00	0
0.167	100	621.0	1.0	621.0	91.97	0.2
0.5	90	533.5	1.1	592.7	79.01	0.6
1	80	452.1	1.3	565.1	66.95	1.3
3	70	380.7	1.4	543.8	56.38	4.3
7	60	312.3	1.7	520.5	46.26	11.7
10	50	256.6	2.0	513.1	38.00	20.0
16	40	213.1	2.5	532.8	31.57	40.0
40	30	169.8	3.3	565.8	25.14	133.3
80	20	122.4	5.0	611.8	18.12	400
100	10	7.1	10.0	71.4	1.06	1,000
120	1	0.0	100.0	1.2	0.00	12,000

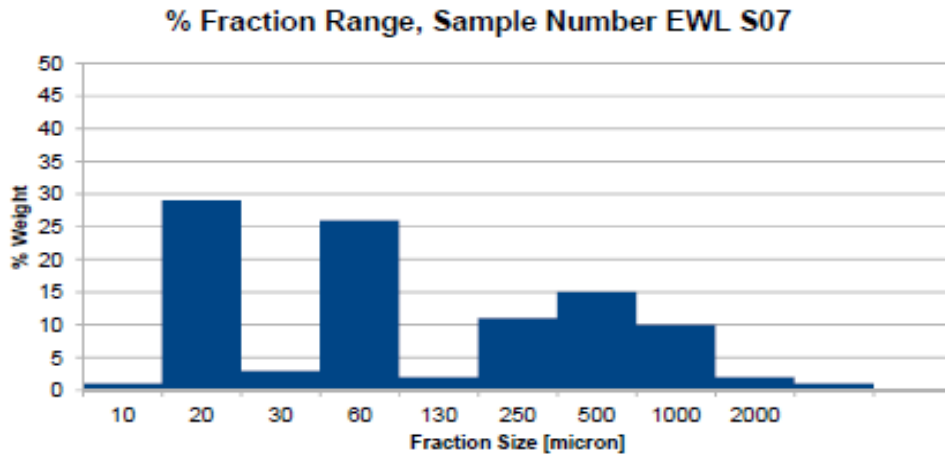
**Table 3b: Sample S07**

<b>Particle Fraction [micron]</b>	<b>% in Fraction [weight]</b>
2	1
4	29
8	3
16	26
31	2
62	11
125	15
250	10
500	2
1,000	1
2,000	0

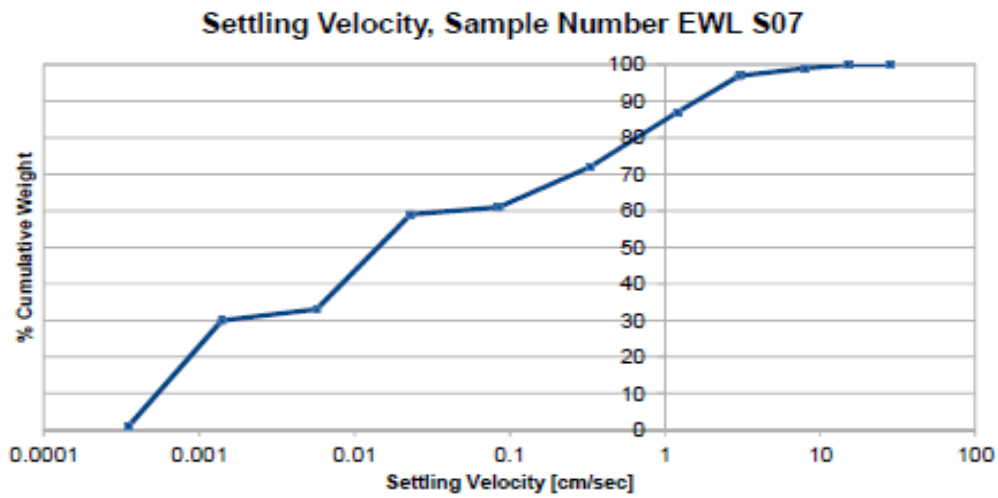
**Table 3c: Sample S07**

<b>Settling Velocity [cm/sec]</b>	<b>% Cumulative Weight</b>
0.00035	1.0
0.0014	30.0
0.0057	33.0
0.023	59.0
0.085	61.0
0.329	72.0
1.2	87.0
3	97.0
8	99.0
15	100.0
28	100.0

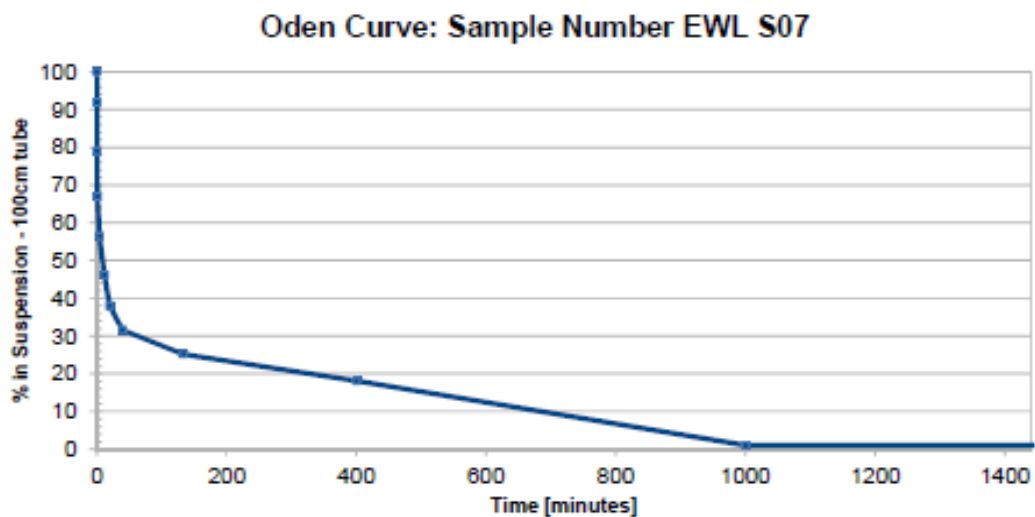
Plot 3a: Sample EWL S07: % Fraction Range



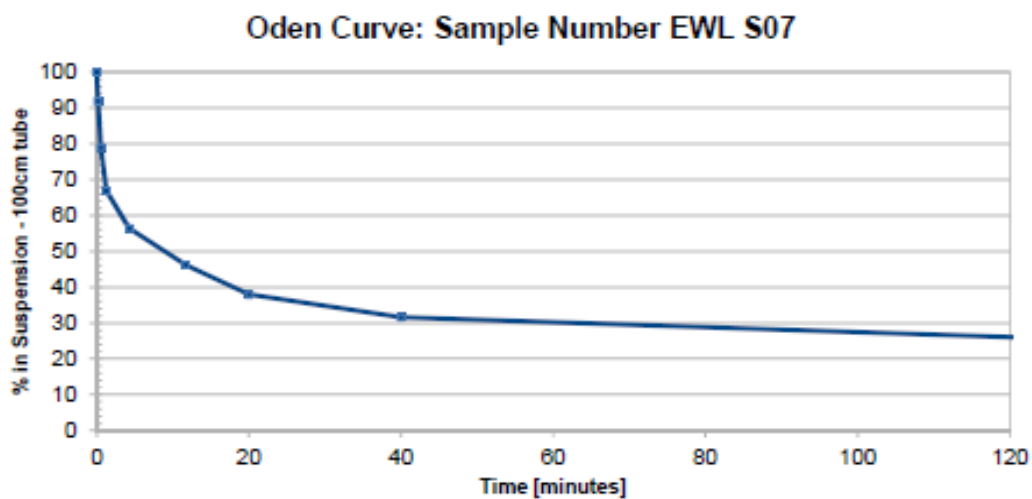
Plot 3b: Sample EWL S07: Settling Velocity



Plot 3c: Sample EWL S07: Oden Curve



Plot 3a: Sample EWL S07: Oden Curve



**Table 4: Sample S53**

Lab Ref	Bed Depth (m)	Vibrocore	Top	Bottom	Sample Number	Material
16:040-3					EWL S53	Sea floor characteristic
Time [min, decimal]	Fall Height [cm]	Cumulative Suspended Sediment (Measured) [mg/L]	Depth Factor to 100cm	Sediment in Suspension 100cm tube (Corrected) [mg/L]	% Sediment in Suspension	Time to Settle 100cm [minutes]
0	110	648.2	0.9	589.3	100.00	0
0.167	100	597.0	1.0	597.0	92.10	0.2
0.5	90	534.6	1.1	504.0	82.48	0.6
1	80	466.3	1.3	582.9	71.94	1.3
3	70	393.9	1.4	562.8	60.78	4.3
7	60	279.8	1.7	466.4	43.17	11.7
10	50	158.2	2.0	316.4	24.41	20.0
16	40	97.9	2.5	244.7	15.10	40.0
40	30	44.4	3.3	148.0	6.85	133.3
80	20	1.2	5.0	5.8	0.18	400
100	10	0.0	10.0	0.3	0.00	1,000
120	1	0.0	100.0	1.8	0.00	12,000

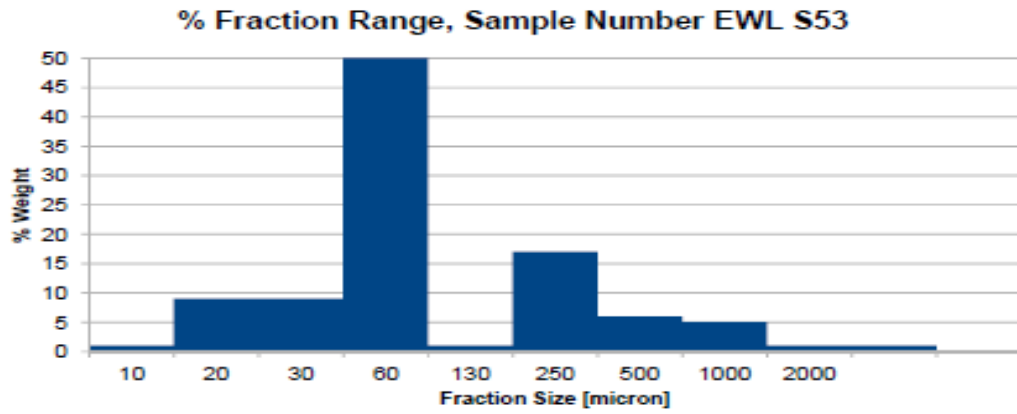
**Table 4b: Sample S53**

<b>Particle Fraction [micron]</b>	<b>% in Fraction [weight]</b>
2	1
4	9
8	9
16	50
31	1
62	17
125	6
250	5
500	1
1,000	1
2,000	0

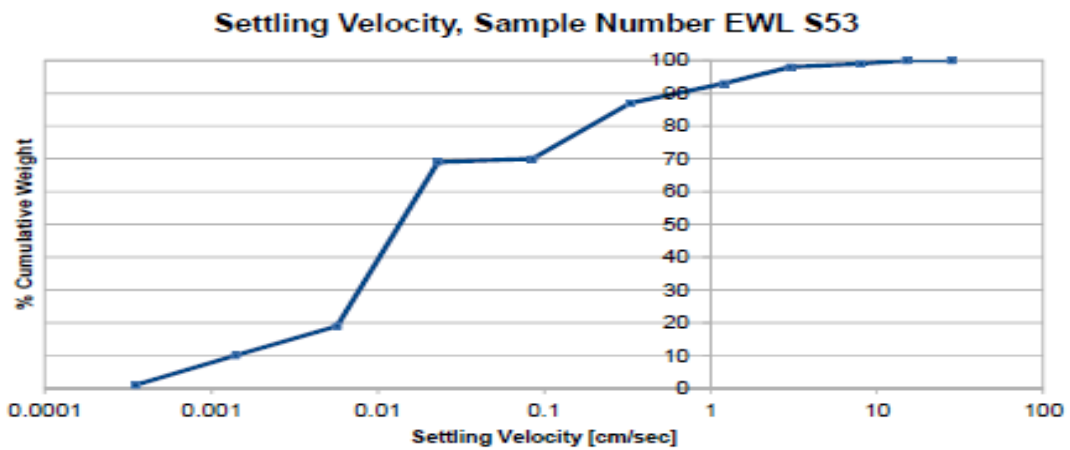
**Table 4c: Sample S53**

<b>Settling Velocity [cm/sec]</b>	<b>% Cumulative Weight</b>
0.00035	1.0
0.0014	10.0
0.0057	19.0
0.023	69.0
0.085	70.0
0.329	87.0
1.2	93.0
3	98.0
8	99.0
15	100.0
28	100.0

Plot 4a: Sample EWL S53: % Fraction Range



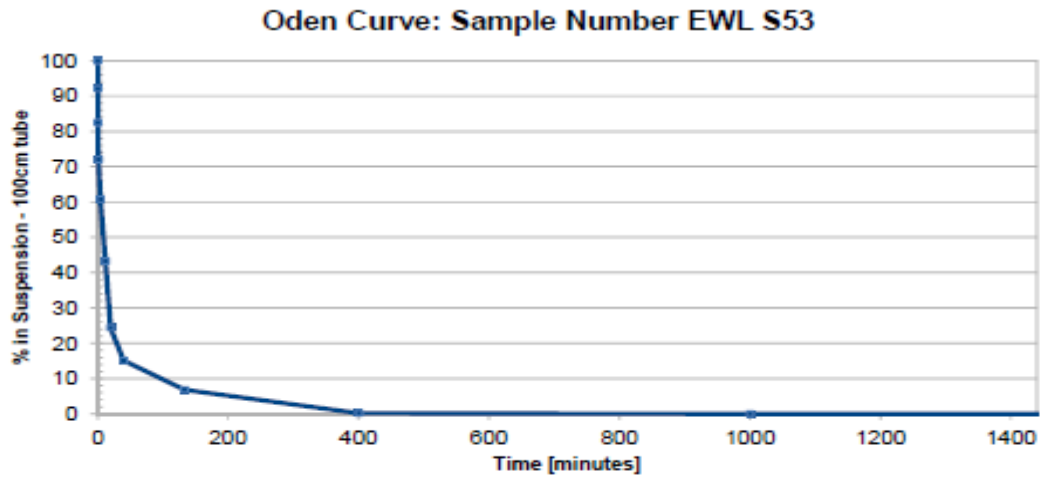
Plot 4b: Sample EWL S53: Settling Velocity



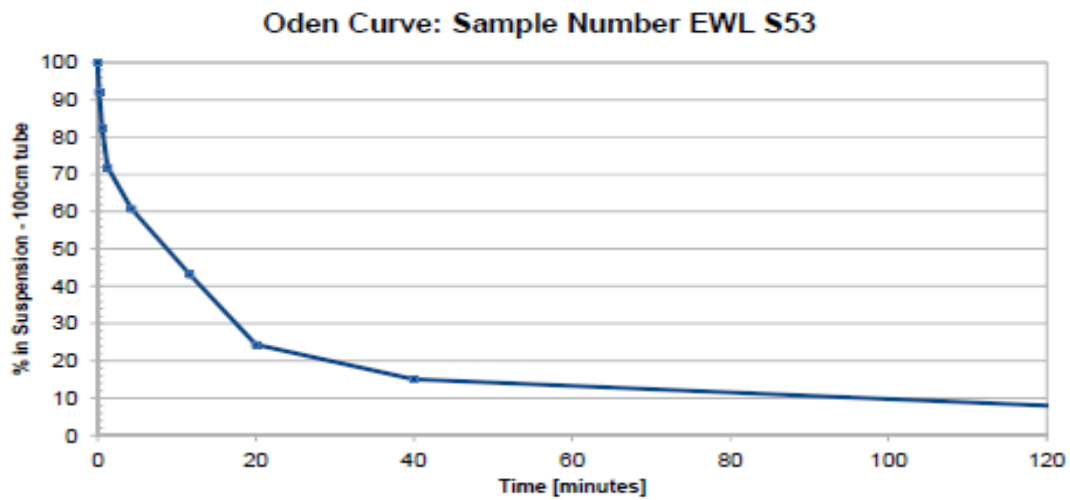
Our Ref: 4216210  
NZ1-12603159-4 0.4



Plot 4c: Sample S53: Oden Curve



Plot 4d: Sample S53: Oden Curve



*This report may not be reproduced, except in full, without the consent of the signatory.*

Yours sincerely,  
**David Steiner**  
Laboratory Assistant

*P.P.*

on behalf of  
**Beca Ltd**  
Direct Dial: +64-9-308 4551  
Email: [david.steiner@beca.com](mailto:david.steiner@beca.com)

Appendix A: Wentworth Scale, 1922

Φ	Φ-φ - mm CONVERSION φ = 30φ <sub>2</sub> (φ in mm) φ <sub>2</sub> in = 2.00φ <sub>2</sub> mm		Fraction mm (round inches)	SIZE TERMS (modified from Wentworth, 1922)	SIEVE SIZES		Intermediate diameters of natural grains equivalent to sieve size	Number of grains per mg		Setting Velocity (Quartz, 20°C)		Threshold Velocity for traction cm/sec	
	ASTM No. (U.S. Standard)	Tyler Mesh No.			Quartz spheres	Natural sand		Spheres (100μ, 10 <sup>3</sup> ) cm/sec	Quartz (100μ)	ft/sec, 100	ft/sec, 100 in flow of 1m depth		
-8	200	256	10.1"	BOULDERS									
-7	100	128	5.04"	COBBLES									
-6	50	64.0	2.52"	PEBBLES	2 1/2	2"						200	
-5	40	50.0	1.26"		very coarse	2 1/2	2"					100	
-4	30	39.1	1.56"	PEBBLES	1 1/2	1 1/2"						100	
-3	20	25.0	0.63"		coarse	1 1/2	1 1/2"					50	
-2	10	11.3	0.32"	PEBBLES	3/4	3/4"						50	
-1	5	6.73	0.15"		medium	3/4	3/4"					30	
0	1	2.00	0.08"	SAND	5	5						20	
1	.5	1.00	0.04"		fine	5	5					10	
2	.25	.500	0.02"	SAND	10	10						5	
3	.125	.250	0.01"		very coarse	10	10					5	
4	.0625	.125	0.005"	SAND	20	20						5	
5	.03125	.0625	0.0025"		coarse	20	20					5	
6	.015625	.03125	0.00125"	SILT	40	40						5	
7	.0078125	.015625	0.000625"		medium	40	40					5	
8	.00390625	.0078125	0.0003125"	SILT	80	80						5	
9	.001953125	.00390625	0.00015625"		fine	80	80					5	
10	.0009765625	.001953125	0.000078125"	CLAY	150	150						5	
					very fine	150	150					5	

Our Ref. 4218210  
NZ1-12803139-4 0.4

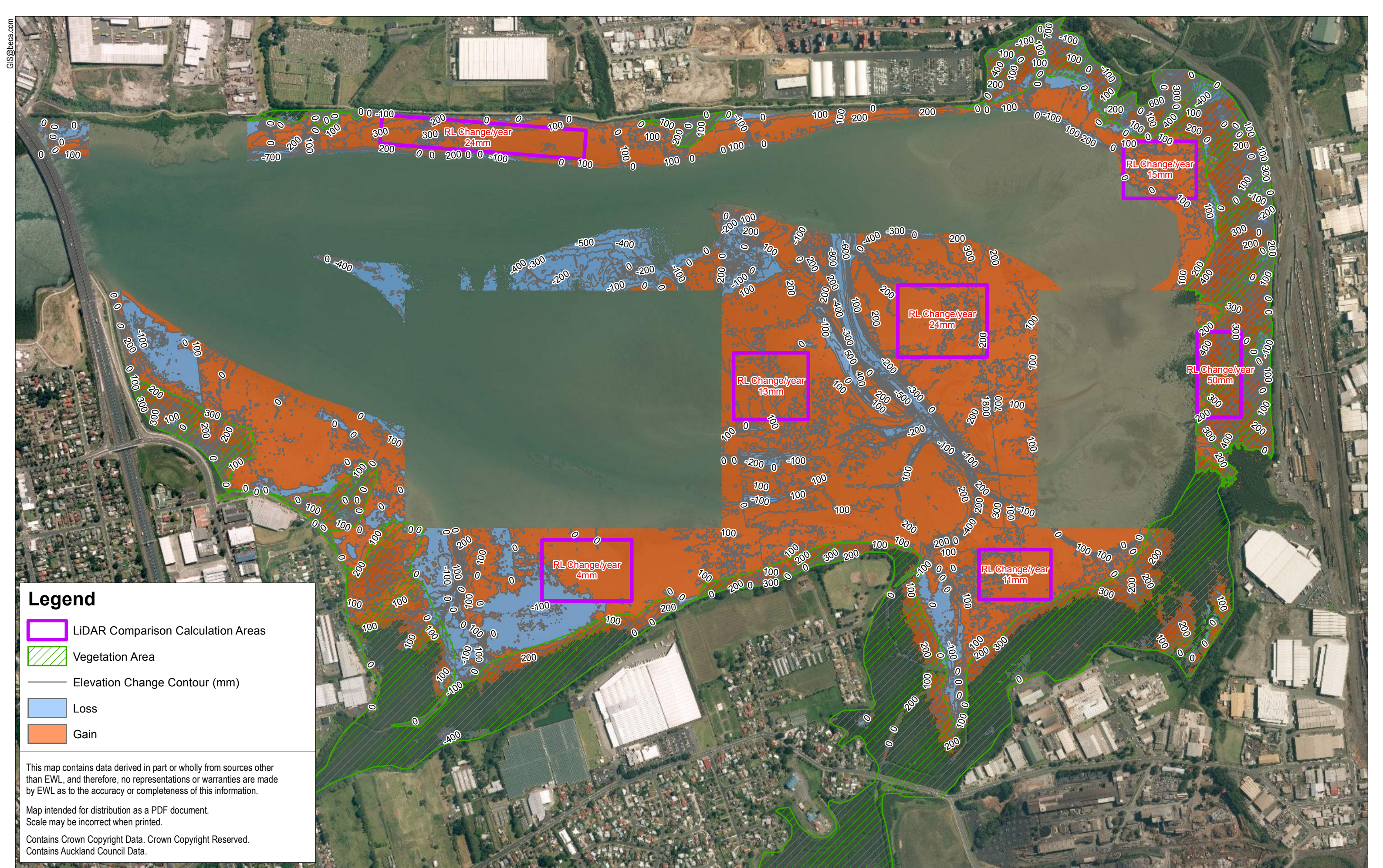
**Appendix A: Values used from the Wentworth Scale**

Fraction	Size Term	Size [mm] (upper boundary)	Size [micron] (upper boundary)	Settling Velocity [cm/sec]	Time to Fall 100cm [minutes]
Sand	Very Coarse	2	2000	28	0.06
	Coarse	1	1000	15	0.11
	Medium	0.5	500	8	0.21
	Fine	0.25	250	3	0.56
	Very Fine	0.125	125	1.2	1.39
Silt	Coarse	0.062	62	0.329	5.1
	Medium	0.031	31	0.085	19.6
	Fine	0.016	16	0.023	72
	Very Fine	0.008	8	0.0057	292
Clay	Clay	0.004	4	0.0014	1190
	Clay Mineral	0.002	2	0.00035	4762

Appendix D

**Sedimentation Rates based on LIDAR Data**





**Legend**

- LiDAR Comparison Calculation Areas
- Vegetation Area
- Elevation Change Contour (mm)
- Loss
- Gain

This map contains data derived in part or wholly from sources other than EWL, and therefore, no representations or warranties are made by EWL as to the accuracy or completeness of this information.

Map intended for distribution as a PDF document.  
Scale may be incorrect when printed.

Contains Crown Copyright Data. Crown Copyright Reserved.  
Contains Auckland Council Data.

A	Original Issue	AYF	BAP	SP	24/03/15
No	Revision	Drawn	Verified	Approved	Date

**DISCLAIMER**  
The information shown on this drawing is solely for the purpose of supporting application under the RMA for resource consents and/or designations. All information shown is subject to final design and review for compliance with any approved consents and/or designations. This Drawing must not be used for construction.



Drawn:	Draft Check:	Reviewed (Design Manager)	Approved (Alliance Manager)	Discipline: Title: Intertidal LiDAR Comparison (2006 & 2013)
Designed:	Design Check:			
Scale: 1:10,000		Original Size: A3	Contract No: PA4041	Drawing No: 7-CP-MAP-001 Rev: A



Appendix E

**Sediment Quality Assessment**

# 1. Sediment Quality Investigation Methodology

## 1.1 Rationale for Sediment Quality Investigation

For these reasons our assessment of contaminants in the marine environment focused on sediment and biota, both of which have potential to accumulate contaminants in the environment. This assessment was augmented with sampling the point sources of contamination (stormwater outfalls) and diffuse pollution sources (groundwater / leachate discharges). The findings of the stormwater and groundwater investigations are covered in Technical Report 12 Surface Water and Technical Report 13 Groundwater Assessment.

The hydrological model presented in Technical Report 13 Groundwater Assessment shows that the Mangere Inlet is the ultimate receiving environment for contamination in stormwater and groundwater derived from the terrestrial environment in Onehunga and Te Papapa.

The marine contamination assessments were focused on establishing the existing contaminant conditions in the receiving environment of Mangere inlet. As recalcitrant organic contaminants<sup>1</sup> have an affinity to the carbon fraction within the sediments, and inorganic contamination, such as metals, will tend to bind to the mineral, finer grained fraction in the sediment. This means that sediment contamination provides a reasonable indication of the level of contamination entering the receiving environment. Analysis of the depth profile of contamination in sediments can also reveal historical and spatial depositional patterns, that may be relate to the various point and diffuse sources around the Mangere Inlet.

Porewater analysis was undertaken to provide a good approximation of the bioavailability<sup>23</sup> of contaminants in sediment. It would also provide a reasonable approximation of the contaminants that may be released into the marine environment through construction activities within the CMA.

The overall approach to the marine contamination assessment was to assess concentrations of contaminants in sediment, porewater and biota, and where possible compare to other relevant data from Mangere inlet and wider Auckland region.

## 1.2 Rationale for Exclusion of Marine Water Quality

Contaminants derived from the land may be discharged to the coastal environment through stormwater pipes, basalt aquifer flow, streams or as shallow groundwater discharges through the foreshore seawalls - sorbed to suspended particles or dissolved in the water.

We considered that analysing the Mangere Inlet sea water had limited value based on the following rationale:

- Some of the contaminants of concern , such as heavy metals and PAHs have strong sorption to soil/sediment particles. Sorption of those contaminants in the matrix of the aquifers and on sediments in discharge zones limits groundwater discharges to the contaminants in the dissolved phase only

---

1 Persistent organic contaminants such as organochlorine pesticides (including DDT family) and polycyclic aromatic hydrocarbons.

2 Forbes, T.L., Forbes, V.E., Giessing, A., Hansen, R. and Kure, L.K., 1998. Relative role of porewater versus ingested sediment in bioavailability of organic contaminants in marine sediments. *Environmental Toxicology and Chemistry*, 17(12), pp.2453-2462.

3 Chapman, P.M., Wang, F., Germano, J.D. and Batley, G., 2002. Porewater testing and analysis: the good, the bad, and the ugly. *Marine Pollution Bulletin*, 44(5), pp.359-366.



- Stormwater discharges will include both dissolved contaminants and sorbed contaminants on suspended solid particles
- The suspended solids with sorbed phase contaminants in discharges (stormwater and groundwater) will tend to flocculate at the saline interface and fall out of suspension and contribute to the marine sediment
- The dissolved phase contaminants in discharges (stormwater and groundwater) will also react to the changed solubility conditions of the saline water. Metals in particular will form low solubility metallic chlorides and sulphides
- The limited solubility of the metals in salt water and the flocculation of suspended solids at the saline interface result in a profile of marine contaminants that will predominate the solid phase rather than dissolved phase (i.e. the water column). Organic contaminants will likewise tend to sorb strongly to the organic fraction of suspended particles and sediment
- There is a large volume of receiving water in the Mangere Inlet with associated dilution factors for contaminants
- The large tidal prism provides tidal cycle flushing. Tidal flushing makes it difficult to determine sources of contamination, as contamination may originate from other areas in the Mangere Inlet and the wider Manukau harbour.

Auckland Council gives a similar view in their 2013 Marine Water Quality Annual Report<sup>4</sup> “A *direct measurement of chemical contaminants in water is unreliable because concentrations are commonly below analytical detection limits, and they vary widely due to water movement and the patchy nature of inputs.*”

### 1.3 Sediment Investigation Methodology

The sediment quality investigations included:

- Intertidal sediments were collected using a 1 m split spoon push tube, with core catcher. Cores were photographed where notable features were observed, and sediment composition and potential presence of contamination (e.g. anoxic layers) recorded. A total of 16 intertidal locations were sampled using the push tube. Sediment samples were collected at regular intervals from the push tube including near surface, 0.3 m, 0.5 m, and 0.7/0.8 m depth.
- Intertidal sediment samples were collected along transects beyond the stormwater outfalls along the Onehunga foreshore intertidal mud flats (Figure x). The purpose was to assess potential contaminant concentration gradients out from the stormwater outfalls. The locations were also aligned with the terrestrial borehole transects to allow continuity of assessment between the terrestrial and marine environments.
- Vibracoring was also undertaken for subtidal areas from a boat at selected locations around Mangere inlet including:
  - Potential dredging zone (Sector 7)
  - Background sediment sampling locations including:
    - Beneath the Manukau Harbour Crossing and the old Mangere Bridge;
    - Immediately east of the proposed dredging location; and
    - Eastern and southern intertidal areas of Mangere inlet
- An additional three sampling locations along the Onehunga foreshore intertidal area to allow for depth delineation of contaminant concentrations, and to augment the push tube sediment sampling to achieve greater depth
- The vibracoring was progressed to a maximum depth of 2.5 m below the sea bed. The effective recovered core was generally 2.2 - 2.3 m in length
- Sediment samples collected from the vibracores generally comprised near surface (sea bed surface), and then approximate 0.3 m intervals to the termination depth
- Selected sediment samples were submitted for laboratory analyses:

---

<sup>4</sup> Auckland Council 2014: Marine Water Quality Annual Report 2013, Auckland Council Technical report, TR2014/030, 2014.

For the samples collected from the proposed dredging area, analysis was completed on two locations composites, comprising a total of five samples

- Near surface samples were generally analysed from every location as these are most relevant benthic infauna and intertidal fauna diversity assessments. Ecological assessments are covered in Technical Report 15 Ecological Impact Assessment.
- Selected samples from varying depth intervals were also analysed to provide some depth delineation across the sediment profile
- Every sample from the three vibrocore locations completed at the Onehunga foreshore were analysed to provide a more comprehensive depth delineation of contaminants in sediment.
- Sediment samples were analysed for:
  - Semi-volatile organic compounds (includes phthalates, and phenols)
  - Polycyclic aromatic hydrocarbons
  - Organochlorine pesticides
  - Broad suite of metals
  - Nutrients
  - Organic carbon
  - Petroleum hydrocarbons
  - Particle size distribution for selected samples
- A data review of existing sediment quality information from Mangare Inlet and the wider Auckland region was also undertaken. This review formed the basis for comparisons with the data collected during the sediment investigations for the EWL project.

Sediment sampling locations are included in the Marine Survey Location figure included in this appendix.

### 1.3.1 Porewater Contamination Investigation

The porewater sampling was undertaken using the following methodology:

- Bulk sediment samples were collected from six locations across the intertidal mudflats of the Onehunga foreshore using the split spoon push tube
- Bulk samples were sent to NIWA in Hamilton for porewater extraction. Sediment samples were placed in a centrifuge to extract porewater. Samples were then sent to RJ Hill Laboratories in Hamilton for chemical analytical testing
- Samples were analysed for metals, polycyclic aromatic hydrocarbons, nutrients, and organochlorine pesticides.
- Data was compiled and compared to ANZECC5 criteria for marine receiving water.

## 1.4 Application of Averaging

An industry accepted practice that is advocated by the MfE6 is to apply averaging across a data set to provide an overview of risk posed by contaminants, rather than focusing on discrete sample location. This is determined through the application of the 95% upper confidence limit (UCL) of the mean concentration. What this determines, with a 95% confidence, is that the mean concentration is likely to be below the calculated number. Strictly speaking, this is generally applied to a data set that is sampled on a systematic grid pattern. The sediment sampling programme, was not sampled using a grid pattern

---

5 Australian and New Zealand Environment and Conservation Council & Agriculture and Resource Management Council of Australia and New Zealand (ANZECC & ARMCANZ), 2000: *Australian and New Zealand Guidelines for Fresh and Marine Water Quality*. National Water Quality Management Strategy

6 Ministry for the Environment, Revised 2011: *Contaminated land management guidelines No. 5: Site investigation and analysis of soils*.

(with the exception of the proposed dredging area), however this approach is still considered applicable due to the relatively homogenous nature of the sediment contaminant distribution.

## 2. Investigation Results

### 2.1 Sediment Quality

The following section provides a summary of the sediment investigation results.

#### 2.1.1 Organics

The results of the sediment quality testing found that concentrations of organic contaminants<sup>7</sup> were generally not detected above laboratory trace analytical detection limits. Trace levels of DDT isomers were detected in one sample, however this is not considered significant due to it being an isolated concentration in the wider data set.

PAH concentrations in sediment were generally below laboratory analytical detection limits. Some discrete locations had low concentrations of PAHs, however these were compliant with ANZECC low criteria, meaning that concentrations are unlikely to pose a risk to environmental receptors. PAH concentrations in sediment were most elevated in the sediments collected from Maimi Stream, at concentrations in excess of the the ANZECC ISQG low indicating that some organisms may be adversely impacted by these concentrations.

Assessments undertaken by Wilcock and Northcott<sup>8</sup> in 1995 identified trace concentrations of PAHs in sediments in the Mangere inlet. Whilst their investigation was limited to two sampling locations, a clear depth profile of PAHs was observed. Their investigations identified that the higher concentrations of PAHs were present in the top 1.6 m of the sediment profile, with highest observed concentrations between 0.9 and 1.2 m depth within the sediment. The suite of PAH analytes used by Wilcock and Northcott (1995) differs to the PAH suite analysed by current methods, and as such direct comparisons are difficult, with the exception of some individual compounds. What is apparent however is that PAH concentrations measured by Wilcock and Northcott (1995) were greater than concentrations measured in the investigations for EWL.

#### 2.1.2 Nutrients

Concentrations of up to (39 mg/kg) ammoniacal nitrogen were measured in some sediment samples. No suitable environmental acceptance criteria are available for the evaluation of nutrients in sediment. Ammoniacal nitrogen bound within sediment influences bioavailability. Ammoniacal nitrogen in porewater (described below) is considered to provide a reasonable approximation of risk posed by ammoniacal nitrogen in sediments as ammonia is highly water soluble, and therefore any ammonia within sediment is likely to readily dissolve into porewater.

#### 2.1.3 Inorganic Contaminants

Figure 1 shows selected inorganic concentrations in sediments from AC studies and the EWL investigation. The mean total arsenic concentration observed during EWL investigations was elevated above the average concentration for both the Waitemata and Manukau harbours. The upper concentration range for arsenic in sediment ranged from 30 mg/kg - 69 mg/kg. Parent soil materials (both volcanic and non-volcanic soils) in the Auckland region have naturally occurring concentrations of between 0.4 - 12 mg/kg. This indicates that a portion of the arsenic measured in sediments is likely due to contamination from anthropogenic sources. Mean arsenic concentrations exceed the ANZECC

---

<sup>7</sup> Such as organochlorine pesticides, polycyclic aromatic hydrocarbons, petroleum hydrocarbons, and semi-volatile organic compounds.

<sup>8</sup> Wilcock, R.J. and Northcott, G.L., 1995. Polycyclic aromatic hydrocarbons in deep cores from Mangere Inlet, New Zealand. *New Zealand journal of marine and freshwater research*, 29(1), pp.107-116.

ISQG Low guideline criteria, indicating that arsenic in sediments may pose a risk to marine environmental receptors.

The mean total copper and lead concentrations in sediment were generally consistent with concentrations for the wider Manukau harbour, and consistent with naturally occurring concentrations in parent soil materials (both volcanic and non-volcanic).

The mean total zinc concentration measured in sediment was below the mean for the Waitemata and Manukau Harbours, and below the ANZECC ISQG Low guideline criteria, indicating that zinc in sediment does not pose a risk to marine receptors.

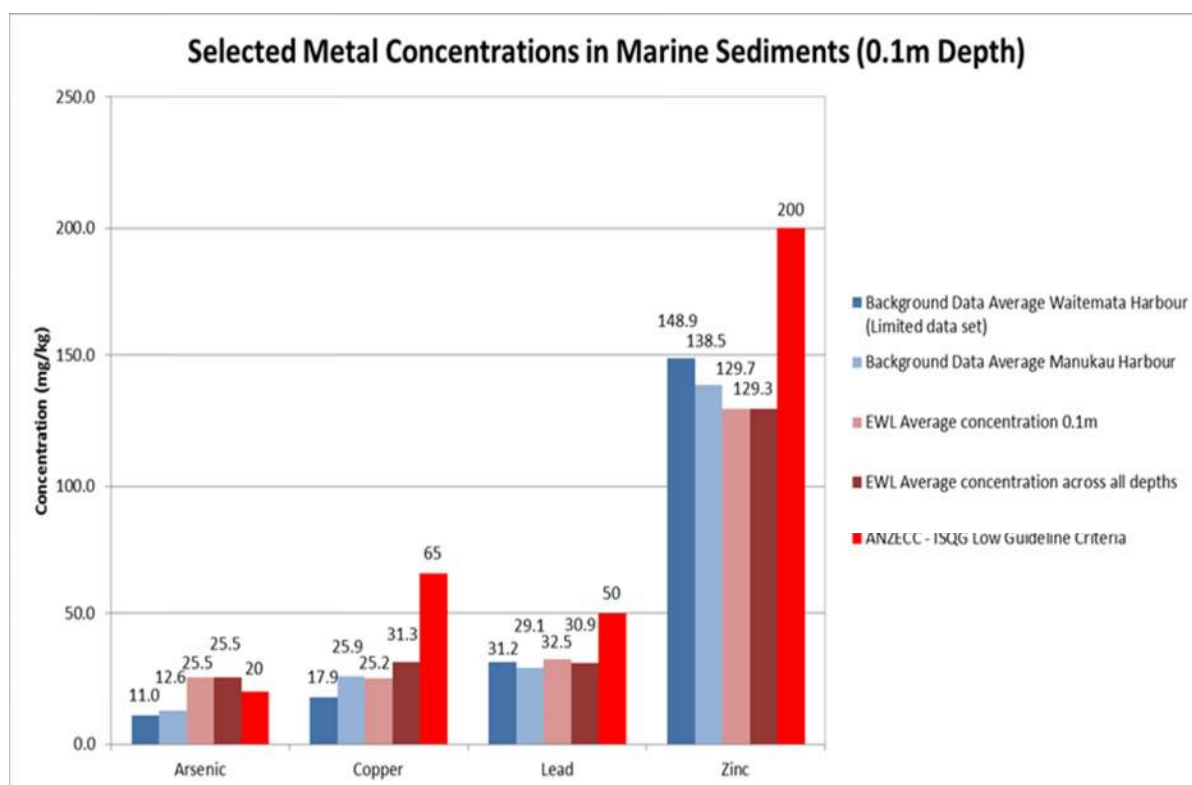


Figure 1 Concentrations of selected contaminants vs ANZECC sediment quality guidelines

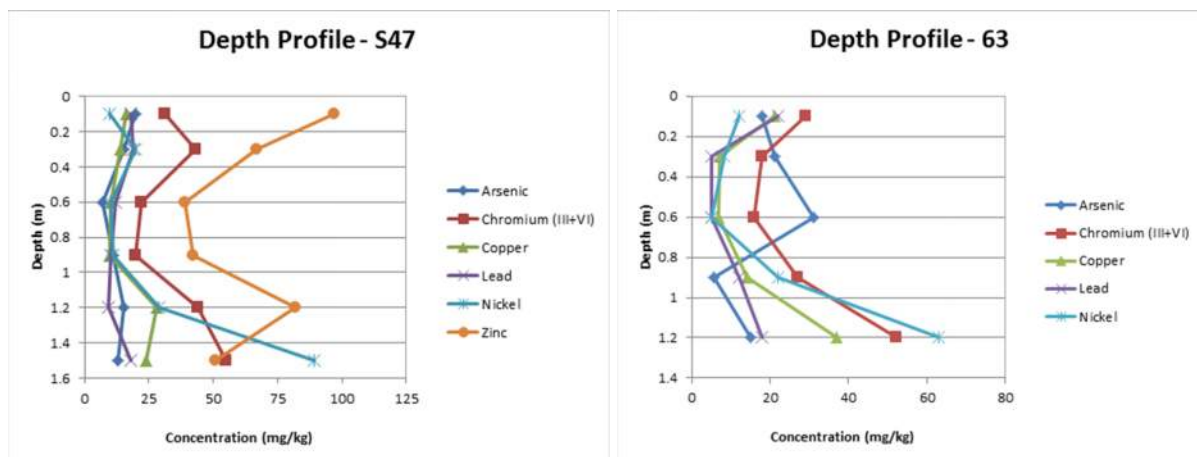
#### 2.1.4 Sediment Contamination Depth Profile

Figure 2 shows the change in inorganic contamination concentrations with depth. These locations are It can be concluded from these metal depth profiles that:

- Contaminant profiles are variable with depth. Some metals appear to follow similar distributions patterns, whereas others do not.
- For location S63, it appears the concentrations increase with depth. S47 was located in the intertidal area adjacent to Galway street landfill and S63 was located south west of Metroport. Depth profiles were undertaken for a number of locations, however S47 was considered relatively representative of the wider sample group and S63 demonstrated a notable trend. S47 does not appear to have any significant trends, with the exception of nickel increasing with depth. S63 shows a general trend of increasing concentrations with depth. Depth profiles were undertaken for a number of locations, however S47 was considered relatively representative of the wider sample group and S63 demonstrated a notable trend, and therefore selected for discussion.

Sediment concentration transects out from stormwater outfalls (3 transect locations) did not show any discernible trends in terms of contaminant concentration gradients – concentrations were reasonably uniform along the gradient.

**Figure 2: Depth profile of metal contamination in sediment**



### 2.1.5 Sediment Contaminant Distribution in Mangere Inlet

A series of maps have been produced to illustrate the patterns of metal concentrations in surface sediment within the inlet (included in Technical Report 16 Ecological Impact Assessment). Where there are ERC and ISQG thresholds for a single contaminant (e.g. copper, lead and zinc), a comparison against both guidelines concentrations has been mapped.

In summary, the review of the distribution of contaminants indicates that:

- Arsenic was found to be elevated in surface sediment across all areas within the inlet and did not seem to vary with depth.
- Chromium was only detected above ISQG guidelines in the intertidal zone.
- Distribution of copper in shallow sediments does not show any trends with location. Deeper samples have higher concentrations in the intertidal zone.
- Lead was consistently more concentrated in the intertidal zone in both shallow and deep sediments than the rest of the inlet.
- Nickel concentrations in shallow samples were generally higher in the transects from the stormwater outfalls in the intertidal zone plus under the Mangere Bridge and locations S09 and S10. Deeper samples had concentrations with more of a widespread distribution.
- Zinc was not detected above effects thresholds at eastern or southern shore sites or in subtidal sediment. However it was detected at concentrations exceeding the ISQG along the intertidal zone, concentrated around existing stormwater discharge points.

Elevated concentrations of metals and PAHs were measured in Maimi Creek sediments.

### 2.1.6 Acid Sulphate Sediments

Acid sulphate soils (ASS) occur naturally in coastal and inland settings and have been found to occur in a range of soil types in Auckland. Potential acid sulphate soils (PASS) are sediments containing un-oxidised sulphides (predominantly iron sulphides), usually located below the water table. If left undisturbed, PASS is unlikely to cause any harm to the environment. If drained, excavated or exposed to air, however, PASS can react with oxygen and water to form sulfuric acid, creating actual acid sulphate soils (AASS). Under acidic conditions, metals such as aluminium and iron as well as trace metal toxicants may be mobilised from the sediment through water infiltration. The acid can in turn mobilise metals to waterways, impacting on marine or freshwater ecosystems. Acid sulphate sediments

and soils are also typically rich in nitrogen and phosphorus compounds, which can be released if the soils are disturbed or dewatered.

The presence of ASS can be problematic for construction projects where PASS or AASS are disturbed. Acidic conditions can also be corrosive to concrete and steel structures (pipes, bridge abutments, underground services and other infrastructure). Ideally disturbance of ASS should be avoided, however in instances where this is not possible, ASS must be carefully managed in order to prevent potential impacts to the environment.

Investigations undertaken for EWL include analysis of three sediment samples collected from intertidal zone of Mangere inlet and two from Otahuhu Creek.

Results indicated that:

- The intertidal samples have mid-range concentrations of oxidisable sulphur (i.e. > 0.5%S), which could be of concern. They also have little to no acid neutralising capacity.
- Sample EWL\_S41\_0.8 has already released some acid, reporting a pHKCl <5.5 and results indicate a small amount of TAA (0.028%S), or acid in the soil.
- The two samples collected from Otahuhu Creek have low-level oxidisable sulphur, and excess acid neutralising capacity, however there is still potential to cause an issue although the risk is considered low.

### **2.1.7 Sediment Porewater Contamination**

Sediment porewater may be released into the environment through the wetland construction activities, or through the loading of sediments during construction activities in the CMA, and therefore it is important to consider contaminants that may be contained within porewater as this will be released into the environment. Porewater contaminants are also considered to provide a reasonable approximation of the bio-availability of contaminants

A number of contaminant concentrations measured in porewater exceeded ANZECC guidelines including ammoniacal nitrogen, copper and zinc. In general, these exceedances are not considered significant as these contaminants would be rapidly be diluted within the water column

The only contaminant of concern measured in porewater was ammoniacal nitrogen. The measured concentrations of ammoniacal nitrogen were an order of magnitude (x10 higher) than the ANZECC 90% protection level. Ammoniacal nitrogen is water soluble, and as such will be readily diluted within the marine environment.

With the exception of copper and zinc, all other heavy metals tested for were below the ANZECC 90% protection level. Zinc exceeded the guideline criteria by approximately two times, while copper was just over three times above the ANZECC 90% protection level criteria. This indicates that, assuming reasonable mixing in the marine environment, it would take approximately three times dilution of porewater to keep concentrations of heavy metals below the ANZECC 90% protection level.

## **2.2 Results Summary**

In summary, the following conclusions can be drawn from the sediment quality investigations:

- Generally, metal concentrations were consistent with that of concentrations measured in sediments in other parts of the Auckland region, and likely to be generally representative of background concentrations
- Some localised concentrations for chromium, copper, zinc, and nickel in excess of the ANZECC ISQG low. These exceedances are not considered statistically significant, and overall concentrations appear to be relatively consistent with concentrations in parent soil / rock material

- The exception to this, was arsenic where some concentrations were elevated above natural concentrations (parent materials), and above ANZECC low acceptance criteria at approximately ½ the locations. This may indicate that that some organisms may be adversely impacted by arsenic concentrations in sediments, if bioavailable
- Low concentrations of organic compounds were detected at some locations. Organic contaminant concentrations were within acceptance criteria
- No significant trends were observed for contaminant distribution within the Mangere inlet, however it can be concluded that contaminant concentrations were higher in the vicinity of stormwater outfalls. No significant trends noted with contaminant depth profiles.
- Contaminant concentrations were most elevated in sediment samples collected from Maimi stream, upstream of the culvert at the foreshore.
- Concentrations of ammoniacal nitrogen in porewater is likely to be rapidly diluted within the marine water within the subtidal areas. Any ammoniacal nitrogen released in the intertidal area is likely to be rapidly diluted within tidal movement of water.
- Acid sulphate soils / sediments within the project area are not considered to pose a risk to environmental receptors.









Sediment Results summary table

Location Code	EXTRA	Otauhu Creek	Otauhu Creek	Miami Downstream	Miami Upstream	S01 & S02	S01 & S02	S01 & S02	S03 & S04	S03 & S04	S03 & S04	S05 & S06	S05 & S06	S05 & S06	S07 & S08	S07 & S08
Sample Depth	0.1	0.1	0.1	0.1	0.1	0.1	0.3	1.2	0.1	0.3	1.8	0.1	0.3	1.5	0.1	0.3
Sampled Date	28/04/2016	13/05/2016	13/05/2016	31/05/2016	31/05/2016	27/04/2016	27/04/2016	27/04/2016	27/04/2016	27/04/2016	27/04/2016	27/04/2016	27/04/2016	27/04/2016	27/04/2016	27/04/2016
Field ID	EWL_EXTRA_0.1 M	MATAROA 1 0.1M	MATAROA 2 0.1M	Miami Downstream	Miami Upstream	COMP 1 (S01_0.1M & S02_0.1M)	COMP 6 (S01_0.3M & S02_0.3M)	COMP 11 (S01_1.2M & S02_1.2M)	COMP 2 (S03_0.1M & S04_0.1M)	COMP 7 (S03_0.3M & S04_0.3M)	COMP 12 (S03_1.8M & S04_1.8M)	COMP 3 (S05_0.1M & S06_0.1M)	COMP 8 (S05_0.3M & S06_0.3M)	COMP 13 (S05_1.5M & S06_1.5M)	COMP 4 (S07_0.1M & S08_0.1M)	COMP 9 (S07_0.3M & S08_0.3M)
Lab Report Number	500018	500607	500607	1594062_1	1594062_1	500018	500018	500018	500018	500018	500018	500018	500018	500018	500018	500018

Chem_Group	ChemName	Units	EQL	ARC - Environmental Response Criteria - Amber	ARC - Environmental Response Criteria - Red	ISQG-High	ISQG-Low														
	Trifluralin	mg/kg	0.5					-	-	-	-	-	-	-	-	-	-	-	-	-	-
	Benzo(a)pyrene TEQ (lower bound) *	mg/kg	0.01					<0.01	0.16	<0.01	-	-	<0.01	<0.01	<0.01	<0.01	<0.01	<0.01	<0.01	<0.01	<0.01
PCBs	Arochlor 1016	mg/kg	0.1					-	-	-	-	-	-	-	-	-	-	-	-	-	-
	Arochlor 1221	mg/kg	0.1					-	-	-	-	-	-	-	-	-	-	-	-	-	-
	Arochlor 1232	mg/kg	0.1					-	-	-	-	-	-	-	-	-	-	-	-	-	-
	Arochlor 1242	mg/kg	0.1					-	-	-	-	-	-	-	-	-	-	-	-	-	-
	Arochlor 1248	mg/kg	0.1					-	-	-	-	-	-	-	-	-	-	-	-	-	-
	Arochlor 1254	mg/kg	0.1					-	-	-	-	-	-	-	-	-	-	-	-	-	-
	Arochlor 1260	mg/kg	0.1					-	-	-	-	-	-	-	-	-	-	-	-	-	-
	PCBs (Sum of Total) - Calc	mg/kg						-	-	-	-	-	-	-	-	-	-	-	-	-	-
PCBs (Total)	mg/kg	0.1					-		0.022												0.023
Phthalates	Butyl benzyl phthalate	mg/kg	0.5					-	-	-	-	-	-	-	-	-	-	-	-	-	-
	Diethylphthalate	mg/kg	0.5					-	-	-	-	-	-	-	-	-	-	-	-	-	-
	Dimethyl phthalate	mg/kg	0.5					-	-	-	-	-	-	-	-	-	-	-	-	-	-
	Di-n-butyl phthalate	mg/kg	0.5					-	-	-	-	-	-	-	-	-	-	-	-	-	-
	Di-n-octyl phthalate	mg/kg	0.5					-	-	-	-	-	-	-	-	-	-	-	-	-	-
Chlorinated Hydrocarbons	2-chloronaphthalene	mg/kg	0.5					-	-	-	-	-	-	-	-	-	-	-	-	-	-
Explosives	2,4-Dinitrotoluene	mg/kg	0.5					-	-	-	-	-	-	-	-	-	-	-	-	-	-
	2,6-dinitrotoluene	mg/kg	0.5					-	-	-	-	-	-	-	-	-	-	-	-	-	-
	Nitrobenzene	mg/kg	0.5					-	-	-	-	-	-	-	-	-	-	-	-	-	-
Herbicides	Pronamide	mg/kg	0.5					-	-	-	-	-	-	-	-	-	-	-	-	-	-
Nitroaromatics	2-Picoline	mg/kg	0.5					-	-	-	-	-	-	-	-	-	-	-	-	-	-
	4-aminobiphenyl	mg/kg	0.5					-	-	-	-	-	-	-	-	-	-	-	-	-	-
	Pentachloronitrobenzene	mg/kg	0.5					-	-	-	-	-	-	-	-	-	-	-	-	-	-





Sediment Results summary table

Location Code	S07 & S08	S09 & S10	S09 & S10	S09 & S10	S11	S12	S14	S15	S16	S17	S18	S19	S20	S21	S22	S23
Sample Depth	0.9	0.1	0.3	0.6	0.1	0.1	0.1	0.1	0.1	0.1	0.1	0.1	0.1	0.1	0.1	0.1
Sampled Date	27/04/2016	27/04/2016	27/04/2016	27/04/2016	28/04/2016	28/04/2016	28/04/2016	28/04/2016	27/04/2016	27/04/2016	27/04/2016	27/04/2016	27/04/2016	27/04/2016	27/04/2016	27/04/2016
Field ID	COMP 14 (S07_0.9M & S08_0.9M)	COMP 5 (S09_0.1M & S10_0.1M)	COMP 10 (S09_0.3M & S10_0.3M)	COMP 15 (S09_0.6M & S10_0.6M)	EWL_S11_0.1M	EWL_S12_0.1M	EWL_S14_0.1M	EWL_S15_0.1M	EWL_S16_0.1M	EWL_S17_0.1M	EWL_S18_0.1M	EWL_S19_0.1M	EWL_S20_0.1M	EWL_S21_0.1M	EWL_S22_0.1M	EWL_S23_0.1M
Lab Report Number	500018	500018	500018	500018	500018	500018	500018	500018	500018	500018	500018	500018	500018	500018	500018	500018

Chem_Group	ChemName	Units	EQL	ARC - Environmental Response Criteria - Amber	ARC - Environmental Response Criteria - Red	ISQG-High	ISQG-Low														
	Trifluralin	mg/kg	0.5					-	-	-	-	-	-	-	-	-	-	-	-	-	-
	Benzo(a)pyrene TEQ (lower bound) *	mg/kg	0.01					<0.01	<0.01	<0.01	<0.01	<0.01	<0.01	<0.01	<0.01	<0.01	<0.01	<0.01	<0.01	<0.01	<0.01
PCBs	Arochlor 1016	mg/kg	0.1					-	-	-	-	-	-	-	-	-	-	-	-	-	-
	Arochlor 1221	mg/kg	0.1					-	-	-	-	-	-	-	-	-	-	-	-	-	-
	Arochlor 1232	mg/kg	0.1					-	-	-	-	-	-	-	-	-	-	-	-	-	-
	Arochlor 1242	mg/kg	0.1					-	-	-	-	-	-	-	-	-	-	-	-	-	-
	Arochlor 1248	mg/kg	0.1					-	-	-	-	-	-	-	-	-	-	-	-	-	-
	Arochlor 1254	mg/kg	0.1					-	-	-	-	-	-	-	-	-	-	-	-	-	-
	Arochlor 1260	mg/kg	0.1					-	-	-	-	-	-	-	-	-	-	-	-	-	-
	PCBs (Sum of Total) - Calc	mg/kg						-	-	-	-	-	-	-	-	-	-	-	-	-	-
	PCBs (Total)	mg/kg	0.1					-	-	-	-	-	-	-	-	-	-	-	-	-	-
																					0.022
Phthalates	Butyl benzyl phthalate	mg/kg	0.5					-	-	-	-	-	-	-	-	-	-	-	-	-	-
	Diethylphthalate	mg/kg	0.5					-	-	-	-	-	-	-	-	-	-	-	-	-	-
	Dimethyl phthalate	mg/kg	0.5					-	-	-	-	-	-	-	-	-	-	-	-	-	-
	Di-n-butyl phthalate	mg/kg	0.5					-	-	-	-	-	-	-	-	-	-	-	-	-	-
	Di-n-octyl phthalate	mg/kg	0.5					-	-	-	-	-	-	-	-	-	-	-	-	-	-
Chlorinated Hydrocarbons	2-chloronaphthalene	mg/kg	0.5					-	-	-	-	-	-	-	-	-	-	-	-	-	-
Explosives	2,4-Dinitrotoluene	mg/kg	0.5					-	-	-	-	-	-	-	-	-	-	-	-	-	-
	2,6-dinitrotoluene	mg/kg	0.5					-	-	-	-	-	-	-	-	-	-	-	-	-	-
	Nitrobenzene	mg/kg	0.5					-	-	-	-	-	-	-	-	-	-	-	-	-	-
Herbicides	Pronamide	mg/kg	0.5					-	-	-	-	-	-	-	-	-	-	-	-	-	-
Nitroaromatics	2-Picoline	mg/kg	0.5					-	-	-	-	-	-	-	-	-	-	-	-	-	-
	4-aminobiphenyl	mg/kg	0.5					-	-	-	-	-	-	-	-	-	-	-	-	-	-
	Pentachloronitrobenzene	mg/kg	0.5					-	-	-	-	-	-	-	-	-	-	-	-	-	-
								-	-	-	-	-	-	-	-	-	-	-	-	-	-





Sediment Results summary table

Location Code	S25	S26	S27	S28	S29	S30	S41	S41	S41	S41	S43	S43	S43	S43	S44	S44
Sample Depth	0.1	0.1	0.1	0.1	0.1	0.1	0.1	0.3	0.5	0.8	0.1	0.3	0.5	0.7	0.1	0.3
Sampled Date	28/04/2016	28/04/2016	28/04/2016	28/04/2016	27/04/2016	26/04/2016	13/04/2016	13/04/2016	13/04/2016	13/04/2016	13/04/2016	13/04/2016	13/04/2016	13/04/2016	13/04/2016	13/04/2016
Field ID	EWL_S25_0.1M	EWL_S26_0.1M	EWL_S27_0.1M	EWL_S28_0.1M	EWL_S29_0.1M	EWL_S30_0.1M	EWL_S41_0.1	EWL_S41_0.3	EWL_S41_0.5	EWL_S41_0.8	EWL_S43_0.1	EWL_S43_0.3	EWL_S43_0.5	EWL_S43_0.7	EWL_S44_0.1	EWL_S44_0.3
Lab Report Number	500018	500018	500018	500018	500018	500018	496898/499392	496898/499392	496898/499392	496898/499392	496898/499392	496898/499392	496898/499392	496898/499392	496898/499392	496898/499392

Chem_Group	ChemName	Units	EQL	ARC - Environmental Response Criteria - Amber	ARC - Environmental Response Criteria - Red	ISQG-High	ISQG-Low	S25	S26	S27	S28	S29	S30	S41	S41	S41	S41	S43	S43	S43	S43	S44	S44
	Trifluralin	mg/kg	0.5					-	-	-	-	-	-	<0.5	<0.5	<0.5	<0.5	<0.5	<0.5	<0.5	<0.5	<0.5	<0.5
	Benzo(a)pyrene TEQ (lower bound) *	mg/kg	0.01					<0.01	<0.01	<0.01	<0.01	<0.01	<0.01	<0.01	<0.01	<0.01	<0.01	<0.01	<0.01	<0.01	<0.01	<0.01	<0.01
PCBs	Arochlor 1016	mg/kg	0.1					-	-	-	-	-	-	<0.1	<0.1	<0.1	<0.1	<0.1	<0.1	<0.1	<0.1	<0.1	<0.1
	Arochlor 1221	mg/kg	0.1					-	-	-	-	-	-	<0.1	<0.1	<0.1	<0.1	<0.1	<0.1	<0.1	<0.1	<0.1	<0.1
	Arochlor 1232	mg/kg	0.1					-	-	-	-	-	-	<0.1	<0.1	<0.1	<0.1	<0.1	<0.1	<0.1	<0.1	<0.1	<0.1
	Arochlor 1242	mg/kg	0.1					-	-	-	-	-	-	<0.1	<0.1	<0.1	<0.1	<0.1	<0.1	<0.1	<0.1	<0.1	<0.1
	Arochlor 1248	mg/kg	0.1					-	-	-	-	-	-	<0.1	<0.1	<0.1	<0.1	<0.1	<0.1	<0.1	<0.1	<0.1	<0.1
	Arochlor 1254	mg/kg	0.1					-	-	-	-	-	-	<0.1	<0.1	<0.1	<0.1	<0.1	<0.1	<0.1	<0.1	<0.1	<0.1
	Arochlor 1260	mg/kg	0.1					-	-	-	-	-	-	<0.1	<0.1	<0.1	<0.1	<0.1	<0.1	<0.1	<0.1	<0.1	<0.1
	PCBs (Sum of Total) - Calc	mg/kg						-	-	-	-	-	-	<0.7	<0.7	<0.7	<0.7	<0.7	<0.7	<0.7	<0.7	<0.7	<0.7
	PCBs (Total)	mg/kg	0.1		0.022		0.023		-	-	-	-	-	<0.1	<0.1	<0.1	<0.1	<0.1	<0.1	<0.1	<0.1	<0.1	<0.1
Phthalates	Butyl benzyl phthalate	mg/kg	0.5					-	-	-	-	-	-	<0.5	<0.5	<0.5	<0.5	<0.5	<0.5	<0.5	<0.5	<0.5	<0.5
	Diethylphthalate	mg/kg	0.5					-	-	-	-	-	-	<0.5	<0.5	<0.5	<0.5	<0.5	<0.5	<0.5	<0.5	<0.5	<0.5
	Dimethyl phthalate	mg/kg	0.5					-	-	-	-	-	-	<0.5	<0.5	<0.5	<0.5	<0.5	<0.5	<0.5	<0.5	<0.5	<0.5
	Di-n-butyl phthalate	mg/kg	0.5					-	-	-	-	-	-	<0.5	<0.5	<0.5	<0.5	<0.5	<0.5	<0.5	<0.5	<0.5	<0.5
	Di-n-octyl phthalate	mg/kg	0.5					-	-	-	-	-	-	<0.5	<0.5	<0.5	<0.5	<0.5	<0.5	<0.5	<0.5	<0.5	<0.5
Chlorinated Hydrocarbons	2-chloronaphthalene	mg/kg	0.5					-	-	-	-	-	-	<0.5	<0.5	<0.5	<0.5	<0.5	<0.5	<0.5	<0.5	<0.5	<0.5
Explosives	2,4-Dinitrotoluene	mg/kg	0.5					-	-	-	-	-	-	<0.5	<0.5	<0.5	<0.5	<0.5	<0.5	<0.5	<0.5	<0.5	<0.5
	2,6-dinitrotoluene	mg/kg	0.5					-	-	-	-	-	-	<0.5	<0.5	<0.5	<0.5	<0.5	<0.5	<0.5	<0.5	<0.5	<0.5
	Nitrobenzene	mg/kg	0.5					-	-	-	-	-	-	<0.5	<0.5	<0.5	<0.5	<0.5	<0.5	<0.5	<0.5	<0.5	<0.5
Herbicides	Pronamide	mg/kg	0.5					-	-	-	-	-	-	<0.5	<0.5	<0.5	<0.5	<0.5	<0.5	<0.5	<0.5	<0.5	<0.5
Nitroaromatics	2-Picoline	mg/kg	0.5					-	-	-	-	-	-	<0.5	<0.5	<0.5	<0.5	<0.5	<0.5	<0.5	<0.5	<0.5	<0.5
	4-aminobiphenyl	mg/kg	0.5					-	-	-	-	-	-	<0.5	<0.5	<0.5	<0.5	<0.5	<0.5	<0.5	<0.5	<0.5	<0.5
	Pentachloronitrobenzene	mg/kg	0.5					-	-	-	-	-	-	<0.5	<0.5	<0.5	<0.5	<0.5	<0.5	<0.5	<0.5	<0.5	<0.5







Sediment Results summary table

Location Code	S44	S44	S45	S45	S45	S45	S46	S46	S46	S46	S47	S47	S47	S47	S47	S47
Sample Depth	0.5	0.7	0.1	0.3	0.5	0.7	0.1	0.3	0.5	0.7	0.1	0.3	0.6	0.9	1.2	1.5
Sample Date	13/04/2016	13/04/2016	13/04/2016	13/04/2016	13/04/2016	13/04/2016	13/04/2016	13/04/2016	13/04/2016	13/04/2016	28/04/2016	28/04/2016	28/04/2016	28/04/2016	28/04/2016	28/04/2016
Field ID	EWL_S44_0.5	EWL_S44_0.7	EWL_S45_0.1	EWL_S45_0.3	EWL_S45_0.5	EWL_S45_0.7	EWL_S46_0.1	EWL_S46_0.3	EWL_S46_0.5	EWL_S46_0.7	EWL_S47_0.1M	EWL_S47_0.3M	EWL_S47_0.6M	EWL_S47_0.9M	EWL_S47_1.2M	EWL_S47_1.5M

Lab Report Number	496898/499392	496898/499392	496898/499392	496898/499392	496898/499392	496898/499392	496898/499392	496898/499392	496898/499392	496898/499392	500018	501450	501450	501450	500018	501450
-------------------	---------------	---------------	---------------	---------------	---------------	---------------	---------------	---------------	---------------	---------------	--------	--------	--------	--------	--------	--------

Chem_Group	ChemName	Units	EQL	ARC - Environmental Response Criteria - Amber	ARC - Environmental Response Criteria - Red	ISQG-High	ISQG-Low														
	Trifluralin	mg/kg	0.5					<0.5	<0.5	<0.5	<0.5	<0.5	<0.5	<0.5	<0.5	-	-	-	-	-	-
	Benzo(a)pyrene TEQ (lower bound) *	mg/kg	0.01					<0.5	<0.5	<0.5	<0.5	<0.5	<0.5	<0.5	<0.5	<0.01	<0.01	<0.01	<0.01	<0.01	<0.01
PCBs	Arochlor 1016	mg/kg	0.1					<0.1	<0.1	<0.1	<0.1	<0.1	<0.1	<0.1	<0.1	-	-	-	-	-	-
	Arochlor 1221	mg/kg	0.1					<0.1	<0.1	<0.1	<0.1	<0.1	<0.1	<0.1	<0.1	-	-	-	-	-	-
	Arochlor 1232	mg/kg	0.1					<0.1	<0.1	<0.1	<0.1	<0.1	<0.1	<0.1	<0.1	-	-	-	-	-	-
	Arochlor 1242	mg/kg	0.1					<0.1	<0.1	<0.1	<0.1	<0.1	<0.1	<0.1	<0.1	-	-	-	-	-	-
	Arochlor 1248	mg/kg	0.1					<0.1	<0.1	<0.1	<0.1	<0.1	<0.1	<0.1	<0.1	-	-	-	-	-	-
	Arochlor 1254	mg/kg	0.1					<0.1	<0.1	<0.1	<0.1	<0.1	<0.1	<0.1	<0.1	-	-	-	-	-	-
	Arochlor 1260	mg/kg	0.1					<0.1	<0.1	<0.1	<0.1	<0.1	<0.1	<0.1	<0.1	-	-	-	-	-	-
	PCBs (Sum of Total) - Calc	mg/kg						<0.7	<0.7	<0.7	<0.7	<0.7	<0.7	<0.7	<0.7	-	-	-	-	-	-
	PCBs (Total)	mg/kg	0.1		0.022		0.023	<0.1	<0.1	<0.1	<0.1	<0.1	<0.1	<0.1	<0.1	-	-	-	-	-	-
Phthalates	Butyl benzyl phthalate	mg/kg	0.5					<0.5	<0.5	<0.5	<0.5	<0.5	<0.5	<0.5	<0.5	-	-	-	-	-	-
	Diethylphthalate	mg/kg	0.5					<0.5	<0.5	<0.5	<0.5	<0.5	<0.5	<0.5	<0.5	-	-	-	-	-	-
	Dimethyl phthalate	mg/kg	0.5					<0.5	<0.5	<0.5	<0.5	<0.5	<0.5	<0.5	<0.5	-	-	-	-	-	-
	Di-n-butyl phthalate	mg/kg	0.5					<0.5	<0.5	<0.5	<0.5	<0.5	<0.5	<0.5	<0.5	-	-	-	-	-	-
	Di-n-octyl phthalate	mg/kg	0.5					<0.5	<0.5	<0.5	<0.5	<0.5	<0.5	<0.5	<0.5	-	-	-	-	-	-
Chlorinated Hydrocarbons	2-chloronaphthalene	mg/kg	0.5					<0.5	<0.5	<0.5	<0.5	<0.5	<0.5	<0.5	<0.5	-	-	-	-	-	-
Explosives	2,4-Dinitrotoluene	mg/kg	0.5					<0.5	<0.5	<0.5	<0.5	<0.5	<0.5	<0.5	<0.5	-	-	-	-	-	-
	2,6-dinitrotoluene	mg/kg	0.5					<0.5	<0.5	<0.5	<0.5	<0.5	<0.5	<0.5	<0.5	-	-	-	-	-	-
	Nitrobenzene	mg/kg	0.5					<0.5	<0.5	<0.5	<0.5	<0.5	<0.5	<0.5	<0.5	-	-	-	-	-	-
Herbicides	Pronamide	mg/kg	0.5					<0.5	<0.5	<0.5	<0.5	<0.5	<0.5	<0.5	<0.5	-	-	-	-	-	-
Nitroaromatics	2-Picoline	mg/kg	0.5					<0.5	<0.5	<0.5	<0.5	<0.5	<0.5	<0.5	<0.5	-	-	-	-	-	-
	4-aminobiphenyl	mg/kg	0.5					<0.5	<0.5	<0.5	<0.5	<0.5	<0.5	<0.5	<0.5	-	-	-	-	-	-
	Pentachloronitrobenzene	mg/kg	0.5					<0.5	<0.5	<0.5	<0.5	<0.5	<0.5	<0.5	<0.5	-	-	-	-	-	-





Sediment Results summary table

Location Code	S48	S48	S48	S48	S48	S48	S49	S49	S50	S50	S51	S52	S52	S53	S53	S54
Sample Depth	0.1	0.3	0.6	0.9	1.2	1.5	0.1	0.5	0.1	0.3	0.1	0.1	0.7	0.1	Depth Composite	0.1
Sampled Date	28/04/2016	28/04/2016	28/04/2016	28/04/2016	28/04/2016	28/04/2016	14/04/2016	14/04/2016	14/04/2016	14/04/2016	14/04/2016	14/04/2016	14/04/2016	14/04/2016	14/04/2016	14/04/2016
Field ID	EWL_S48_0.1M	EWL_S48_0.3M	EWL_S48_0.6M	EWL_S48_0.9M	EWL_S48_1.2M	EWL_S48_1.5M	EWL_S49_0.1	EWL_S49_0.5	EWL_S50_0.1	EWL_S50_0.3	EWL_S51_0.1	EWL_S52_0.1	EWL_S52_0.7	EWL_S53_0.1	EWL_S53	EWL_S54_0.1
Lab Report Number	501450	500018	501450	500018	501450	501450	497549/499395	497549/499395	497549/499395	497549/499395	497549/499395	497549/499395	497549/499395	497549/499395	497549	497549/499395

Chem_Group	ChemName	Units	EQL	ARC - Environmental Response Criteria - Amber	ARC - Environmental Response Criteria - Red	ISQG-High	ISQG-Low	S48	S48	S48	S48	S48	S48	S48	S49	S49	S50	S50	S51	S52	S52	S53	S53	S54
	Trifluralin	mg/kg	0.5					-	-	-	-	-	-	-	-	-	-	-	-	-	-	-	-	-
	Benzo(a)pyrene TEQ (lower bound) *	mg/kg	0.01					<0.01	<0.01	<0.01	<0.01	<0.01	<0.01	<0.01	<0.01	<0.01	<0.01	<0.01	<0.01	<0.01	<0.01	<0.01	<0.01	<0.01
PCBs	Arochlor 1016	mg/kg	0.1					-	-	-	-	-	-	-	-	-	-	-	-	-	-	-	-	-
	Arochlor 1221	mg/kg	0.1					-	-	-	-	-	-	-	-	-	-	-	-	-	-	-	-	-
	Arochlor 1232	mg/kg	0.1					-	-	-	-	-	-	-	-	-	-	-	-	-	-	-	-	-
	Arochlor 1242	mg/kg	0.1					-	-	-	-	-	-	-	-	-	-	-	-	-	-	-	-	-
	Arochlor 1248	mg/kg	0.1					-	-	-	-	-	-	-	-	-	-	-	-	-	-	-	-	-
	Arochlor 1254	mg/kg	0.1					-	-	-	-	-	-	-	-	-	-	-	-	-	-	-	-	-
	Arochlor 1260	mg/kg	0.1					-	-	-	-	-	-	-	-	-	-	-	-	-	-	-	-	-
	PCBs (Sum of Total) - Calc	mg/kg						-	-	-	-	-	-	-	-	-	-	-	-	-	-	-	-	-
PCBs (Total)	mg/kg	0.1			0.022	0.023	-	-	-	-	-	-	-	-	-	-	-	-	-	-	-	-	-	
Phthalates	Butyl benzyl phthalate	mg/kg	0.5					-	-	-	-	-	-	-	-	-	-	-	-	-	-	-	-	-
	Diethylphthalate	mg/kg	0.5					-	-	-	-	-	-	-	-	-	-	-	-	-	-	-	-	-
	Dimethyl phthalate	mg/kg	0.5					-	-	-	-	-	-	-	-	-	-	-	-	-	-	-	-	-
	Di-n-butyl phthalate	mg/kg	0.5					-	-	-	-	-	-	-	-	-	-	-	-	-	-	-	-	-
	Di-n-octyl phthalate	mg/kg	0.5					-	-	-	-	-	-	-	-	-	-	-	-	-	-	-	-	-
Chlorinated Hydrocarbons	2-chloronaphthalene	mg/kg	0.5					-	-	-	-	-	-	-	-	-	-	-	-	-	-	-	-	-
Explosives	2,4-Dinitrotoluene	mg/kg	0.5					-	-	-	-	-	-	-	-	-	-	-	-	-	-	-	-	-
	2,6-dinitrotoluene	mg/kg	0.5					-	-	-	-	-	-	-	-	-	-	-	-	-	-	-	-	-
	Nitrobenzene	mg/kg	0.5					-	-	-	-	-	-	-	-	-	-	-	-	-	-	-	-	-
Herbicides	Pronamide	mg/kg	0.5					-	-	-	-	-	-	-	-	-	-	-	-	-	-	-	-	-
Nitroaromatics	2-Picoline	mg/kg	0.5					-	-	-	-	-	-	-	-	-	-	-	-	-	-	-	-	-
	4-aminobiphenyl	mg/kg	0.5					-	-	-	-	-	-	-	-	-	-	-	-	-	-	-	-	-
	Pentachloronitrobenzene	mg/kg	0.5					-	-	-	-	-	-	-	-	-	-	-	-	-	-	-	-	-







Sediment Results summary table

Location Code	S54	S54	S55	S55	S55	S56	S56	S56	S56	S56	S56	S56	S56	S57	S57	S58	S58
Sample Depth	0.7	Depth Composite	0.1	0.9	Depth Composite	0.1	0.3	0.6	0.9	1.2	1.5	1.8	0.1	0.3	0.1	0.5	
Sampled Date	14/04/2016	14/04/2016	14/04/2016	14/04/2016	14/04/2016	27/04/2016	27/04/2016	27/04/2016	27/04/2016	27/04/2016	27/04/2016	27/04/2016	27/04/2016	15/04/2016	15/04/2016	15/04/2016	15/04/2016
Field ID	EWL_S54_0.7	EWL_S54	EWL_S55_0.1	EWL_S55_0.9	EWL_S55	EWL_S56_0.1M	EWL_S56_0.3M	EWL_S56_0.6M	EWL_S56_0.9M	EWL_S56_1.2M	EWL_S56_1.5M	EWL_S56_1.8M	EWL_S57_0.1	EWL_S57_0.3	EWL_S58_0.1	EWL_S58_0.5	
Lab Report Number	497549/499395	497549	497549/499395	497549/499395	497549	500018	501450	501450	500018	501450	501450	501450	497549/499395	497549/499395	497549/499395	497549/499395	

Chem_Group	ChemName	Units	EQL	ARC - Environmental Response Criteria - Amber	ARC - Environmental Response Criteria - Red	ISQG-High	ISQG-Low													
	Trifluralin	mg/kg	0.5	-	-	-	-	-	-	-	-	-	-	-	-	-	-	-	-	-
	Benzo(a)pyrene TEQ (lower bound) *	mg/kg	0.01	<0.01	-	<0.01	<0.01	-	-	<0.01	<0.01	<0.01	<0.01	<0.01	<0.01	<0.01	<0.01	<0.01	-	<0.01
PCBs	Arochlor 1016	mg/kg	0.1	-	-	-	-	-	-	-	-	-	-	-	-	-	-	-	-	-
	Arochlor 1221	mg/kg	0.1	-	-	-	-	-	-	-	-	-	-	-	-	-	-	-	-	-
	Arochlor 1232	mg/kg	0.1	-	-	-	-	-	-	-	-	-	-	-	-	-	-	-	-	-
	Arochlor 1242	mg/kg	0.1	-	-	-	-	-	-	-	-	-	-	-	-	-	-	-	-	-
	Arochlor 1248	mg/kg	0.1	-	-	-	-	-	-	-	-	-	-	-	-	-	-	-	-	-
	Arochlor 1254	mg/kg	0.1	-	-	-	-	-	-	-	-	-	-	-	-	-	-	-	-	-
	Arochlor 1260	mg/kg	0.1	-	-	-	-	-	-	-	-	-	-	-	-	-	-	-	-	-
	PCBs (Sum of Total) - Calc	mg/kg	-	-	-	-	-	-	-	-	-	-	-	-	-	-	-	-	-	-
	PCBs (Total)	mg/kg	0.1	-	0.022	-	0.023	-	-	-	-	-	-	-	-	-	-	-	-	-
Phthalates	Butyl benzyl phthalate	mg/kg	0.5	-	-	-	-	-	-	-	-	-	-	-	-	-	-	-	-	-
	Diethylphthalate	mg/kg	0.5	-	-	-	-	-	-	-	-	-	-	-	-	-	-	-	-	-
	Dimethyl phthalate	mg/kg	0.5	-	-	-	-	-	-	-	-	-	-	-	-	-	-	-	-	-
	Di-n-butyl phthalate	mg/kg	0.5	-	-	-	-	-	-	-	-	-	-	-	-	-	-	-	-	-
	Di-n-octyl phthalate	mg/kg	0.5	-	-	-	-	-	-	-	-	-	-	-	-	-	-	-	-	-
Chlorinated Hydrocarbons	2-chloronaphthalene	mg/kg	0.5	-	-	-	-	-	-	-	-	-	-	-	-	-	-	-	-	-
Explosives	2,4-Dinitrotoluene	mg/kg	0.5	-	-	-	-	-	-	-	-	-	-	-	-	-	-	-	-	-
	2,6-dinitrotoluene	mg/kg	0.5	-	-	-	-	-	-	-	-	-	-	-	-	-	-	-	-	-
	Nitrobenzene	mg/kg	0.5	-	-	-	-	-	-	-	-	-	-	-	-	-	-	-	-	-
Herbicides	Pronamide	mg/kg	0.5	-	-	-	-	-	-	-	-	-	-	-	-	-	-	-	-	-
Nitroaromatics	2-Picoline	mg/kg	0.5	-	-	-	-	-	-	-	-	-	-	-	-	-	-	-	-	-
	4-aminobiphenyl	mg/kg	0.5	-	-	-	-	-	-	-	-	-	-	-	-	-	-	-	-	-
	Pentachloronitrobenzene	mg/kg	0.5	-	-	-	-	-	-	-	-	-	-	-	-	-	-	-	-	-
				-	-	-	-	-	-	-	-	-	-	-	-	-	-	-	-	-





Sediment Results summary table

Location Code	S59	S59	S60	S61	S61	S62	S62	S63	S63	S63	S63	S63
Sample Depth	0.1	0.8	0.1	0.3	0.5	0.1	Depth Composite	0.1	0.3	0.6	0.9	1.2
Sampled Date	15/04/2016	15/04/2016	15/04/2016	15/04/2016	15/04/2016	15/04/2016	15/04/2016	27/04/2016	27/04/2016	27/04/2016	27/04/2016	27/04/2016
Field ID	EWL_S59_0.1	EWL_S59_0.8	EWL_S60_0.1	EWL_S61_0.3	EWL_S61_0.5	EWL_S62_0.1	EWL_S62	EWL_S63_0.1M	EWL_S63_0.3M	EWL_S63_0.6M	EWL_S63_0.9M	EWL_S63_1.2M
Lab Report Number	497549/499395	497549/499395	497549/499395	497549/499395	497549	497549/499395	497549	500018	501450	500018	501450	501450

Chem_Group	ChemName	Units	EQL	ARC - Environmental Response Criteria - Amber	ARC - Environmental Response Criteria - Red	ISQG-High	ISQG-Low										
	Trifluralin	mg/kg	0.5					-	-	-	-	-	-	-	-	-	-
	Benzo(a)pyrene TEQ (lower bound) *	mg/kg	0.01					-	<0.01	<0.01	-	-	<0.01	-	<0.01	<0.01	<0.01
PCBs	Arochlor 1016	mg/kg	0.1					-	-	-	-	-	-	-	-	-	-
	Arochlor 1221	mg/kg	0.1					-	-	-	-	-	-	-	-	-	-
	Arochlor 1232	mg/kg	0.1					-	-	-	-	-	-	-	-	-	-
	Arochlor 1242	mg/kg	0.1					-	-	-	-	-	-	-	-	-	-
	Arochlor 1248	mg/kg	0.1					-	-	-	-	-	-	-	-	-	-
	Arochlor 1254	mg/kg	0.1					-	-	-	-	-	-	-	-	-	-
	Arochlor 1260	mg/kg	0.1					-	-	-	-	-	-	-	-	-	-
	PCBs (Sum of Total) - Calc	mg/kg						-	-	-	-	-	-	-	-	-	-
	PCBs (Total)	mg/kg	0.1		0.022		0.023	-	-	-	-	-	-	-	-	-	-
Phthalates	Butyl benzyl phthalate	mg/kg	0.5					-	-	-	-	-	-	-	-	-	-
	Diethylphthalate	mg/kg	0.5					-	-	-	-	-	-	-	-	-	-
	Dimethyl phthalate	mg/kg	0.5					-	-	-	-	-	-	-	-	-	-
	Di-n-butyl phthalate	mg/kg	0.5					-	-	-	-	-	-	-	-	-	-
	Di-n-octyl phthalate	mg/kg	0.5					-	-	-	-	-	-	-	-	-	-
Chlorinated Hydrocarbons	2-chloronaphthalene	mg/kg	0.5					-	-	-	-	-	-	-	-	-	-
Explosives	2,4-Dinitrotoluene	mg/kg	0.5					-	-	-	-	-	-	-	-	-	-
	2,6-dinitrotoluene	mg/kg	0.5					-	-	-	-	-	-	-	-	-	-
	Nitrobenzene	mg/kg	0.5					-	-	-	-	-	-	-	-	-	-
Herbicides	Pronamide	mg/kg	0.5					-	-	-	-	-	-	-	-	-	-
Nitroaromatics	2-Picoline	mg/kg	0.5					-	-	-	-	-	-	-	-	-	-
	4-aminobiphenyl	mg/kg	0.5					-	-	-	-	-	-	-	-	-	-
	Pentachloronitrobenzene	mg/kg	0.5					-	-	-	-	-	-	-	-	-	-
								-	-	-	-	-	-	-	-	-	-





Sediment Results summary table

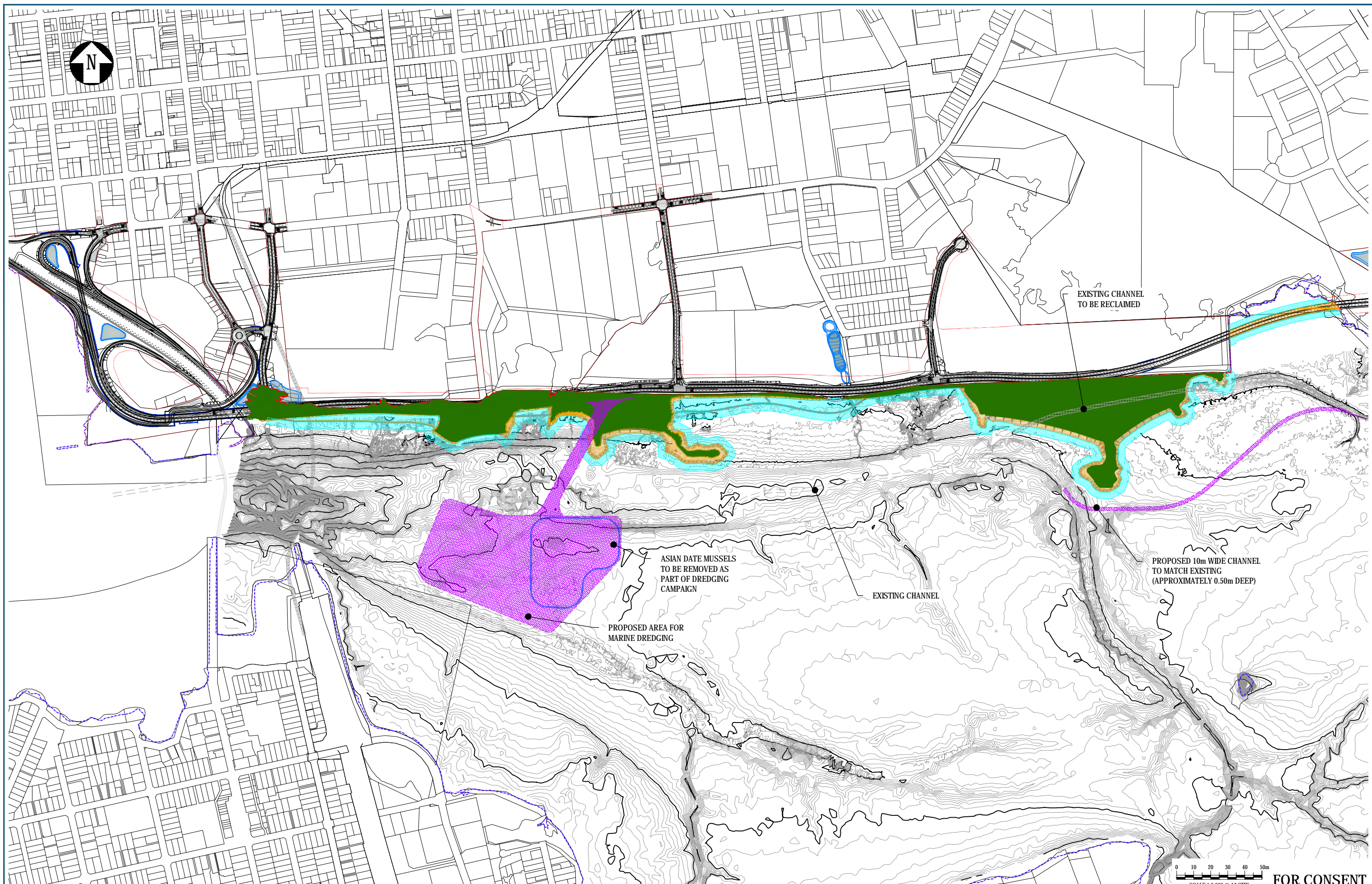
Location Code
Sample Depth
Sampled Date
Field ID

Lab Report Number

Chem_Group	ChemName	Units	EQL	ARC - Environmental Response Criteria - Amber	ARC - Environmental Response Criteria - Red	ISQG-High	ISQG-Low	Statistical Summary										
								Number of	Number of	Minimum	Minimum	Maximum	Maximum	Average	Median	Standard	Number of	Number of
	Trifluralin	mg/kg	0.5					20	0	<0.5	ND	<0.5	ND	0.25	0.25	0	0	0
	Benzo(a)pyrene TEQ (lower bound) *	mg/kg	0.01					94	1	<0.01	0.16	<0.5	0.16	0.059	0.005	0.1	0	0
PCBs	Arochlor 1016	mg/kg	0.1					20	0	<0.1	ND	<0.1	ND	0.05	0.05	0	0	0
	Arochlor 1221	mg/kg	0.1					20	0	<0.1	ND	<0.1	ND	0.05	0.05	0	0	0
	Arochlor 1232	mg/kg	0.1					20	0	<0.1	ND	<0.1	ND	0.05	0.05	0	0	0
	Arochlor 1242	mg/kg	0.1					20	0	<0.1	ND	<0.1	ND	0.05	0.05	0	0	0
	Arochlor 1248	mg/kg	0.1					20	0	<0.1	ND	<0.1	ND	0.05	0.05	0	0	0
	Arochlor 1254	mg/kg	0.1					20	0	<0.1	ND	<0.1	ND	0.05	0.05	0	0	0
	Arochlor 1260	mg/kg	0.1					20	0	<0.1	ND	<0.1	ND	0.05	0.05	0	0	0
	PCBs (Sum of Total) - Calc	mg/kg						20	0	<0.7	ND	<0.7	ND	0.35	0.35	0	0	0
	PCBs (Total)	mg/kg	0.1		0.022		0.023	20	0	<0.1	ND	<0.1	ND	0.05	0.05	0	20	0
Phthalates	Butyl benzyl phthalate	mg/kg	0.5					20	0	<0.5	ND	<0.5	ND	0.25	0.25	0	0	0
	Diethylphthalate	mg/kg	0.5					20	0	<0.5	ND	<0.5	ND	0.25	0.25	0	0	0
	Dimethyl phthalate	mg/kg	0.5					20	0	<0.5	ND	<0.5	ND	0.25	0.25	0	0	0
	Di-n-butyl phthalate	mg/kg	0.5					20	0	<0.5	ND	<0.5	ND	0.25	0.25	0	0	0
	Di-n-octyl phthalate	mg/kg	0.5					20	0	<0.5	ND	<0.5	ND	0.25	0.25	0	0	0
Chlorinated Hydrocarbons	2-chloronaphthalene	mg/kg	0.5					20	0	<0.5	ND	<0.5	ND	0.25	0.25	0	0	0
Explosives	2,4-Dinitrotoluene	mg/kg	0.5					20	0	<0.5	ND	<0.5	ND	0.25	0.25	0	0	0
	2,6-dinitrotoluene	mg/kg	0.5					20	0	<0.5	ND	<0.5	ND	0.25	0.25	0	0	0
	Nitrobenzene	mg/kg	0.5					20	0	<0.5	ND	<0.5	ND	0.25	0.25	0	0	0
Herbicides	Pronamide	mg/kg	0.5					20	0	<0.5	ND	<0.5	ND	0.25	0.25	0	0	0
Nitroaromatics	2-Picoline	mg/kg	0.5					20	0	<0.5	ND	<0.5	ND	0.25	0.25	0	0	0
	4-aminobiphenyl	mg/kg	0.5					20	0	<0.5	ND	<0.5	ND	0.25	0.25	0	0	0
	Pentachloronitrobenzene	mg/kg	0.5					20	0	<0.5	ND	<0.5	ND	0.25	0.25	0	0	0

**Appendix F**  
**Dredging Assessment**





0	ISSUED FOR CONSENT	AR			
No.	Issued Status	Drawn	Check'd	App'd	Date

**DISCLAIMER**  
 This drawing is for the purpose of supporting applications under the RMA for resource consents and designations. All information shown is subject to final design. Areas and measurements are subject to survey. Where the designs conflict with conditions the conditions will prevail. This Drawing must not be used for construction.

**East West Link**

Drawn	A RAM	Drafting Check	Reviewed Design Manager	Approved Alliance Manager
Designed	J MURAHIDY	Design Check		
Scale:	Original Scale (A1)	Reduced Scale (A3)	AS SHOWN	Contract No. PA4014

Drawing Title	COASTAL OCCUPATION AREA OF MARINE DREDGING	
Drawing Number	AEE-CMA-401	Rev No. 0

SCALE 1:2,000 @ A3 SIZE    **FOR CONSENT**



## F1 Scope and Extent of Dredging

It is proposed to use 'mudcrete' to build parts of the Foreshore Works. Mudcrete is a material made from mixing dredged material with ordinary Portland cement. Advantages of using mudcrete for this Project are:

- Dredged material can be won nearby which reduces the number of vehicles delivering alternative materials (e.g. quarry run) to the site;
- Mudcrete forms a relatively strong material within 24 hours and can be used to effectively form an impermeable barrier. Such a barrier can isolate landfill leachate from the tide and vice versa;
- It can be placed in any weather and underwater and does not need to be reworked in order to compact it; and
- It is natural looking material and can be left in place as a soft protection structure.

Mudcrete has been used on major coastal and harbour projects such as Waitemata Upper Harbour Bridge, Fergusson Container Terminal Expansion, Americas Cup (Viaduct) Harbour, Kohimarama and St Heliers Beaches.

The required quantities of mudcrete include:

- 36,000m<sup>3</sup> of in-situ material under the outer bunds to form a stable foundation;
- 200,000m<sup>3</sup> which needs to be won externally, and of which some 120,000m<sup>3</sup> would form the outer bund to contain the wetlands. The remaining quantity of 80,000m<sup>3</sup> would be used on the internal bunds; and
- Material won from within the wetland footprint can be used to form a mudcrete seal or liner for the wetlands and to create the main bund for the Project road, but that operation would not be exposed to the tide;

It is understood that it is preferable to win dredged material from the sub-tidal area rather than the inter-tidal area which is inhabited by wading birds and which is ecologically important. Furthermore it is preferred to take the material from the sub-tidal area infested with Asian date mussels. This area is shown on Figure F1 and covers about 8 ha. As 200,000m<sup>3</sup> of dredged material is required for the project, a 15% contingency will be applied for the application to cover unforeseen conditions. If the dredged depth were limited to 1.5m and 230,000m<sup>3</sup> of material is required then some 15ha needs to be dredged. The area of marine dredging is shown in *Volume 2: Drawing Set, Plan Set 4: Coastal Occupation* drawing referenced. AEE-CMA-101 and Figure F1. This area encapsulates the area of Asia date mussels.

---

It is intended that the mixing plant for the mudcrete, probably a pug mill, would be located near the Waikaraka Park construction site, as illustrated on Figure F1. In order to have an efficient operation, a navigation channel would be dredged to -3.5m RL from the dredging area to the mixing plant. See Figure F1. This channel would be 25m wide with side slope of 1(V):5(H). It would enable the dredging operation to provide material continuously to the mixing plant without having to work around a tidal window.

From the mixing plant mudcrete would be transported to the working area via either a conveyor system or vehicles. The mudcrete would initially be placed at existing seabed levels then gradually built up for later reshaping. Prior to this operation the seabed would be stabilised with mudcrete to form the foundation for the bund which could be achieved a number of ways. It could be stabilised in-situ with specialised equipment. Or it could be dredged, mixed in an adjacent basin or barge, and placed back into the dredged area. Or it could be dredged, conveyed to the mixing plant (at Waikaraka Park), mixed and conveyed back into the dredged area.

It is intended that the outer bund would be completed as the first stage. This would encapsulate the Project area, thereby limiting the potential for sediment plumes from the placing of mudcrete material and potentially allowing the remainder of the Project to be completed in the dry.

## **F2 Sediment fate assessment of dredging operation during construction**

### **F2.1 Description of the Physical Effects of Dredging**

In preparing this assessment, the following assumptions were made:

- 200,000m<sup>3</sup> of dredging from a dedicated dredged area (external to the Project) as shown in Figure F1, exposed to the tide 100% of the time;
- 36,000m<sup>3</sup> of dredging for outer bund foundation conditions (i.e. below seabed level), exposed to the tide 50% of the time;
- 7,000m<sup>3</sup> of dredging for the new tidal channel at the eastern end of the foreshore works, exposed to the tide for 100% of the time.
- 120,000m<sup>3</sup> of mudcrete placement in the outer bund (i.e. above seabed level), exposed to the tide 50% of the time;
- Use of a mechanical dredger (see Figure F2) so that the dredged material remains relatively intact for the mudcreting process (i.e. minimal water is mixed with the dredged material);
- Production rate of dredger of 750m<sup>3</sup>/day over 10 hours/day (i.e. dredging of 200,000m<sup>3</sup> would take 267 days) for the external dredged area and 300m<sup>3</sup>/day over 10 hours/day for dredging bund foundations and new tidal channel. These production rates assume no disruption in the supply chain and minimal downtime due to equipment malfunction. (pers. communication, Greg Kroef of Heron Construction)
- Capacity of receiving barges is 250m<sup>3</sup>;
- The dredged material is 85% mud (clay/silt) and has a dry density of 750 kg/m<sup>3</sup>. The dry density of the mudcrete is 1,000kg/m<sup>3</sup>.

Sources of sediment from the dredging/placing operation that could cause a sediment plume which would be dispersed around the Inlet/harbour (referred to as far field) are:

- From the dredger bucket;
- Overflow from the receiving barge;
- Placement of the mudcrete material.

The assessment of the dispersion of dredging and mudcrete operations is based on sediment release rates in the literature (Becker et al, 2014) and from local experiments. NIWA (in Appendix C) has modelled the suspended solids plume and subsequent deposition based on a release rate of 1kg of sediment/second (1 kg/s) for 10 hours per day. This modelling was for 3 discrete locations as depicted on Figure F1 (Sources 1, 2, 3). Based on the actual release rate for the different types of operation, the results have been pro-rated to provide an overall assessment of the levels of suspended solids and deposition within the Māngere Inlet. (See Section F2.4).

**Figure F2: Mechanical (backhoe) Dredger loading a Receiving Barge**



**F2.2 Sediment Release from the External Dredging Operation (at Source 1)**

One of the benefits of mechanical dredging is that most of dislodged material remains intact and falls back into the dredged area. From monitoring and modelling studies (Becker et al, 2014), it is estimated that a maximum amount of about 4% of the silt /clay fraction of the sediment becomes a passive source that can be dispersed into the far field. On this basis the release rate of material (Sr) is:

$$\begin{aligned}
 \text{Sr (kg/d)} &= \text{Production rate x dry density x silt/clay fraction x 0.04} \\
 &= 750 \times 750 \times 0.85 \times 0.04 \\
 &= 19,125 \text{ kg/d} \\
 &= 0.53 \text{ kg/s}
 \end{aligned}$$

In addition there will be some overflow from the receiving barge as it becomes full. It is estimated that a maximum amount of about 20% of the silt /clay fraction of the overflowed sediment (Becker et al, 2014) becomes a passive source that can be dispersed into the far field. If it overflowed for 5 minutes while loading, the release rate of material is:

$$\begin{aligned}
 \text{Sr(kg/d)} &= \text{Product rate x dry density x silt/clay fraction x overflow} \\
 &\quad \text{period x 0.2/time to fill the barge}
 \end{aligned}$$

$$\begin{aligned}
&= 750 \times 750 \times 0.85 \times 5 \times 0.2 / [10(60) (250/750)] \\
&= 2,390 \text{ kg/d} \\
&0.07 \text{ kg/s}
\end{aligned}$$

The average daily release of sediment is therefore  $0.53+0.07=0.6$  kg/s. The total release of dredged sediment into the water column over the Project would therefore be  $(19.1+2.4) 267=5740$  tonne.**F2.3 Sediment Release of Internal Dredging and Mudcreting Operation (Sources 2 and 3).**

Dredging for the bund foundation will be within a box cut, predominately outside of the tidal channel and tidal inundation will only occur for about 50% of the time. Because it is within a box cut the sediment discharge will be confined and less than for dredging in an open area. It is therefore appropriate, but probably conservative, to adopt the average release of 2% of the silt /clay fraction of the sediment from monitoring and modelling studies (Becker et al, 2014). Assuming no overflow due to the confined location, the release rate of material (Sr) is:

$$\begin{aligned}
\text{Sr (kg/d)} &= \text{Production rate} \times \text{dry density} \times \text{silt/clay fraction} \times 0.02 \times \% \\
&= \text{time when tidally inundated.} \\
&= 300 \times 750 \times 0.85 \times 0.02 \times 0.5 \\
&= 1,912 \text{ kg/d} \\
&= 0.05 \text{ kg/s}
\end{aligned}$$

The total release of dredged sediment into the water column over the Project for the bund foundations would therefore be  $(1.9 \times 36,000)/300=228$  tonne.

Dredging for the new tidal channel at the eastern end will be undertaken within a tidal window at higher tide levels. Over a single tidal cycle, allowing say 1m clearance for the dredger, dredging would only take place 25% of the time. From monitoring and modelling studies (Becker et al, 2014), it is estimated that a maximum amount of about 4% of the silt /clay fraction of the sediment becomes a passive source that can be dispersed into the far field. Assuming no overflow, the release rate of material (Sr) is:

$$\begin{aligned}
\text{Sr (kg/d)} &= \text{Production rate} \times \text{dry density} \times \text{silt/clay fraction} \times 0.02 \times \% \\
&= \text{time when tidally inundated.} \\
&= 300 \times 750 \times 0.85 \times 0.04 \times 0.25 \\
&= 1,912 \text{ kg/d} \\
&= 0.05 \text{ kg/s}
\end{aligned}$$

The total release of dredged sediment into the water column over the Project for the new tidal channel would therefore be  $(1.9 \times 7,000)/300=44$  tonne.

Mudcrete is hydroscopic in that it tends to attract seawater into it due to the dehydration process. The clay/silt/cement mixture is quite sticky and binds together rather than releasing material into the water column. Experiments have been undertaken to measure the amount of sediment that is released from mudcrete within the Port of Auckland. A sample of mudcrete (about  $0.05\text{m}^3$ ) was prepared, placed on a steel tray and lowered into the tide (with a measured current of 0.2 knots). It was kept submerged for 24 hours and then removed. The volume of the sample was measured before and after the experiment. It was found that the measured volumes were similar with some increase (of about 1%). No visual plumes were observed during the experiment. For the purpose of this assessment, it will be assumed that 0.5% of the mudcrete could be dispersed into the far field.

Some 120,000m<sup>3</sup> of mudcrete will be used to construct the outer bund above the seabed with 36,000m<sup>3</sup> of under bund mudcrete placed below seabed level not directly exposed to the tide. Sediment associated with the mudcrete could be dispersed at a rate of:

$$\begin{aligned}
 \text{Sr(kg/d)} &= \text{Placement rate (same as production rate for external} \\
 &= \text{dredging) x dry density x silt/clay fraction x \% time when} \\
 &= \text{tidally inundated x 0.025} \\
 &= 750 (1000) 0.85 (0.005)0.5 \\
 &= 1595\text{kg/d} \\
 &= 0.04 \text{ kg/s}
 \end{aligned}$$

The average daily discharge of sediment for the dredging and mudcreting of the outer bund is therefore 0.05+0.04=0.09 kg/s. For the whole project the total release of mudcrete would be 120,000(1.6)/750 =256 tonnes, or 528 tonnes if the sediment from the under bund and new tidal channel dredging operations were included.

#### F2.4 Sediment Fate of Dredging and Mudcreting Operations (Sources 1, 2 and 3).

As the sediment plume moves away from its source the plume expands or disperses outwards. The average concentration of total suspended solids (TSS) is dependent on the sediment release rate (Sr), the rate of dispersion, the depth of water and the velocity of the flow. In other dredging programmes (e.g. Rangitoto channel), a mixing zone of 200m has been used to establish the extent of elevated TSS with an exceedence trigger level of 25 g/m<sup>3</sup>.

Detailed sediment fate studies have been undertaken by NIWA to assess likely changes in total suspended concentrations away from the dredger and rates of deposition within the Inlet and harbour. That assessment is contained in Appendix C (Section 8 – Figures 8.1 to 8.6) and by applying their findings the dispersal and fate of the sediment plumes is discussed below.

When dredging in the main tidal channel (Source 1) as indicated on Figure F1, the TSS was estimated to be:

- At 100m to the west the TSS would be (25 x 0.6) 15 g/m<sup>3</sup> under south westerly conditions. Similarly 200m to the west would be (18 x 0.6) 11g/m<sup>3</sup>, 100m to the east would be (50 x 0.6) 30 g/m<sup>3</sup>, and 200m to the east would be (40 x 0.6) 24 g/m<sup>3</sup>.

When dredging and mudcreting at Source 2 as indicated on Figure F1, the TSS was estimated to be:

- At 100m to the west the TSS would be (40 x 0.09) 4 g/m<sup>3</sup> under north easterly conditions. Similarly 200m to the west would be (30 x 0.09) 3 g/m<sup>3</sup>, 100m to the east would be (136 x 0.09) 12 g/m<sup>3</sup>, and 200m to the east would be (106 x 0.09) 10 g/m<sup>3</sup>. It is noted that these plume extents are mainly contained within the project area.

When dredging and mudcreting at Source 3 as indicated on Figure F1, the TSS was estimated to be:

- At 100m to the west the TSS would be (870 x 0.09) 78 g/m<sup>3</sup> under calm conditions. Similarly 200m to the west would be (830 x 0.09) 75 g/m<sup>3</sup>, 100m to the east would be (570 x 0.09) 51 g/m<sup>3</sup>, and 200m to the east would be (340 x 0.09) 31 g/m<sup>3</sup>. It is noted that the plume extents to the west are mainly contained within the project area, while those to the east are towards Anns Creek.

Based on the daily deposition rates generated by 1 kg/s of sediment release over 10hrs per day, the maximum and average annual deposition rates can be established. See Figures 8.2, 8.4 and 8.6 in Appendix C.

- When dredging in the main tidal channel (Source 1) as indicated on Figure F1, the maximum deposition (away from the source location) was estimated to be 5 mm/ year with an average deposition of 3mm/year.
- When dredging at Source 2 as indicated on Figure F1, the maximum deposition (away from the source location) was estimated to be 0.3 mm/ year with an average deposition of 0.2mm/year.
- When dredging at Source 3 as indicated on Figure F1, the maximum deposition (away from the source location) was estimated to be 0.7 mm/ year with an average deposition of 0.4mm/year.

Overall the dredging operation at the dedicated dredging site (Source 1) dominates the overall deposition, with a maximum deposition of 6mm/year and an average deposition of 4mm/year.

## F2.5 Assessment of Effects of the Dredging Operation

Maximum sediment concentration away from the Project area and from the dredging operation at 200m is estimated to be 31 g/m<sup>3</sup> for the dredging and mudcrete operations at the eastern end of the Foreshore Works (Source 3). This is for a short period (less than 0.5 hr) and would average 15 g/m<sup>3</sup> over 1.5 hrs. For comparison the ambient median sediment concentration in the Manukau Harbour is 26g/m<sup>3</sup> with a wide variation (10 to 150g/m<sup>3</sup>). Average sediment concentration in the Māngere Inlet is about 30g/m<sup>3</sup>. These values are representative of median/average concentrations which would persist over the whole tidal cycle.

The dredging operation at the main dredging site (Source 1) dominates the overall deposition, with a maximum overall deposition of 6mm/year and an average deposition of 4mm/year. This is representative of what would occur in the Anns Creek area where the annual deposition is about 5-15 mm/year (see Figure 5-13 of Appendix C).

The fate of the sediment will be predominantly into the Inlet as naturally occurs. The total release of sediment from the Project is about 6,300 tonne or 9 tonnes per tide. The sediment flux for a spring tide is 700 tonnes per tide and for the neap tide is 350 tonnes per tide. Overall it is concluded that the sediment plumes and deposition associated with the dredging operation will be to a lesser extent than the ambient levels of total suspended solids (TSS), sediment fluxes and deposition. It will be temporary, persisting for a period of about 1 year. If the dredging operation were over a longer period the TSS level will reduce slightly and the total deposition will remain the same.

In the context of the Manukau Harbour which is noted for having high natural levels of TSS and deposition, the sediment plumes from the dredging and mudcrete operation will have a minor adverse effect.

## F2.6 Recommendations

### Proposed monitoring/mitigation/design changes

- The embankment construction should be staged so that the outer embankment is completed initially to encapsulate the remainder of the Project;
- The dredged channel should be infilled as part of the project so as to minimise adverse effects on the Inlet morphology. This will require filling the channel with some 25,000m<sup>3</sup> of material from the dredged area;
- Monthly average production rates for external dredging operation should be limited to 750 m<sup>3</sup>/day and for internal dredging operation should be limited to 300m<sup>3</sup>/day;
- No dredger overflows from receiving barges when dredging within 200m of the eastern end of the Foreshore Works;
- There should be regular (weekly) water quality monitoring of the dredging and mudcrete operations;
- There should be a contingency plan for trigger level exceedances; and
- On completion of the Project, using the latest LiDAR data and monitoring plates, assess the sediment deposition rates. This should be repeated 5 and 10 years after completion.



---

The above measures should be included in the special conditions of consent.

## F2.7 Conclusions

With the measures in Section F2.3 in place the adverse effects of the dredging and mudcrete operations will be minor, and will provide a basis for responding to measured adverse effects.

## F3 Assessment of Effects of Dredged Area (Long-term)

The ideal location of a dredged area would be within the central intertidal area as it would be in a lower tidal current location, away from the entrance, and likely to accumulate sediments in the long term. That option was not viable, however, due to the intertidal area being ecologically important.

The proposed dredged area shown in Figure F1. On completion of the project it will cover an area of about 15 ha, with the removal of about 200,000m<sup>3</sup> of sediment at an average depth below existing seabed levels of 1.35m (for 230,000m<sup>3</sup> the average depth would be 1.55m). As part of the dredging operation the area of Asian date mussels will be removed.

NIWA has modelled the dredged area with the reclamation in place and the results are described in Section 7 of Appendix C. (It is noted that the modelled area (20 ha) is larger than the area shown in Figure F1 (15 ha). Overall it is concluded that:

- The tidal velocities will reduce through the dredged area; and
- The central part of the dredged area will slightly erode and the flanks will accumulate sediment.
- Compared with the Project without the dredged channel, the overall net deposition is similar throughout the Inlet.

Modelling has indicated that while sedimentation is likely on the flanks of the dredged area the central part of it will remain as a basin. This is likely to be a remnant feature long term.

An elevated lip around the edge of the dredged area was left in place so as to encourage some degree of sedimentation long-term. Modelling has shown that this is only effective at promoting sedimentation on the flanks.

Overall the effect of the dredged area on coastal processes is considered to be minor. There will be a remnant dredged basin but this will be submerged and will not extend into the intertidal area. If the lip around the edge of the basin were removed then it would provide better navigability into the Inlet.

## F4 Assessment of Effects of Mudcrete (Long-term)

If left exposed, mudcrete will slowly fritter at a rate similar to soft Waitematā Sandstone Series, probably at 10 to 50mm/year. Given the low energy environment, mudcrete loss will probably be around 20mm/year. It is not intended to have mudcrete exposed in the long term. It will be covered by either beach material, rock, or a hardened surface.

The mudcrete is made up of the native material. This material contains some contaminants which are elevated but not unusually high (see Appendix E). Laboratory testing of mudcrete for some target contaminants, including potential leaching, has been undertaken and is appended. All contaminants tested were below ANZECC 90% level of protection for marine water, except for copper for which the highest value was 9mg/m<sup>3</sup> (compared to 3mg/m<sup>3</sup> for ANZECC value).

One of the benefits of mudcrete is it has low permeability, with an average measured value (k) of  $3 \times 10^{-9}$  m/s. In addition the hydraulic head to promote flow through the mudcrete is minimal. The following gives an example that the natural environment is not at risk from the leachate from mudcrete.

If it is assumed that there is a hydraulic head of 1.5m and the flow path length of 30m to promote the movement of water, the hydraulic gradient is  $1.5/30 = 0.05$ . The flow (Q) through a depth of 2.0m would



---

be  $Q = kiA = 3 \times 10^{-9} (0.05)^2 (1000) = 0.026$  L/day/m length of exposure or a seepage depth of 0.013mm/day. If the seawater had a copper concentration of  $1 \text{ mg/m}^3$ , then a dilution of  $9/(3-1) = 4.5$  is required to reduce the leachate to ANZECC guidelines. The following average daily phenomena are present in the environment:

- Seawater from the tides: 450mm (dilution of 1:35,000);
- Rainfall: 3.2mm (dilution 1:240); and
- Evaporation: 2.5mm (no discharge).

The above example is somewhat academic as the hydraulic head for the wetland arrangement is such that any leachate would be encouraged to migrate into the wetland. But it does illustrate the low risk to the natural environment from mudcrete leachate.

Overall it is considered that the long term effects from the use of mudcrete are negligible.

Transport Infrastructure - BL  
 21 Pitt Street  
 PO Box 6345  
 Auckland 1141  
 New Zealand

26 July 2016

**Attention: Stephen Priestley**

**Report 16:040 (amended)**

Dear Stephen,

**Results of Manukau Harbour Marine Sediment Mudcrete Trials - May 2016**

Beca Ltd trading as Envirolab has been commissioned by the NZ Transport Agency as part of the East West Link Alliance (East West) to conduct analysis and a series of mudcrete trials on marine sediment samples collected from the Manukau Harbour. This letter presents the final results of the mudcrete testing programme conducted in May 2016 (*amended to include nitrogen nutrients in the SPLP results and a figure showing sampling locations*).

This report relates only to the samples as tested, sampling was undertaken by others.

**Method**

As part of the East West testing programme a series of marine sediment samples were collected by GHD personnel and supplied to Beca's Envirolab laboratory. The individual samples were grouped and composited in equal volume to form five bulk samples, each representative of a different area of the harbour. The grouping of the individual samples to form the bulk samples is given in **Table 1**. The individual sample locations and composite grouping of the samples is shown in a GIS map appended to this letter (drawing number GIS-CP-AEE-001 dated 21 July 2016).

**Table 1**

**Sample Numbers As Received From GHD Grouped Into Their Respective Composite for Mudcrete**

Parameter		Unconfined Compressive Strength (UCS) Results in Triplicate						
Sample	Envirolab Prefix	GHD Sample Reference					Composite Sample Ref	Mudcrete Ref
Batch 1	16:040	S41	S46	S53	S54	S55	16:040-S1	16:040-M1
Batch 2	16:040	S05	S06	S07	S09	S10	16:040-S2	16:040-M2
Batch 3	16:040	S01	S02	S03	S12	----	16:040-S3	16:040-M3
Batch 4	16:040	S04	S16	S18	S20	----	16:040-S4	16:040-M4
Batch 5	16:040	S56	S61	S62	S63	----	16:040-S5	16:040-M5

An initial subsample was taken from each of the bulk samples. The remainder of each bulk marine sediment samples was then mixed with Portland cement at a rate of 80kg per m<sup>3</sup> to form 'mudcrete'. The mudcrete made from each of the bulk samples was placed in moulds to form five core samples suitable for UCS testing. The core samples were allowed to set for approximately 2-days before being removed from the mould and placed underwater to cure.

### Testing Suite(s)

#### ■ **Particle Size Distribution testing**

Each of the five subsamples collected from the composite bulk samples prior to forming mudcrete was subjected to particle size distribution testing. The results of the particle size testing are presented in the original laboratory report from Geotest (report N° 1880L:02, dated 13 June 2016) which is appended to this letter.

#### ■ **Marine Sediment chemical analysis**

Each of the five subsamples collected from the composite bulk samples prior to forming mudcrete was subjected to chemical analysis for heavy metals and saline water leaching. The samples were dispatched to R.J. Hill Laboratories Ltd (Hill Laboratories) for chemical analyses. Chemical analysis consisted of total heavy metals and synthetic precipitation leaching procedure (SPLP) undertaken using saline water, the saline leachate water then being analysed for the same suite of heavy metals as the initial solid material. The results of the Marine Sediment chemical testing are presented in **Table 3**. The original laboratory report from Hill Laboratories (report N° 1588470 SPv3, dated 01 July 2016) is appended to this letter.

#### ■ **Unconfined Compressive Strength (UCS) testing**

Three out of each set of five mudcrete cores were subjected to unconfined compressive strength (UCS) testing. One core after 7-days curing and two after 28-days of curing. The results of the UCS testing are presented in **Table 2**. The original laboratory report from Geotest (report N° 1880L:05, dated 13 June 2016) is appended to this letter.

#### ■ **Permeability testing**

Three permeability tests were undertaken, one test on one core from each of the first three sets of five mudcrete cores. Permeability testing was undertaken by Opus International Consultants Ltd (Opus), Hamilton. The results of the permeability testing are presented in **Table 2**. The original laboratory report from Opus (report N° HA146, dated 13 June 2016) is appended to this letter.

#### ■ **Mudcrete Core chemical analysis**

One core from each of the five sets of mudcrete cores was subjected to chemical analysis for heavy metals and saline water leaching. The samples were dispatched to Hill Laboratories for chemical analyses. Chemical analysis consisted of total heavy metals and synthetic precipitation leaching procedure (SPLP) undertaken using saline water, the saline leachate water then being analysed for the same suite of heavy metals as the initial solid material. The results of the Mudcrete Core chemical testing are presented in **Table 3**. The original laboratory report from Hill Laboratories (report N° 1594833 SPv3, dated 01 July 2016) is appended to this letter.

## Results

Copies of the original laboratory reports and/or certificates for all the analyses presented in this report are appended to this letter. Results of the mudcrete core strength testing are given in **Table 2**. Results for the marine sediment and mudcrete chemical testing are presented in **Table 3**.

**Table 2**

**Results of Manukau Harbour Mudcrete Strength Testing After 7-days and 28-days Curing**

Parameter	Unconfined Compressive Strength (UCS) Results in Triplicate			Permeability (m/s)	
	After 7-days curing (kPa)	After 28-days curing (kPa)		Head 35kPa	Head 70kPa
16:040-M1 (Batch 1)	300	420	360	$1.7 \times 10^{-9}$	$2.1 \times 10^{-9}$
16:040-M1 (Batch 2)	84	120	46	$4.1 \times 10^{-9}$	$4.3 \times 10^{-9}$
16:040-M3 (Batch 3)	210	140	110	$2.5 \times 10^{-9}$	$6.5 \times 10^{-9}$
16:040-M1 (Batch 4)	130	220	300	----	----
16:040-M1 (Batch 5)	140	220	220	----	----

**Table 3 Comparison of the Analytical Testing Results for the Manukau Harbour Marine Sediment and Mudcrete Cores Against ANZECC 2000 guidelines**

Analytical Parameter	ANZECC (2000) ISQG-High	ANZECC 90% (2000)	Marine sediment					Mudcrete				
			16:040 S1	16:040 S2	16:040 S3	16:040 S4	16:040 S5	16:040 M1	16:040 M2	16:040 M3	16:040 M4	16:040 M5
<b>Sediment/Mudcrete – Total Metals (mg/kg dry wt)</b>												
Arsenic	70	----	11	14	14	13	13	7	10	8	10	9
Cadmium	10	----	0.26	0.1	0.06	0.14	0.07	0.17	<0.10	<0.10	0.14	<0.10
Chromium	370	----	37	33	25	35	29	29	32	20	30	24
Copper	270	----	25	17	13	20	16	18	17	12	20	13
Lead	220	----	30	10.1	9.2	17.7	10.4	18.9	9.1	6.6	17.3	8.3
Mercury	1.0	----	0.080	0.055	0.041	0.085	0.062	<0.10	<0.10	<0.10	<0.10	<0.10
Nickel	52	----	13	34	17	34	29	11	34	15	20	21
Silver	3.7	----	0.61	0.07	0.04	0.16	0.06	0.5	<0.4	<0.4	<0.4	<0.4
Tin	----	----	2.6	1.2	0.9	2.1	1.2	1.7	<1.0	<1.0	1.7	<1.0
Zinc	410	----	125	61	48	92	55	100	63	42	122	47
Sulphate (mg/kg dry wt)	----	----	1,810	1,890	1,930	2,200	1,950	2,300	2,400	2,200	2,200	2,100
Total Organic Carbon (g/100g dry wt)	----	----	0.94	0.80	0.98	1.16	0.77	0.72	0.74	0.69	0.86	0.62
<b>Saline SPLP Leachate – Total Metals (g/m<sup>3</sup>)</b>												
Arsenic	----	----	<0.004	<0.004	0.008	<0.004	<0.004	0.006	0.004	0.006	0.004	0.005
Cadmium	----	0.014	<0.0002	<0.0002	<0.0002	<0.0002	<0.0002	<0.0002	<0.0002	<0.0002	<0.0002	<0.0002
Chromium	----	0.020 <sup>1</sup>	<0.001	<0.001	<0.001	<0.001	<0.001	0.002	0.008	0.002	0.004	0.004
Copper	----	0.003	<0.001	<0.001	<0.001	<0.001	<0.001	0.009	0.004	0.002	0.007	0.003
Lead	----	0.0066	<0.001	<0.001	<0.001	<0.001	<0.001	<0.001	<0.001	<0.001	<0.001	<0.001
Mercury	----	0.0007	TBC	TBC	TBC	TBC	TBC	<0.00008	<0.00008	<0.00008	<0.00008	<0.00008
Nickel	----	0.200	<0.007	0.011	<0.007	<0.007	<0.007	0.015	0.008	<0.007	0.017	<0.007
Silver	----	0.0018	<0.0004	<0.0004	<0.0004	<0.0004	<0.0004	<0.0004	<0.0004	<0.0004	<0.0004	<0.0004
Tin	----	----	<0.002	<0.002	<0.002	<0.002	<0.002	<0.002	<0.002	<0.002	<0.002	<0.002
Zinc	----	0.023	<0.004	<0.004	<0.004	<0.004	<0.004	<0.004	<0.004	<0.004	<0.004	<0.004
pH	----	----	7.4	7.6	7.7	7.5	7.6	9.0	9.0	9.1	9.1	9.0
Total Ammoniacal-N	----	1.2	0.79	----	----	1.7	0.87	0.54	----	----	0.71	0.43
Nitrite-N	----	----	0.03	----	----	< 0.02	< 0.02	< 0.02	----	----	< 0.2	< 0.2
Nitrate-N	----	3.4 <sup>2</sup>	0.05	----	----	0.05	0.05	0.06	----	----	< 0.2	< 0.2
Nitrate-N + Nitrite-N	----	3.4 <sup>2</sup>	0.09	----	----	0.07	0.06	0.07	----	----	< 0.2	< 0.2

<sup>1</sup>Guideline value for ANZECC 90% chromium as Cr(VI)

<sup>2</sup>Guideline value for ANZECC 90% Nitrate-N freshwater

**Results exceeding ANZECC Guideline**

Should you have any queries regarding this report, please contact the undersigned.

*This report may not be reproduced, except in full, without the written consent of the signatory.*

Yours sincerely

**Brian Mills**

Senior Environmental Scientist

on behalf of

**Beca Ltd**

Direct Dial: +64-9-308 0869

Email: [brian.mills@beca.com](mailto:brian.mills@beca.com)